

AD _____

Award Number: DAMD17-99-1-9078

TITLE: Studies of Vascular Endothelial Growth Factor (VEGF)
Signaling in Breast Cancer Cells

PRINCIPAL INVESTIGATOR: Hava Avraham, Ph.D.

CONTRACTING ORGANIZATION: Beth Israel Deaconess Medical Center
Boston, Massachusetts 02215

REPORT DATE: July 2002

TYPE OF REPORT: Final

PREPARED FOR: U.S. Army Medical Research and Materiel Command
Fort Detrick, Maryland 21702-5012

DISTRIBUTION STATEMENT: Approved for Public Release;
Distribution Unlimited

The views, opinions and/or findings contained in this report are those of the author(s) and should not be construed as an official Department of the Army position, policy or decision unless so designated by other documentation.

20030411 052

REPORT DOCUMENTATION PAGEForm Approved
OMB No. 074-0188

Public reporting burden for this collection of information is estimated to average 1 hour per response, including the time for reviewing instructions, searching existing data sources, gathering and maintaining the data needed, and completing and reviewing this collection of information. Send comments regarding this burden estimate or any other aspect of this collection of information, including suggestions for reducing this burden to Washington Headquarters Services, Directorate for Information Operations and Reports, 1215 Jefferson Davis Highway, Suite 1204, Arlington, VA 22202-4302, and to the Office of Management and Budget, Paperwork Reduction Project (0704-0188), Washington, DC 20503

1. AGENCY USE ONLY (Leave blank)		2. REPORT DATE July 2002	3. REPORT TYPE AND DATES COVERED Final (1 Jul 99 - 30 Jun 02)	
4. TITLE AND SUBTITLE Studies of Vascular Endothelial Growth Factor (VEGF) Signaling in Breast Cancer Cells			5. FUNDING NUMBERS DAMD17-99-1-9078	
6. AUTHOR(S) Hava Avraham, Ph.D.				
7. PERFORMING ORGANIZATION NAME(S) AND ADDRESS(ES) Beth Israel Deaconess Medical Center Boston, Massachusetts 02215 E-Mail: havraham@caregroup.harvard.edu			8. PERFORMING ORGANIZATION REPORT NUMBER	
9. SPONSORING / MONITORING AGENCY NAME(S) AND ADDRESS(ES) U.S. Army Medical Research and Materiel Command Fort Detrick, Maryland 21702-5012			10. SPONSORING / MONITORING AGENCY REPORT NUMBER	
11. SUPPLEMENTARY NOTES Original contains color plates. All DTIC reproductions will be in black and white.				
12a. DISTRIBUTION / AVAILABILITY STATEMENT Approved for Public Release; Distribution Unlimited				12b. DISTRIBUTION CODE
13. Abstract (Maximum 200 Words) (abstract should contain no proprietary or confidential information) Our proposal aims to investigate the function of VEGF in breast cancer cell growth and signaling. Our data suggest that breast cancer cells secrete various levels of VEGF and express in addition to the Flt-1 and Flk-1/KDR receptors, a novel VEGF receptor type which needs to be identified and characterized. These data lead us to hypothesize that VEGF, secreted by breast cancer cells, is a multi-functional protein which acts in an autocrine fashion and can simultaneously activate specific VEGF receptor signaling pathways in breast cancer cells, thereby regulating breast cancer cell growth, tumor angiogenesis and subsequently tumor growth. In order to test this hypothesis, we propose to focus on two basic aims: (a) To identify and characterize the VEGF receptors expressed in breast cancer cell, and to analyze their expression on primary breast tissues. We will elucidate the signaling events upon VEGF stimulation in breast cancer cells and identify which activated signaling molecules are essential for the VEGF-mediated effects on breast cancer cell growth; and (b) To study the effects of VEGF and VEGF receptor expression on the regulation of tumor angiogenesis and signal transduction pathways in breast cancer cells.				
14. SUBJECT TERMS breast cancer, VEGF				15. NUMBER OF PAGES 115
				16. PRICE CODE
17. SECURITY CLASSIFICATION OF REPORT Unclassified	18. SECURITY CLASSIFICATION OF THIS PAGE Unclassified	19. SECURITY CLASSIFICATION OF ABSTRACT Unclassified	20. LIMITATION OF ABSTRACT Unlimited	

FOREWORD

Opinions, interpretation, conclusions and recommendations are those of the author and are not necessarily endorsed by the U. S. Army.

____ Where copyrighted material is quoted, permission has been obtained to use such material.

_____ Where material from documents designated for limited distribution is quoted, permission has been obtained to use the material.

____ Citations of commercial organizations and trade names in this report do not constitute an official Department of Army endorsement or approval of the products or services of these organizations.

x In conducting research using animals, the investigator(s) adhered to the "Guide for the Care and Use of Laboratory Animals," prepared by the Committee on Care and use of Laboratory Animals of the Institute of Laboratory Resources, national Research Council (NIH Publication No. 86-23, Revised 1985).

x For the protection of human subjects, the investigator(s) adhered to policies of applicable Federal Law 45 CFR 46.

N/A In conducting research utilizing recombinant DNA technology, the investigator(s) adhered to current guidelines promulgated by the National Institutes of Health.

N/A In the conduct of research utilizing recombinant DNA, the investigator(s) adhered to the NIH Guidelines for Research Involving Recombinant DNA Molecules.

N/A In the conduct of research involving hazardous organisms, the investigator(s) adhered to the CDC-NIH Guide for Biosafety in Microbiological and Biomedical Laboratories.

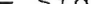



 PI - Signature Date

TABLE OF CONTENTS

	Page #
FRONT COVER	1
STANDARD FORM (SF) 298	2
FOREWORD	3
TABLE OF CONTENTS	4
INTRODUCTION	5
BODY	5-10
KEY RESEARCH ACCOMPLISHMENTS	10
REPORTABLE OUTCOMES	11
CONCLUSIONS	11
REFERENCES	
APPENDICES	

FINAL REPORT FOR AWARD #: DAMD17-99-1-9078
Year 3 of 3

Title: Studies of Vascular Endothelial Growth Factor (VEGF) Signaling in Breast Cancer Cells

P.I.: Hava Avraham, Ph.D.

INTRODUCTION

The overall goal of our proposal is to investigate the function of VEGF in breast cancer cell growth and signaling. The first step in VEGF action is binding to its high affinity tyrosine kinase receptors Flt-1 and Flk-1/KDR, found primarily in endothelial cells. Our data suggest that breast cancer cells secrete various levels of VEGF and express in addition to the Flt-1 and Flk-1/KDR receptors, a novel VEGF receptor type which needs to be identified and characterized. These data lead us to hypothesize that VEGF, secreted by breast cancer cells, is a multi-functional protein which acts in an autocrine fashion and can simultaneously activate specific VEGF receptor signaling pathways in breast cancer cells, thereby regulating breast cancer cell growth, tumor angiogenesis and subsequently tumor growth. In order to test this hypothesis, we propose to focus on two basic aims: (a) To identify and characterize the VEGF receptors expressed in breast cancer cell, and to analyze their expression in primary breast tissues. We will elucidate the signaling events upon VEGF stimulation in breast cancer cells and identify which activated signaling molecules are essential for the VEGF-mediated effects on breast cancer cell growth; and (b) To study the effects of VEGF and VEGF receptor expression on the regulation of tumor angiogenesis and signal transduction pathways in breast cancer cells. Specifically, we will investigate effects of conditional ectopic expression of VEGF and VEGF receptors in MCF-7 breast cancer cells and in MCF-10A normal mammary epithelial cells and will analyze the effects of their overexpression on the regulation of tumor angiogenesis and signal transduction pathways in breast cancer cells.

HYPOTHESIS/PURPOSE

This overall goal of this proposal is to investigate the function of VEGF in breast cancer cell growth and signaling. We hypothesize that VEGF, secreted by breast cancer cells, is a multifunctional protein which acts in an autocrine fashion and can simultaneously activate specific VEGF receptor signaling pathways, thereby regulating breast cancer cell growth, invasion, tumor angiogenesis and subsequently tumor growth.

TECHNICAL OBJECTIVES

In this proposal, we elucidated VEGF signaling pathways in breast cancer cells (BCs) and identified which activated signaling molecules are essential for the VEGF-mediated effects on breast cancer cell growth. In addition, we characterized the VEGF receptors expressed in BCs that mediate the specific effects of VEGF and investigated the effects of conditional ectopic expression of VEGF and VEGF receptors on the regulation of tumor angiogenesis and signal transduction pathways in breast cancer cells. Toward this goal, the following specific aims were proposed:

Specific Aim 1: To characterize signaling events upon VEGF stimulation in breast cancer cells.

A. To identify and characterize the VEGF receptors in breast cancer cells, and analyze their expression in primary breast tumors.

B. To elucidate the receptor-activated signaling molecules in response to VEGF stimulation.

Specific Aim 2: To study the effects of VEGF and VEGF receptor expression on the regulation of tumor angiogenesis and signal transduction pathways in breast cancer cells.

RESULTS

Specific Aim 1 was completed, as was reported in my previous report.

Specific Aim 2: We have attempted to generate VEGF stable transfected breast cancer cells MCF-7 and normal mammary epithelial cells MCF-10A. However, we failed to generate these stable clones. Overexpression of VEGF in these cells affected their survival. Therefore, we decided to use an alternative approach of downregulation of VEGF expression in MDA-MB-231 cells and analyzed the effects on apoptosis, survival and migration. MDA-MB-231 cells are human breast cancer that secrete high levels of VEGF and are highly tumorigenic. We generated stable clones of MDA-MB-231 cells that overexpress sense and antisense VEGF and analyzed these clones as described below. Since some of the breast cancer patients develop breast metastasis to the brain, we also analyzed the autocrine and paracrine role of VEGF in breast cancer metastasis using these clones.

VEGF/VPF Increases Penetration of MDA-MB-231 Cells across an HBMEC Monolayer---To test whether VEGF/VPF increases tumor cell penetration, DiI-labeled MDA-MB-231 cells were added to an HBMEC monolayer cultured onto a Transwell apical chamber, and then penetrating MDA-MB-231 cells were assessed under a fluorescent microscope. VEGF/VPF treatment led to a dose-dependent increase in the penetration of MDA-MB-231 cells across the HBMEC monolayer as compared to the untreated control (Fig. 1). However, basic fibroblast growth factor (bFGF), which is also known as a potent endothelial cell growth factor that does not increase vascular permeability, failed to significantly increase the transendothelial migration of the cells. These data indicate the possibility that increased transmigration of MDA-MB-231 cells is due to the endothelial cell retraction induced by VEGF/VPF and not due to the mitogenic effect of VEGF/VPF.

MDA-MB-231 cells failed to migrate toward either the basolateral side of the formaldehyde-fixed HBMEC monolayer or the fibronectin-coated polycarbonate filter without the HBMEC monolayer (data not shown), indicating that the living endothelial monolayer is needed to induce the migration of tumor cells toward the basolateral side of the filter as reported previously. To further characterize whether VEGF/VPF is related directly to the increased transendothelial migration of MDA-MB-231 cells, the HBMEC monolayer was treated with VEGF/VPF monoclonal antibodies and with SU-1498, an antagonist of VEGF/VPF receptor (Flk-1/KDR). As shown in Fig. 3, both treatments against VEGF/VPF significantly inhibited the transendothelial migration of MDA-MB-231 cells at 20 μ g/ml and 50 μ M, respectively.

VEGF/VPF Increases the Adhesion of MDA-MB-231 Cells to an HBMEC Monolayer---Metastatic tumor cells attach more preferentially to SEB membrane components than to the apical surface of an intact endothelial monolayer. The same phenomenon was observed in this study with MDA-MB-231 cells which attached preferentially to areas where the SEB of the endothelial cell was exposed (Fig. 2, right panel). Therefore, the increased transendothelial migration of MDA-MB-231 cells induced by VEGF/VPF might result from increased adhesion of the cells to the SEB membrane components of endothelial cells which were exposed. To test this possibility, DiI-labeled MDA-MB-231 cells were added to an HBMEC monolayer cultured onto 24-well plates with or without VEGF/VPF and cell adhesion was then assessed under a fluorescent microscope. At a concentration of 30 ng/ml, VEGF/VPF increased the adhesion of MDA-MB-231 cells to the HBMEC monolayer by 3-fold as compared to the untreated control (Fig. 2, left panel), and this effect was blocked by VEGF/VPF monoclonal antibodies and SU-1498 (Fig. 4). However, bFGF failed to significantly increase the adhesion of tumor cells to the monolayer as compared to the untreated control (Fig. 2). These results indicate that the increased transendothelial migration of MDA-MB-231 cells induced by VEGF/VPF was at least in part derived from enhanced tumor cell adhesion onto the exposed SEB membrane components.

VEGF/VPF Increases the Transendothelial Migration and Adhesion of MDA-MB-231 Cells through Calcium Signaling---VEGF/VPF stimulates several molecules mediating intracellular signals in endothelial cells, including mitogen-activated protein/extracellular signal-regulated kinase (ERK) kinase (MEK), phosphatidylinositol 3-kinase (PI3-kinase), and calcium. To examine which signaling pathways of VEGF/VPF in endothelial cells are responsible for the increased transendothelial migration and

adhesion of MDA-MB-231 cells, the effects of specific inhibitors for various VEGF/VPF signaling pathways were tested. As shown in Figs. 3 and 4, the intracellular calcium chelator (BAPTA-AM) inhibited the increased transendothelial migration and adhesion of MDA-MB-231 cells stimulated by VEGF/VPF while the MEK inhibitor (PD98059) and the PI3-kinase inhibitor (Wortmannin) had no effect, indicating that VEGF/VPF increases the transendothelial migration and adhesion of MDA-MB-231 cells through activation of endothelial calcium signaling.

VEGF/VPF Increases the Permeability of the HBMEC Monolayer---Endothelial cell retraction induces the breakdown of intercellular junctions and leads to an increase in vascular permeability. Therefore, we measured the extent of endothelial cell retraction induced by VEGF/VPF as the degree of permeability change of [³H] inulin through the HBMEC monolayer. As expected, VEGF/VPF meaningfully increased the permeability of the monolayer as compared to the untreated control, and this effect was blocked by VEGF/VPF monoclonal antibody and SU-1498 (Fig. 5). Furthermore, the increased vascular permeability caused by VEGF/VPF was abolished by BAPTA-AM but not by PD98059 and Wortmannin (Fig. 5), indicating that calcium signaling mediates the increased permeability induced by VEGF/VPF.

VEGF/VPF Induces Cytoskeletal Rearrangement of HBMECs---We then assessed the mechanism that leads to increased endothelial cell permeability. One important regulatory mechanism for the integrity of endothelial cell junction maintenance is the distribution of actin to a cortical pattern, precluding stress fiber formation. As shown in Fig. 6A, VEGF/VPF caused a marked redistribution of actin fibers which condensed toward the center of the cell, with resulting stress fiber formation. The actin condensation in the endothelial cells occurred within 15 min after VEGF/VPF treatment. Actin redistribution induced by VEGF/VPF was substantially reversed by co-incubation with VEGF/VPF monoclonal antibody and SU-1498 (data not shown). These data indicated that VEGF/VPF was responsible for the architectural change within the endothelial cell, leading to increased vascular permeability. Since we found that calcium signaling contributed to the increased permeability stimulated by VEGF/VPF, we assessed its contribution to the redistribution of actin. We found that BAPTA-AM potentially blocked the effect of VEGF/VPF in stimulating actin redistribution (Fig. 6A), suggesting a molecular mechanism for the role of calcium in modulating the permeability of the HBMEC monolayer.

We also examined adherens junction protein alignment at the HBMEC monolayer (Fig. 6B). The specific endothelial adherens junctional protein VE-cadherin has been shown to maintain and perhaps regulate endothelial barrier properties. VE-cadherin was disrupted to a zig-zag form within 15 min after treatment with VEGF/VPF. After 2 hours, gaps between adjacent endothelial cells could be seen where junctional protein staining was lost (Fig. 6B). Co-incubation of monolayers with BAPTA-AM failed to show disorganization of VE-cadherin or promote the appearance of inter-endothelial gap formation (Fig. 6B), indicating that calcium signaling governs the endothelial junction disorganization produced by VEGF/VPF.

These data suggest that the increased transendothelial migration of MDA-MB-231 cells induced by VEGF/VPF occurs through the loss of junctional proteins, with concomitant gap formation in endothelial monolayer, as shown in Fig. 6C.

Down-Regulation of VEGF/VPF Expression Induces Apoptosis and Inhibits the Transendothelial Migration of MDA-MB-231 Cells ---In addition to its vascular permeability activity in endothelial cells, VEGF/VPF induces intracellular signaling that mediates the proliferation and invasion of breast cancer cells. To examine the possibility that the endogenous VEGF/VPF in MDA-MB-231 cells modulates the transendothelial migration of these cells, we have generated MDA-MB-231 clones stably transfected with antisense VEGF/VPF cDNA constructs (AS-VEGF-C1 and -C2). In these clones, VEGF/VPF expression was down-regulated significantly as compared to the parental cells (Fig. 7A). When these cells were added to the HBMEC monolayer and examined for transendothelial migration, the two stable clones showed reduced migration toward the bottom of the HBMEC monolayer as compared to the

parental or control vector expressing cells (pZeoSV, Fig. 7B). Next, using cell cycle analysis and TUNEL assay, we investigated whether the reduced transendothelial migration of AS-VEGF-C1 and -C2 clones resulted from the increased apoptosis of these cells. As shown in Fig. 8A and B, the apoptosis rates of AS-VEGF-C1 and -C2 clones were significantly increased over the parental or pZeoSV cells, indicating that endogenous VEGF/VPF acts as a survival factor in MDA-MB-231 cells. Furthermore, apoptosis gene array analysis revealed that apoptosis-related genes such as TRAIL, Cox-2, caspase-7, and -8 were up-regulated significantly in AS-VEGF-C1 and -C2 clones as compared to the parental or pZeoSV cells (Fig. 8C, Table 1), strongly suggesting that the reduced transendothelial migration of AS-VEGF-C1 and -C2 resulted from the increased apoptosis of these cells.

VEGF/VPF Promotes the Survival of MDA-MB-231 Cells Through the PI3-kinase Pathway---Since VEGF/VPF can stimulate the PI3-kinase pathway, we examined whether VEGF/VPF mediates the survival of MDA-MB-231 cells through phosphorylation of the serine/threonine kinase Akt/PKB, a downstream target of PI3-kinase. To test this possibility, the AS-VEGF-C1 clone was treated with VEGF/VPF (100 ng/ml) for 15 min and the phosphorylation of Akt was analyzed by Western blotting. VEGF/VPF increased significantly the phosphorylation of Akt as compared to the untreated control (Fig. 9A), but failed to increase the phosphorylation of ERK (data not shown). Epidermal growth factor (EGF) did not increase significantly the phosphorylation of Akt as compared to the untreated control. In addition, VEGF-Ad-infected cells showed increased PI3-kinase activity and Akt phosphorylation as compared to the parental or CTL-Ad-infected cells (Fig. 9B, C, and D). However, no change in the ERK phosphorylation of VEGF-Ad-infected cells was observed (Fig. 9E). These data indicate that VEGF/VPF mediates the survival of MDA-MB-231 cells via the PI3-kinase/Akt pathway.

FIGURE LEGENDS

Fig. 1. VEGF/VPF increases transendothelial migration of MDA-MB-231 cells across an HBMEC monolayer. HBMECs were added to fibronectin-coated 24-well Transculture inserts with pore sizes of 8 μ m (Costar Corp.) and grown for 5 days in 5% CO₂ at 37 °C. 40,000 DiI-labeled MDA-MB-231 cells were added to the apical chamber. To exclude the chemoattractant effect of the added growth factor, bFGF or VEGF/VPF was added evenly to the apical and basolateral chambers. After incubation for 6 hours, the apical chamber was fixed with 3.7% formaldehyde and washed extensively with PBS. The apical side of the apical chamber was scraped gently with cotton wool. Only the migrating tumor cells were observed by a fluorescent microscope and counted from 10 random fields of 200 magnification. The results are presented as the mean \pm SD of duplicate samples and are representative of 5 individual studies. CTL, control

Fig. 2. VEGF/VPF increases Adhesion of MDA-MB-231 cells onto the HBMEC monolayer. HBMECs were added to attachment factor-coated 24-well culture plates and grown for 5 days in 5% CO₂ at 37 °C. 100,000 DiI-labeled MDA-MB-231 cells in 500 μ l of the same medium were added to each well with or without test samples. After incubation for 2 hours, the wells were fixed with 3.7% formaldehyde and washed extensively with PBS to remove floating tumor cells. Attached tumor cells were observed by a fluorescent microscope and counted from 10 random fields of 200 magnification. Alternatively, to detach the endothelial monolayer, the monolayers were treated with 50 mM NH₄OH solution for 5 min and washed extensively with PBS before adding the DiI-labeled MDA-MB-231 cells. The results are presented as the mean \pm SD of triplicate samples. CTL, control; EC, endothelial cells; SEB, sub-endothelial basement

Fig. 3. BAPTA/AM inhibits transendothelial migration of MDA-MB-231 cells across an HBMEC monolayer. HBMECs were added to fibronectin-coated 24-well Transculture inserts with pore sizes of 8 μ m (Costar Corp.) and grown for 5 days in 5% CO₂ at 37 °C. The monolayers were pre-treated for 30 min with the indicated inhibitors and washed twice with culture medium. 40,000 DiI-labeled MDA-MB-

231 cells were added to the apical chamber. To exclude the chemoattractant effect of the added growth factor, VEGF/VPF was added evenly to the apical and basolateral chambers. After incubation for 6 hours, the apical chamber was fixed with 3.7% formaldehyde and washed extensively with PBS. The apical side of the apical chamber was scraped gently with cotton wool. Only the migrating tumor cells were observed by a fluorescent microscope and counted from 10 random fields of 200 magnification. The results are presented as the mean \pm SD of triplicate samples. CTL, control; VEGF-Ab, VEGF/VPF antibody (20 μ g/ml); SU, SU-1498 (50 μ M); PD, PD98059 (10 μ M); WM, Wortmannin (1 μ M); BAPTA, BAPTA-AM (10 μ M)

Fig. 4. BAPTA/AM inhibits adhesion of MDA-MB-231 cells onto the HBMEC monolayer. HBMECs were added to attachment factor-coated 24-well culture plates and grown for 5 days in 5% CO₂ at 37 °C. The monolayers were pre-treated for 30 min with the indicated inhibitors and all inhibitors except VEGF/VPF monoclonal antibodies and SU-1498 were removed from the monolayers by washing twice with culture medium. 100,000 DiI-labeled MDA-MB-231 cells in 500 μ l of the same medium were added to each well with or without VEGF/VPF. After incubation for 2 hours, the wells were fixed with 3.7% formaldehyde and washed extensively with PBS to remove floating tumor cells. Attached tumor cells were observed by a fluorescent microscope and counted from 10 random fields of 200 magnification. The results are presented as the mean \pm SD of triplicate samples. CTL, control; VEGF-Ab, VEGF/VPF antibody (20 μ g/ml); SU, SU-1498 (50 μ M); PD, PD98059 (10 μ M); WM, Wortmannin (1 μ M); BAPTA, BAPTA-AM (10 μ M)

Fig. 5. VEGF/VPF increases the permeability of the HBMEC monolayer. Approximately 100,000 HBMECs were added to fibronectin-coated 24-well Transculture inserts with pore sizes of 0.4 μ m (Falcon Corp.) and grown for 5 days in 5% CO₂ at 37°C. After the removal of culture medium, 0.4 ml of the fresh culture medium containing [³H] inulin (1 μ Ci) was added to the apical chamber. The basolateral chamber was filled with 0.6 ml of the same medium without [³H] inulin and then VEGF/VPF (30 ng/ml) was added to the apical and basolateral chambers. For the inhibitor treatment, the monolayers were pre-treated for 30 min with various inhibitors as indicated before VEGF/VPF treatment. After the incubation for 2 hours, 30 μ l of medium from the basolateral chamber were collected and the amount of [³H] inulin across the monolayers was determined by scintillation counting. The data represent the mean values of total cpm of three separate experiments. CTL, control; VEGF-Ab, VEGF/VPF antibody (20 μ g/ml); SU, SU-1498 (50 μ M); PD, PD98059 (10 μ M); WM, Wortmannin (1 μ M); BAPTA, BAPTA-AM (10 μ M)

Fig. 6. VEGF/VPF induces actin redistribution and VE-cadherin disruption in HBMECs. *Panel A*, HBMECs were added to fibronectin-coated 24-well Transculture inserts with pore sizes of 0.4 μ m and grown for 5 days in 5% CO₂ at 37°C. After assaying for 2 hours, the cells were fixed with 3.7% formaldehyde in PBS, and then permeabilized with 0.5% Triton X-100. The F-actin in the cells was stained and observed by a fluorescent microscope. *Panel B*, HBMECs were grown as in A. After assaying, the cells were fixed with 3.7% formaldehyde in PBS, and then permeabilized with 0.5% Triton X-100. The VE-Cadherin of the cells was stained and viewed under a confocal microscope. *Panel C*, HBMECs were grown as in A. Approximately 1,000 BCECF-AM-labeled MDA-MB-231 cells were added to each well with or without VEGF/VPF. After incubation for 2 hours, the cells were fixed with 3.7% formaldehyde in PBS. VE-cadherin in the HBMECs was stained and viewed under a confocal microscope. MDA-MB-231 cells are visualized by green color, whereas VE-cadherin is viewed as red color, respectively. CTL, control; VEGF/VPF, 30 ng/ml; BAPTA-AM, 10 μ M

Fig. 7. Down-regulation of endogenous VEGF/VPF induces the reduced transendothelial migration of MDA-MB-231 cells. *Panel A*, antisense VEGF/VPF transfectants were stably generated. MDA-MB-231 cells were transfected with antisense VEGF vector and selected in the presence of

Zeocin (1 mg/ml). VEGF/VPF expression of MDA-MB-231 transfectants was analyzed by Western blotting using a polyclonal anti-VEGF/VPF antibody. Total protein extracts were analyzed by Western blotting using anti-Csk antibody as an internal control. *Panel B*, HBMECs were added to fibronectin-coated 24-well Transculture inserts with pore sizes of 8 μ m (Costar Corp.) and grown for 5 days in 5% CO₂ at 37 °C. 40,000 DiI-labeled parental or transfected MDA-MB-231 cells were added to the apical chamber. After incubation for 6 hours, the apical chamber was fixed with 3.7% formaldehyde and washed extensively with PBS. The apical side of the apical chamber was scraped gently with cotton wool. Only the migrating tumor cells were observed by a fluorescent microscope and counted from 10 random fields of 200 magnification. The results are presented as the mean \pm SD of triplicate samples.

Fig. 8. Down-regulation of endogenous VEGF/VPF induces apoptosis of MDA-MB-231 cells. *Panel A*, parental or transfected MDA-MB-231 cells were grown subconfluently in 6-well plates in culture medium containing 10% FBS. The cells were harvested, centrifuged and fixed with 70% cold ethanol. Ethanol-fixed cells were centrifuged and suspended in 1 ml of PI/Triton X-100 staining solution and incubated for 15 min at 37 °C. Samples were analyzed by flow cytometry, and apoptosis was measured as the percentage of cells with a sub G₀/G₁ DNA content in the PI intensity-area histogram plot. *Panel B*, parental or transfected MDA-MB-231 cells were grown on chamber slides and stained with the fluorescein in situ cell death detection kit (Boehringer Mannheim) according to the protocol of the manufacturer. After washing with PBS, the cells were mounted and intracellular fluorescein-labeled fragmented DNA was observed by a fluorescent microscope. *Panel C*, parental or transfected MDA-MB-231 cells were grown subconfluently in 6-well plates in culture medium containing 10% FBS. Total RNA preparation and hybridization were performed. The hybridized membranes were exposed on a Phosphorimager and analyzed by using ArrayVisionTM software. 1, TRAIL; 2, Cox-2

Fig. 9. VEGF/VPF induces PI3-kinase activation in MDA-MB-231 cells. *Panel A*, the AS-VEGF-C1 clone was grown subconfluently in 6-well plates in culture medium containing 10% FBS. The medium was replaced by culture medium containing 0.5% FBS and, after starvation for 24 hours, the cells were stimulated by VEGF/VPF (100 ng/ml) or EGF (100 ng/ml) for 15 min. The cells were then lysed, and 50 μ g of total protein was resolved by 12% SDS-PAGE and subjected to Western blot analysis by using anti-human phospho-Akt antibody. To verify the amount of loaded proteins, blots were reprobed with anti-human Akt antibody. *Panels B-E*, MDA-MB-231 cells were grown subconfluently in 6-well plates in culture medium containing 10% FBS. The medium was replaced by culture medium containing 0.5% FBS and after starvation overnight, the cells were infected with VEGF-Ad. After incubation for 24 hours, the cells were lysed, and 50 μ g of total protein was resolved by 12% SDS-PAGE and subjected to Western blot analysis by using anti-human VEGF/VPF antibody (*B*), anti-human phospho-Akt antibody (*D*), or anti-mouse phospho-ERK antibody (*E*). Total protein extracts were analyzed by Western blotting using anti-Csk antibody (*B*), anti-human Akt antibody (*D*), or anti-mouse ERK monoclonal antibody (*E*) as an internal control. Alternatively, a PI3-kinase assay was performed. Briefly, cell lysates containing 1 mg of protein were incubated overnight at 4°C with anti-human p85 subunit specific PI3-kinase antibody and Protein G Sepharose. After washing, the beads were incubated in reaction buffer containing 5 μ g of PI, 50 μ M ATP, and 5 μ Ci [γ -³²P]ATP for 10 min at room temperature. Lipid extracts were resolved on thin layer chromatography plates and then the plate was exposed to X-ray film (*C*, upper panel). The PI3-P was eluted from the plate and the amount was determined by scintillation counting (*C*, lower panel). CTL, control; PI3-P, phosphatidyl inositol-3 phosphate

KEY RESEARCH ACCOMPLISHMENTS;

The effects of VEGF on Signaling, migration, survival and breast metastasis to the brain have been analyzed in breast cancer cells. In addition, we determined the role of the extracellular matrix (ECM) in mediating VEGF's function in breast cancer cells.

REPORTABLE OUTCOMES

We published several papers on this project.

1. Price DJ, Miralem T, Jiang S, Steinberg R, Avraham H. Role of VEGF in the stimulation of cellular invasion and signaling of breast cancer cells. *Cell Growth and Differentiation* 2001; 12:129-135.
2. Miralem T, Steinberg R, Price D, Avraham H. VEGF165 requires extracellular matrix components to induce mitogenic effects and migratory response in breast cancer cells. *Oncogene*. 2001. 20:5511-5524.
3. Lee, T. H., Avraham, H., Lee, S-H., and Avraham, S. Vascular endothelial growth factor modulates neutrophil transendothelial migration via upregulation of interleukin-8 in human brain microvascular endothelial cells. *J Biol Chem*. 2002;277:10445-10451.
4. Price, D.J., Avraham, S., Feuerstein J., Fu, Y., and Avraham, H. The Invasive phenotype in HMT-3522 cells requires increased EGF Receptor signaling through both PI-3kinase and E-RK 1, 2 pathways. *Cell Communication and Adhesion*. 9 (2):87-102.
5. Lee, T.H., Avraham, H.K. Nam, M.J., and Avraham, S. The Autocrine and Paracrine of Vascular Endothelial Growth Factor in Breast cancer Metastasis. *J Biol Chem*. (In Press, 2002).

CONCLUSIONS

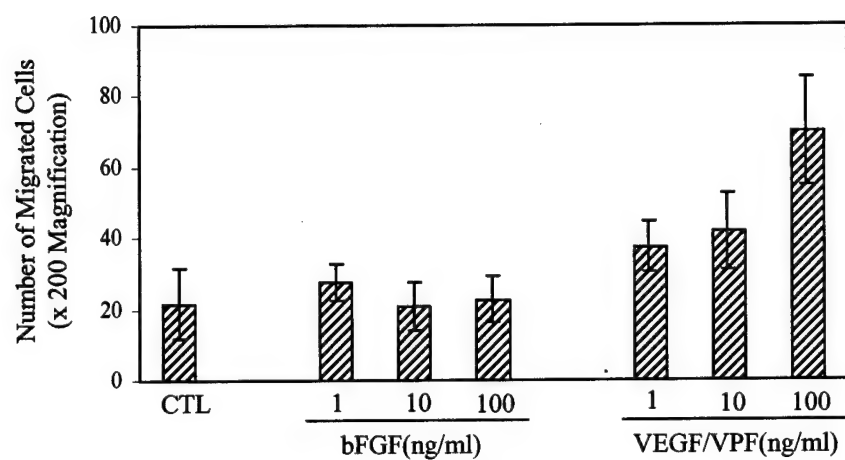
- 1) VEGF stimulation of breast cancer cells resulted in increase in cellular invasion and played a role in signaling in breast cancer cells.
- 2) VEGF required the extracellular matrix components to induce mitogenic effects and migratory response in breast cancer cells.
- 3) VEGF plays an important role in breast metastasis to the brain. Breast tumors that secrete VEGF are likely to be also metastatic tumors.

Table 1. Expression of apoptosis related-genes in antisense VEGF/VPF transfected MDA-MB-231 cells

The human apoptotic cDNA membranes were hybridized with total RNA isolated from antisense VEGF/VPF-transfected MDA-MB-231 cells. The membranes were exposed on a Phosphorimager and analyzed using ArrayVision™ software. The sVOL is the subtracted volume value derived by subtracting the background volume value from the volume value of the spot. Genomic DNA and GAPDH represent the positive controls for the hybridizations.

Apoptosis related-genes	Control sVOL [(Parental + PzeoSV)/2]	Data sVOL [(VEGF-C1+ C2)/2]	Data/Control ratio (VOL)
TRAIL	0.38	10.30	27.10
Cox-2	0.48	5.91	12.31
GM-CSF	0.38	2.06	5.42
IL-1beta	1.32	5.11	3.87
DAP kinase	0.84	3.17	3.77
VEGI	0.80	2.85	3.56
p27	1.42	4.83	3.40
IAP-1	3.68	11.81	3.20
M-CSF	8.84	27.75	3.13
P21	1.23	3.40	2.76
BimEL	1.17	3.15	2.69
Caspase-7	2.93	7.86	2.68
Rb2/p130	2.34	6.19	2.63
NAIP	2.07	5.37	2.59
GALECTIN-3	7.77	19.86	2.55
IGF-I R	1.71	4.18	2.44
IL-12 p35	1.02	2.46	2.41
Caspase-8	2.23	5.18	2.32
RAR-epsilon	1.97	4.57	2.31
TANK	3.42	7.55	2.20
HLA hc	20.14	43.79	2.17
IFN-gamma R1	3.17	6.85	2.16
BDNF	3.98	8.57	2.15
p100/NF-kappa B2	10.01	21.39	2.13
GAPDH	175.01	226.77	1.29
Genomic DNA	88.79	102.63	1.15

Fig.1



CTL



VEGF/VPF(100 ng/ml)

Fig. 2

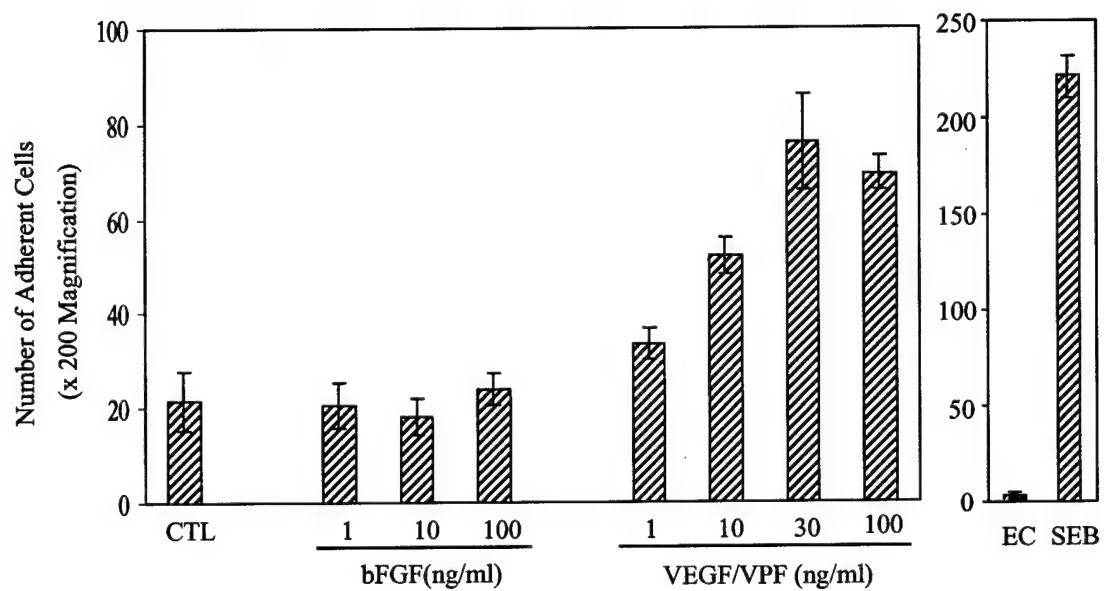


Fig. 3

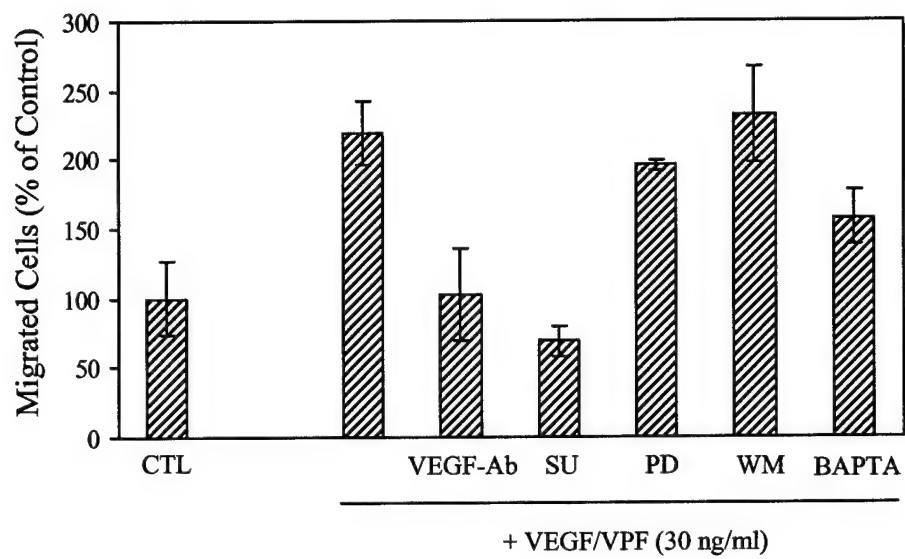


Fig. 4

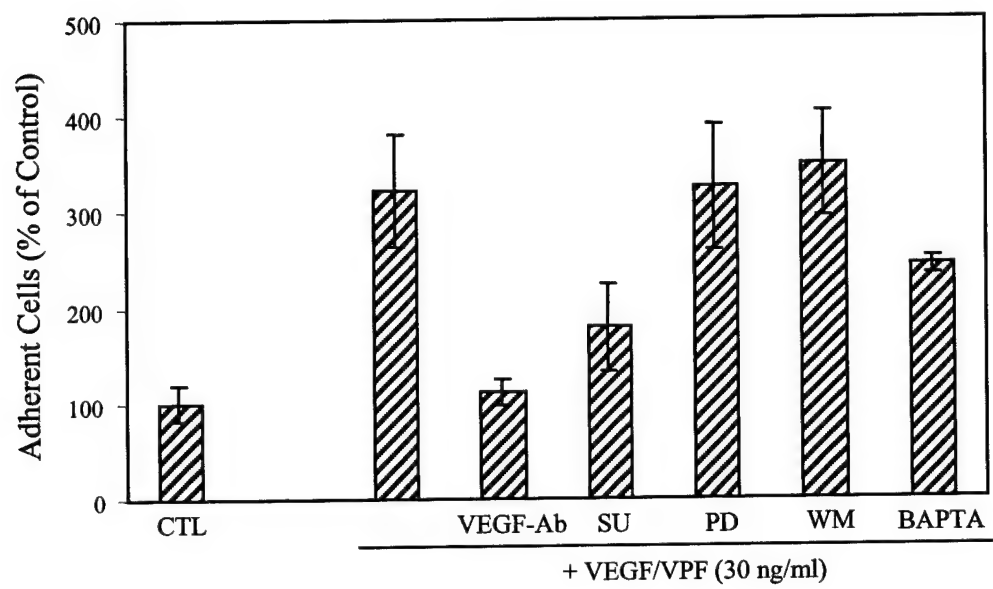


Fig. 5

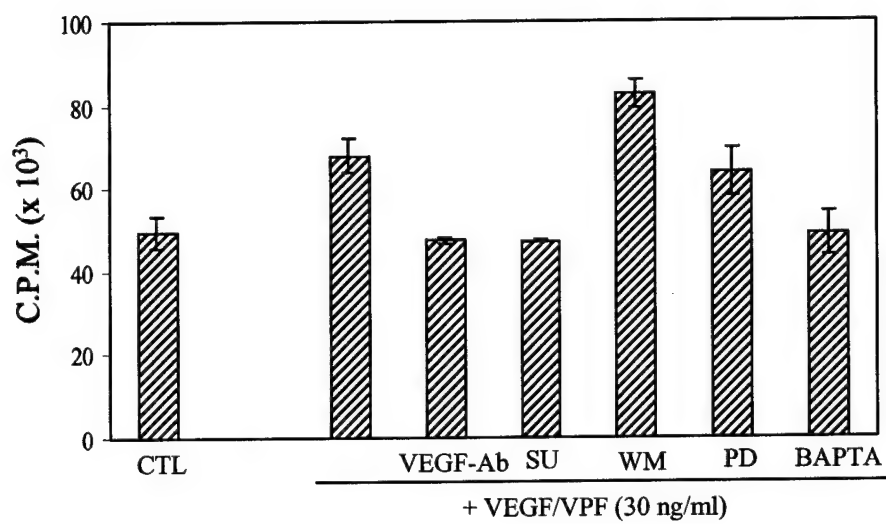


Fig. 6

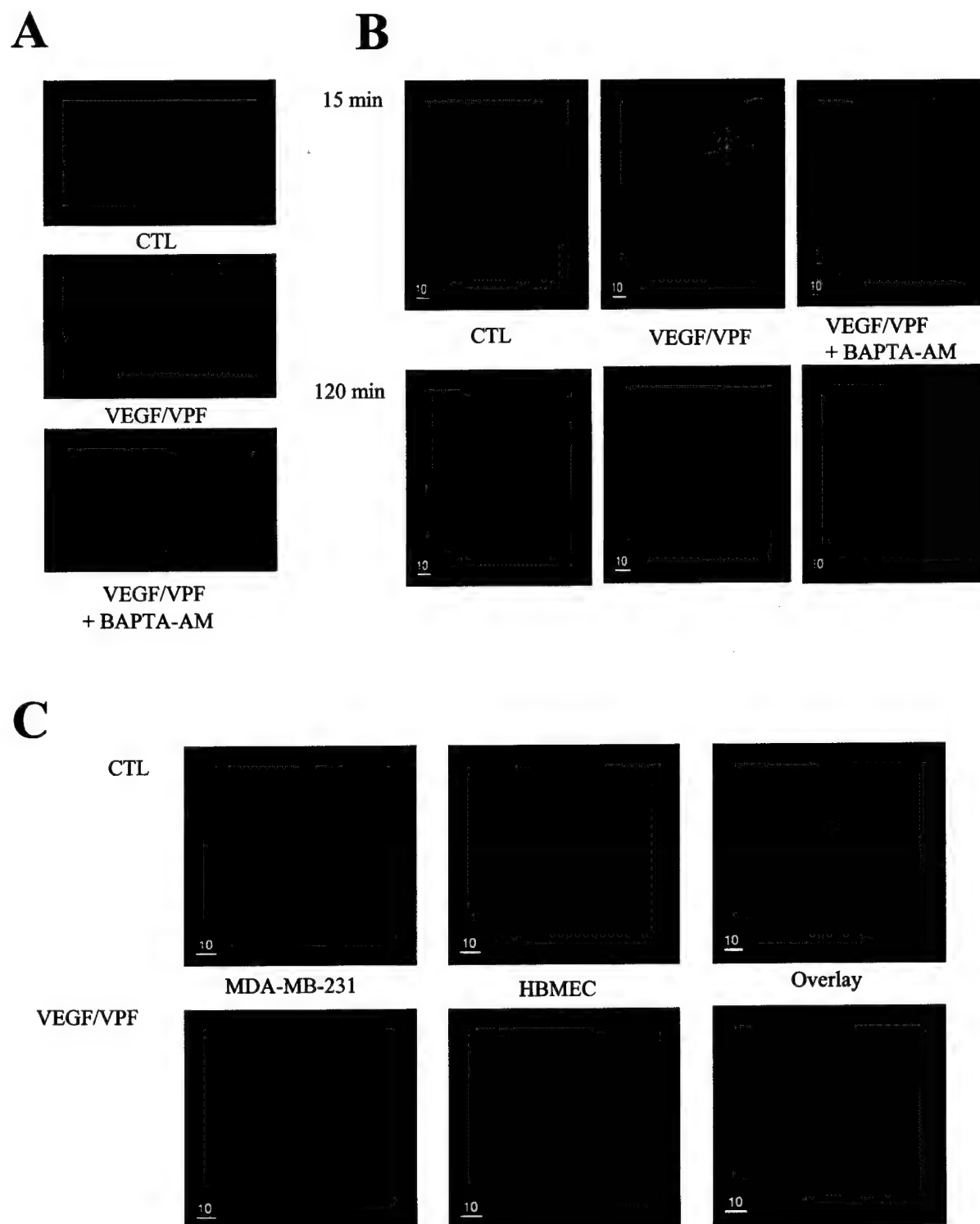
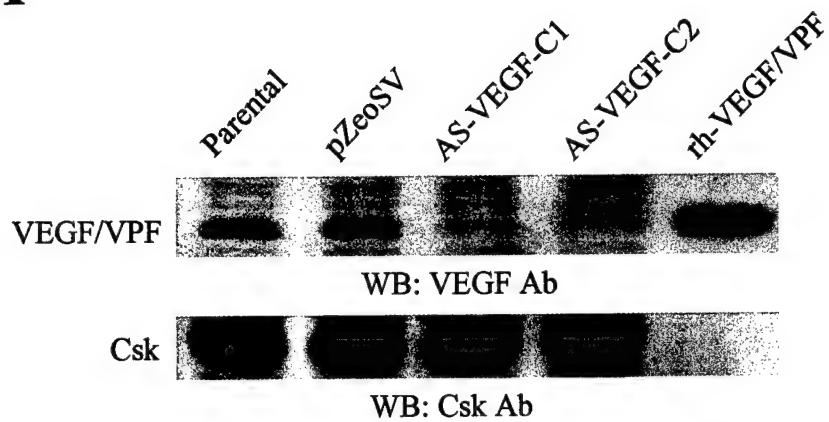


Fig. 7

A



B

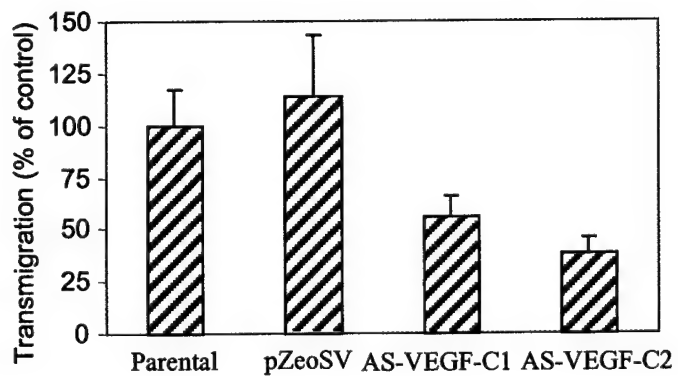


Fig. 8

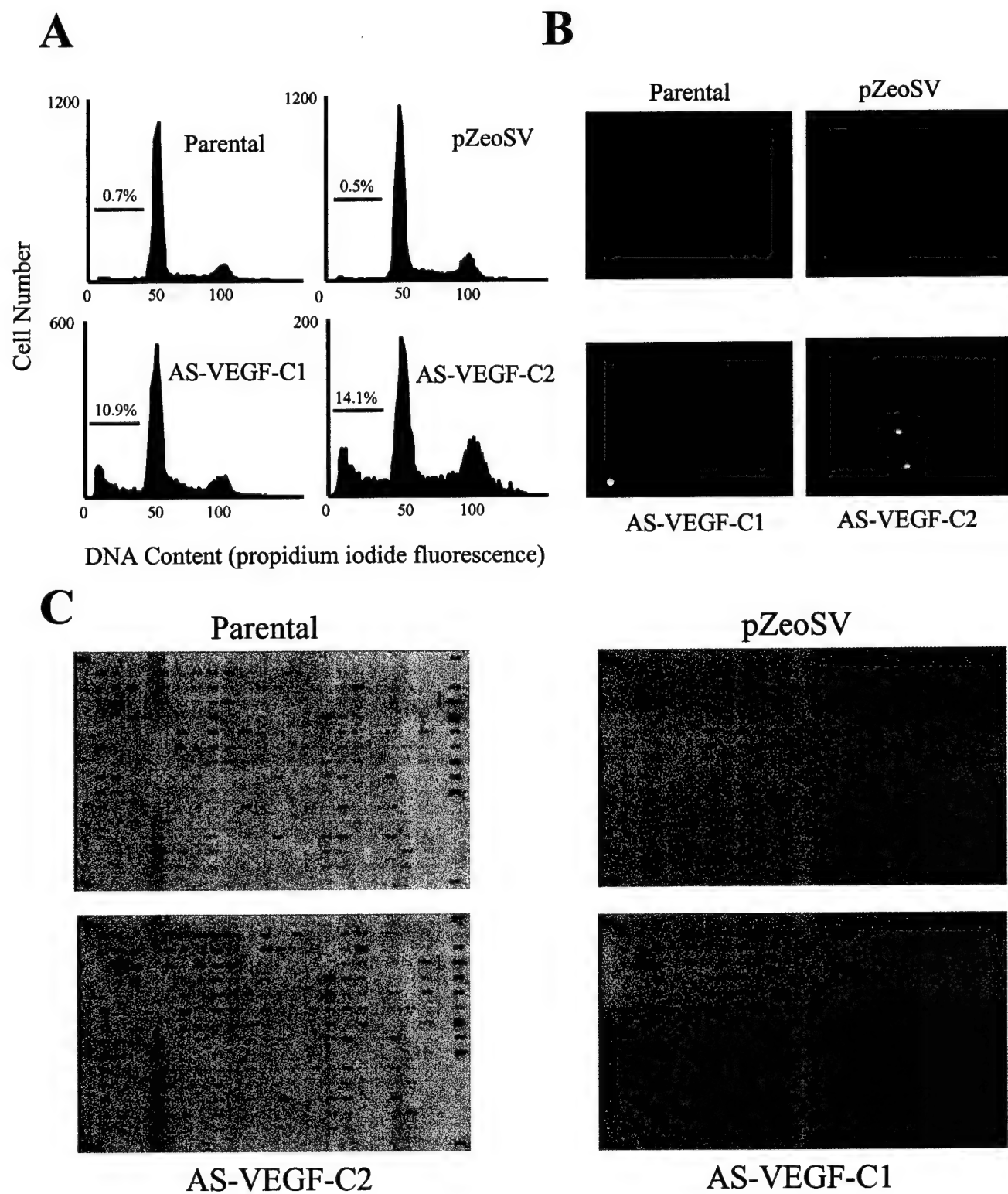
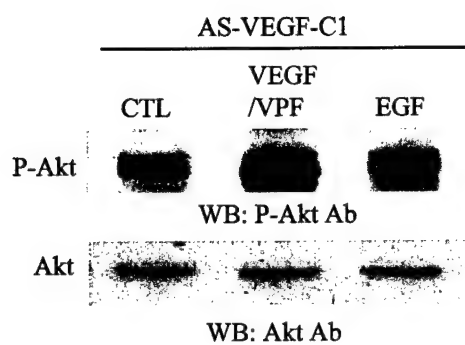
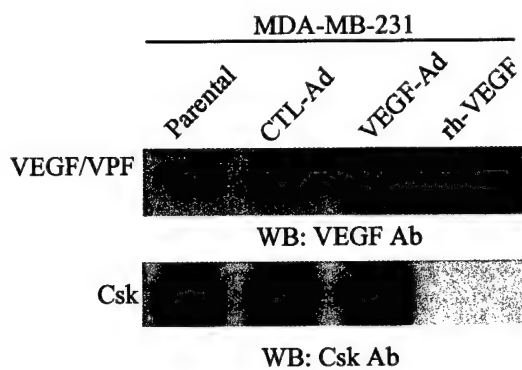


Fig. 9

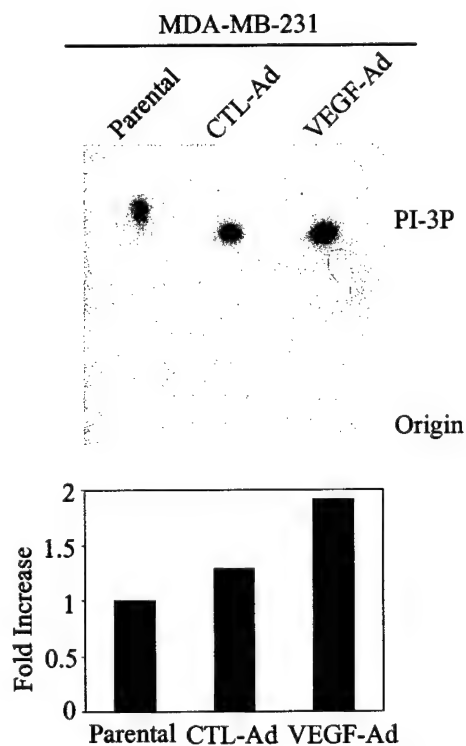
A



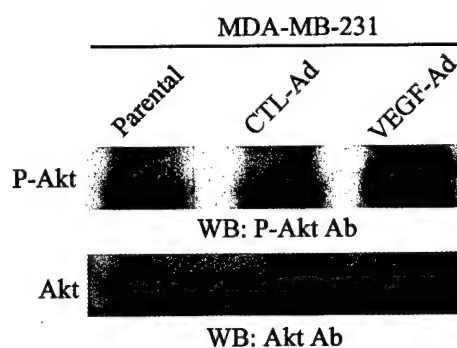
B



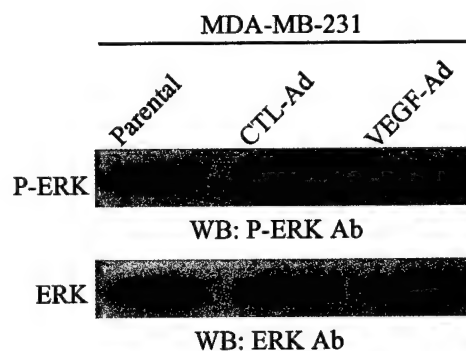
C



D



E



Role of Vascular Endothelial Growth Factor in the Stimulation of Cellular Invasion and Signaling of Breast Cancer Cells¹

Daniel J. Price, Tihomir Miralem, Shuxian Jiang, Robert Steinberg, and Hava Avraham²

Division of Experimental Medicine, Beth Israel-Deaconess Medical Center, Harvard Institutes of Medicine, Boston, Massachusetts 02115

Abstract

The expression of vascular endothelial growth factor (VEGF) by breast tumors has been previously correlated with a poor prognosis in the pathogenesis of breast cancer. Furthermore, VEGF secretion is a prerequisite for tumor development. Although most of the effects of VEGF have been shown to be attributable to the stimulation of endothelial cells, we present evidence here that breast tumor cells are capable of responding to VEGF. We show that VEGF stimulation of T-47D breast cancer cells leads to changes in cellular signaling and invasion. VEGF increases the cellular invasion of T-47D breast cancer cells on Matrigel/fibronectin-coated transwell membranes by a factor of two. Northern analysis for the expression of the known VEGF receptors shows the presence of moderate levels of Flt-1 and low levels of Flk-1/KDR mRNAs in a variety of breast cancer cell lines. T-47D breast cancer cells bind ¹²⁵I-labeled VEGF with a K_d of 13×10^{-9} M. VEGF induces the activation of the extracellular regulated kinases 1,2 as well as activation of phosphatidylinositol 3'-kinase, Akt, and Forkhead receptor L1. These findings in T-47D breast cancer cells strongly suggest an autocrine role for VEGF contributing to the tumorigenic phenotype.

Introduction

VEGF³ is widely recognized to be significant as a stimulator of tumor angiogenesis (1–5). A variety of studies have shown

the importance of VEGF as a prognostic indicator of the severity of breast cancer (6–10). VEGF occurs in a number of isoforms, including polypeptides of 121, 145, 165, 189, and 206 amino acids, which are produced by the alternate splicing of a single gene containing eight exons (11–14). Although VEGF-121 and VEGF-165 are the isoforms most commonly secreted by tumor cells, it is the VEGF-165 isoform that acts most strongly on endothelial cells, leading to the formation of new capillaries (15, 16). This effect of VEGF-165 on endothelial cells has been shown to be through defined cytoplasmic receptors (Flt-1, Flk-1/KDR, and Neuropilin-1; Refs. 17–22). Among its other effects, the stimulation of endothelial cells by VEGF-165 is known to lead to cell proliferation and migration (20, 23). These functions are likely to be important in the formation of neovasculature during tumor formation. In support of this, murine embryonic fibroblasts with targeted deletion of VEGF were significantly less tumorigenic in an *in vivo* model, and this was shown to be related to decreased vascular density and decreased vascular permeability (1).

VEGF has been shown to be present in breast tumors at levels that are, on average, 7-fold higher than in normal adjacent tissue (24). Expression of the VEGF receptor, Flt-1, was not increased in these tumors. Other investigators have found selective expression of VEGF and Flk-1/KDR in breast carcinomas (25). Immunocytochemistry showed that Flk-1/KDR was primarily present in the endothelium and epithelium of the mammary ducts. A number of studies have shown that VEGF secretion by the tumor cells is a prerequisite of tumor development. It was shown recently by Yoshiji *et al.* (26) that VEGF was required for the initial stages of breast cancer tumorigenesis, and that this initial effect was related to the development of neovascular stroma. Other studies have shown that the inhibition of vascular angiogenesis by such agents as angiostatin and endostatin resulted in reduced tumorigenesis and even regression of established tumors (27–30).

Although the significance of VEGF in the development of tumor vasculature is well documented, there is also a great amount of information to suggest an autocrine effect of VEGF on the tumor cells. There have been reports of VEGF signaling in melanoma cells (31, 32) and in prostate carcinoma cells (33). Both VEGF and Flt-1 have been shown to be expressed in angiosarcoma cells by immunohistochemistry and *in situ* hybridization (34). In another study, De Jong *et al.* (35) have used immunohistochemistry to measure VEGF and VEGF receptors in breast cancer. They also investigated EGF, PDGF α and β , TGF β , and their respective receptors. By carrying out double staining for the receptor/ligand combinations, they were able to distinguish possible autocrine and paracrine mechanisms for VEGF acting on the cells of the tumor. These investigators concluded that in 22–24% of cases, VEGF could act in an autocrine manner, whereas in 38–40% of the cases, it would be able to act in a paracrine

Received 11/30/00; revised 2/9/01; accepted 2/9/01.

The costs of publication of this article were defrayed in part by the payment of page charges. This article must therefore be hereby marked advertisement in accordance with 18 U.S.C. Section 1734 solely to indicate this fact.

¹ This paper is supported by NIH Grants CA 76226 and R21CA87290, DAMD 17-98-1-8032, and DAMD 17-99-1-9078, by Experienced Breast Cancer Research Grant 34080057089, by the Milheim Foundation, by the Massachusetts Department of Public Health (to H. A.), and by DAMD 17-001-0152 (to T. M.). This work was done during the tenure of an established investigatorship from the American Heart Association (H. A.).

² To whom requests for reprints should be addressed, at Division of Experimental Medicine, Beth Israel-Deaconess Medical Center, Harvard Institutes of Medicine, 4 Blackfan Circle, Boston, MA 02115. Phone: (617) 667-0073; Fax: (617) 975-6373; E-mail: havraham@caregroup.harvard.edu.

³ The abbreviations used are: VEGF, vascular endothelial growth factor; HRG, heregulin; MTR, Matrigel; PI 3-kinase, phosphatidylinositol 3'-kinase; ERK, extracellular regulated kinase; FKH, Forkhead; FKHRL1, Forkhead receptor L1; HUVEC, human vascular endothelial cell; MAP, mitogen-activated protein; GSK-3, glycogen synthase kinase-3.

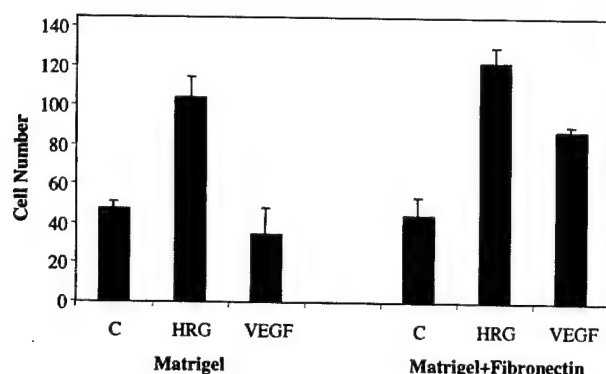


Fig. 1. Invasion of T-47D cells in response to VEGF or heregulin. Comparisons are to medium alone (C). Migrations were conducted on membranes coated with Matrigel alone (left) or Matrigel plus fibronectin (right).

manner. In the studies presented here, we show that VEGF-165 is able to stimulate the invasion of T-47D breast cancer cells into Matrigel. However, there was no effect of VEGF-165 on T-47D cell proliferation. We also show the presence of Flk-1/KDR and Flt-1 mRNAs in a number of breast cancer cell lines. Stimulation of T-47D cells with VEGF-165 led to tyrosine phosphorylation of multiple proteins in crude extracts, activation of ERK1,2 and also activation of the PI 3-kinase signaling pathway. Because T-47D cells are known to secrete VEGF (26), this effect on T-47D cells suggests a possible autocrine component for VEGF, leading to increased tumorigenesis.

Results

VEGF-165 Stimulation Leads to Increased Invasion of T-47D Cells. It was recently reported that VEGF⁴ modulates the chemotaxis and migration of endothelial cells (20). In addition, cellular invasion of MCF7 breast cancer cells in response to heregulin has been shown to be mediated through a PI 3-kinase-dependent pathway (36). Therefore, we asked whether VEGF signaling in T-47D breast cancer cells might also affect the invasion of these cells. As is shown in Fig. 1 (left panel), initial experiments on Matrigel alone showed no invasion in response to VEGF-165, whereas a >2-fold increase in invasion in response to heregulin was observed. However, when fibronectin was added to the Matrigel coating on the transwell membrane, VEGF-165 caused an ~2-fold increase in invasion that was ~72% of the invasion observed in response to heregulin under these conditions (Fig. 1, right panel). These results indicate that VEGF-165 induced the invasion of breast cancer cells in the presence of fibronectin.

Breast Cancer Cell Lines Express Primarily Flt-1 mRNA. We tested for the possible expression of VEGF receptor mRNAs in human breast tumor and normal breast cell lines. Using Northern blotting, we analyzed the expression of Flt-1, Flk-1/KDR, and Neuropilin-1 mRNAs in a number of

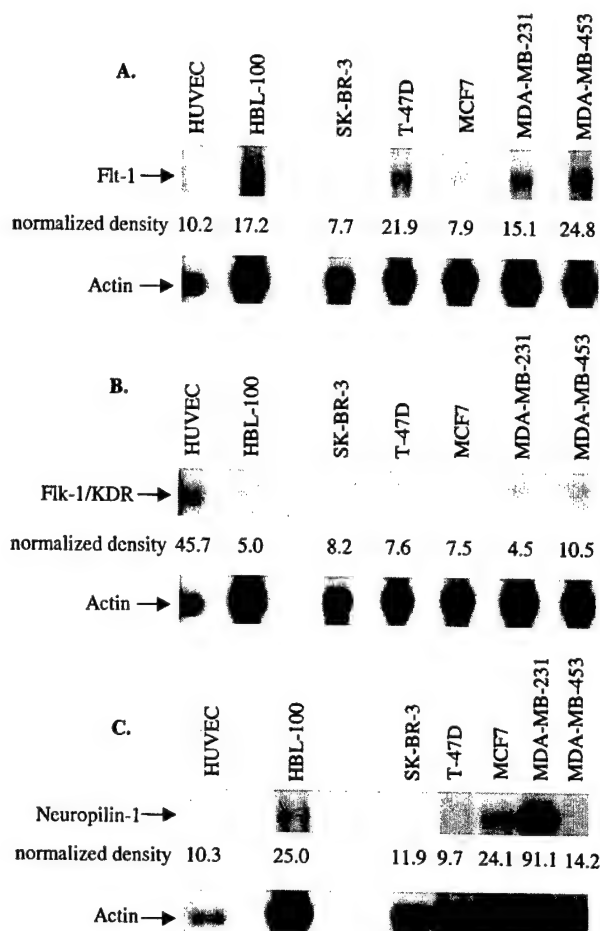


Fig. 2. Northern blotting for (A) Flt-1, (B) Flk-1/KDR, and (C) Neuropilin-1 mRNAs. Cell lines tested are indicated above. Control actin mRNA probe is shown in each panel. Densitometry of the Flt-1, Flk-1/KDR, and Neuropilin-1 bands was normalized to the corresponding actin signals.

cell lines. These included SK-BR-3, T-47D, MCF7, MDA-MB-231, and MDA-MB-453 breast cancer lines as well as an HL-100 nonmalignant breast line and HUVECs. As shown in Fig. 2A, all of the breast cancer lines except SK-BR-3 and MCF7 expressed a moderate level of Flt-1. HUVECs expressed a comparatively low level of this mRNA. HUVECs expressed a comparatively high level of Flk-1/KDR, whereas all of the breast cancer cells expressed low levels of this mRNA (Fig. 2B). MDA-MB-231 cells expressed a high level of Neuropilin-1, and MCF7 cells expressed a lower level of this mRNA (Fig. 2C). Other breast cancer lines failed to express Neuropilin-1 mRNA. These findings indicate that there is variable expression of VEGF receptors (Flt-1, Flk-1/KDR, and Neuropilin-1) in breast cancer. Although T-47D cells and three other breast lines expressed primarily Flt-1, only one of the cell lines (MDA-MB-231) expressed a high level of Neuropilin-1. Flk-1/KDR expression was uniformly low in all of the breast cell lines studied.

VEGF-165 Binds to T-47D Cells with a Lower Affinity Compared with the Known VEGF Receptors. To characterize the possible cellular receptors for VEGF on breast

⁴ Notation: Unless otherwise stated, all notation of VEGF refers to the VEGF-165 isoform.

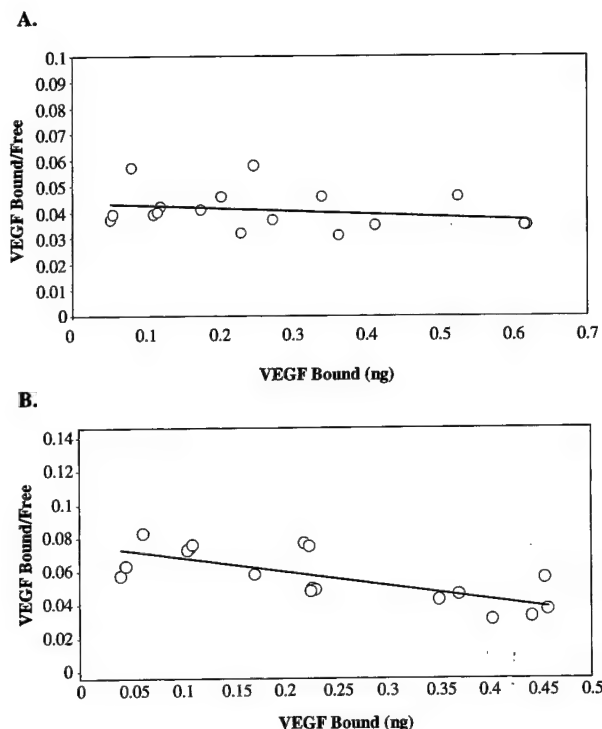


Fig. 3. Scatchard analysis of binding of ^{125}I -VEGF to MDA-MB-231 cells (A) and T-47D cells (B). Lines indicate a least square fit of the data points.

cancer cells, we determined the binding of ^{125}I -labeled VEGF to either T-47D cells or to MDA-MB-231 cells as a control. From Scatchard analysis of this data (Fig. 3), we calculated the binding of VEGF to T-47D cells as having a K_d of $\sim 13 \times 10^{-9} \text{ M}$ and $\sim 0.63 \times 10^5$ binding sites/cell. Binding of VEGF to MDA-MB-231 cells showed a K_d of $\sim 17.4 \times 10^{-10} \text{ M}$ and $\sim 1.53 \times 10^5$ binding sites/cell. Thus, MDA-MB-231 cells had a VEGF binding that was similar to that determined previously by Soker *et al.* (Ref. 21; $K_d \sim 2.8 \times 10^{-10} \text{ M}$; $0.95\text{--}1.1 \times 10^5$ binding sites/cell) reflecting the binding primarily to Neuropilin-1. To confirm our binding data obtained for detached cells, we repeated the experiments following more closely the method of Soker *et al.* (21), who determined binding to cells on tissue culture wells. Using this method, we obtained K_d values for VEGF binding to MDA-MB-231 and T-47D cells that were similar (within a factor of 2–3) to the values obtained by our method with detached cells (data not shown). Waltenberger *et al.* (20) have characterized VEGF binding to Flt-1 to have a K_d of $1.6 \times 10^{-11} \text{ M}$ and VEGF binding to Flk-1/KDR to have a K_d of $7.6 \times 10^{-10} \text{ M}$. Our experiments with T-47D cells, on the other hand, showed a binding that was lower in affinity as compared with all of the known VEGF receptors.

VEGF-165 Stimulates the Tyrosine Phosphorylation of a Number of Proteins in T-47D Breast Cancer Cells. We next asked whether VEGF might have an effect on the signaling of receptor tyrosine kinases to intracellular components in T-47D cells. Thus, we stimulated these cells with VEGF-165 and measured the changes in total tyrosine phos-

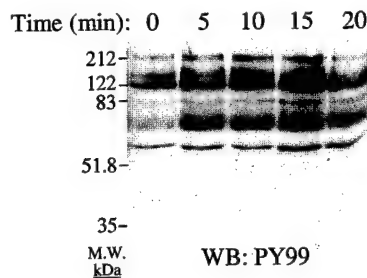


Fig. 4. Stimulation of T-47D cells with VEGF and western immunoblotting of total cell extracts with an anti-phosphotyrosine antibody.

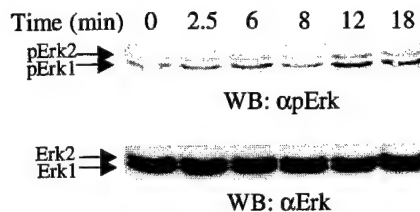


Fig. 5. Stimulation of T-47D cells with VEGF and Western immunoblotting of total cell extracts with anti-phospho-ERK antibody (upper panel). Lower panel indicates immunoblotting with an antibody to total ERK 1 protein.

phorylation. When serum-starved T-47D cells were treated with 100 ng/ml VEGF-165, we found increased tyrosine phosphorylation of a number of proteins as shown by anti-phosphotyrosine Western blotting of total cell extracts (Fig. 4). These included proteins of molecular weight M_r 60,000, 75,000, 122,000, and 200,000.

VEGF-165 Stimulates the MAP Kinases ERK 1,2 in T-47D Breast Cancer Cells. To analyze whether VEGF might modulate MAP kinase activity in the breast cancer cells, extracts from T-47D cells activated with VEGF were resolved on SDS-PAGE, and transfers were probed to detect activation of ERK 1,2 (Fig. 5). We observed a slight increase in the phosphorylation of ERK 1,2 that was attributable to VEGF at 15–20 min. Blotting for total ERK 1,2 showed that the differences seen were not attributable to differences in protein loading.

VEGF-165 Treatment Leads to Stimulation of PI 3-kinase and Related Pathways in T-47D Breast Cancer Cells. Inasmuch as PI 3-kinase has been shown to be induced by VEGF in endothelial cells (37), we next determined whether VEGF also might activate this pathway in breast cancer cells. PI 3-kinase activity was measured by an *in vitro* kinase assay of extracts from the VEGF-treated cells (Fig. 6A, left panel). There was a clear stimulation of phosphatidylinositol phosphorylation by VEGF at 5–20 min (see arrow). There was no phosphorylation seen in the normal serum control precipitate. As a control, we stimulated T-47D cells with heregulin and measured the PI 3-kinase activity (Fig. 6A, right panel). This showed the position of phosphatidylinositol 3-phosphate in the chromatogram.

Because Akt is known to be a down-stream target of PI 3-kinase (38), we then measured Akt activation in VEGF-

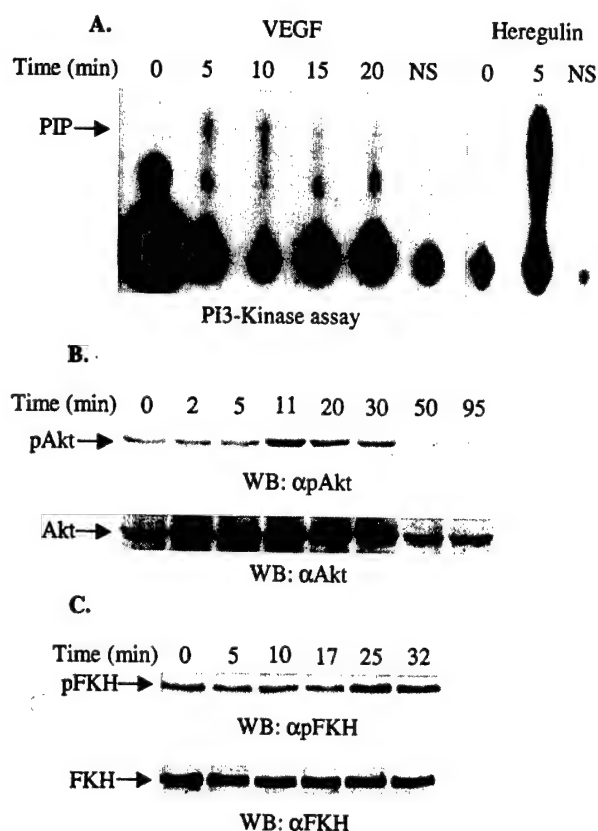


Fig. 6. (A) Stimulation of T-47D cells with VEGF and assay for PI 3-kinase (left panel). Right panel indicates the PI 3-kinase assay of T-47D cells stimulated with heregulin. NS indicates normal serum control precipitate. (B) Stimulation of T-47D cells with VEGF and immunoblotting of extracts with anti-phospho-Ser253 Akt. (C) Stimulation of T-47D cells with VEGF and immunoblotting of extracts with anti-phospho-FKH antibodies. Below each is shown the corresponding blotting of the non-phosphorylated protein.

treated T-47D cells by Western blotting using a phospho-Akt antibody (Fig. 6B). VEGF produced a small but detectable Akt phosphorylation signal that was first seen at 25 min, decreased at 50 min, and reached basal levels by 95 min.

We next tested for possible substrates of Akt, including GSK-3, p70 S6 kinase, and FKHRL1. Whereas stimulation of GSK-3 was seen after heregulin treatment, no stimulation of GSK-3 was detectable after VEGF treatment (data not shown). No change was seen in the phosphorylation of p70 S6K at Thr-421 or Ser-424 after either heregulin or VEGF treatment (data not shown). We then tested to see if there was a change in the phosphorylation of FKHRL1, a Forkhead family member known to be involved in the transcription of apoptosis-related proteins (39–41). We saw increases in the phosphorylation of FKHRL1 at Ser-253 in extracts from cells stimulated by VEGF (Fig. 6C). A similar increase in phosphorylation was also seen at Thr-32 of FKHRL1 (data not shown). These changes in FKHRL1 phosphorylation appeared to follow the changes in Akt phosphorylation, indicating that FKHRL1 was the substrate for Akt upon VEGF stimulation of breast cancer cells.

Taken together, the results indicate that VEGF induces the activation of ERK1,2 and PI 3-kinase signaling pathways in

breast cancer cells, leading to an increased invasiveness of the cells.

Discussion

In this study, we have presented results showing the VEGF-induced invasion and signaling in T-47D breast cancer cells. These studies demonstrate the importance of VEGF in stimulating effects on breast tumor cells in contrast to its effects on endothelial cells. Our studies with mRNA expression show that all breast tumor lines examined, except SK-BR-3, expressed moderate levels of Flt-1 and lower levels of Flk-1/KDR. Thus, we postulate that breast cancer cell lines are representative of human breast tumors in terms of their expressing VEGF receptors. Our studies with T-47D breast cancer cells support the conclusion that these cells are capable of responding to VEGF in terms of changes in intracellular signaling and cellular invasion. Data from our laboratory⁵ and from other investigators (26), have shown that T-47D cells secrete VEGF at the levels that are required for this stimulation. Thus, we postulate that, in many breast cancers, the elements are present for stimulation of an autocrine mechanism leading to increased cell invasion.

We tested to see if VEGF receptors other than Flt-1 and Flk-1/KDR might account for the signaling in the breast cancer cells. By Northern blotting, the VEGF receptor Neuropilin-1 was seen to be expressed in two of the breast cancer cell lines, MDA-MB-231 and MCF7 cells. MDA-MB-231 cells contain the highest level of Neuropilin-1, but VEGF fails to stimulate tyrosine phosphorylation or ERK 1,2 activation.⁶ Thus, it is unlikely that Neuropilin-1 is involved in the effects that we have seen in T-47D cells. Our Northern blotting of breast cancer cell lines showing the presence of Flt-1 and Flk-1/KDR are consistent with the finding of Speirs and Atkin (42), who found that these receptors were present in human breast cancer tumor epithelial cells. It was similarly shown by De Jong *et al.* (35) that in nearly 50% of the breast tumors, there was significant expression of Flt-1 and Flk-1/KDR in the tumor epithelial cells, correlating with the expression of VEGF by these cells. These investigators postulated that VEGF secreted by these epithelial cells could have both autocrine and paracrine roles. The paracrine mechanism for this action is likely to be through the stimulation of endothelial cells, leading to a development of the neovasculature (17–19, 22). However, the mechanism for the autocrine action of VEGF on the epithelial cells of the tumors has not been characterized. On the basis of the results presented here, we propose that VEGF acts in an autocrine manner by stimulating signaling, leading to cellular invasion in breast cancer epithelial cells. The cellular signaling in T-47D cells stimulated by VEGF leads to the stimulation of ERK1,2 and PI 3-kinase pathways. Stimulation of the PI 3-kinase pathway in particular is often related to cellular invasion. As mentioned above, MCF7 breast cancer cells are known to migrate in response to heregulin through a PI 3-kinase-mediated process (36). We have observed the invasion of T-47D cells in

⁵ D. J. Price, H. Kawai, and H. Avraham, unpublished results.

⁶ D. Price, unpublished data.

response to VEGF only when fibronectin is present on the transwell membrane. This is an indication that both the growth factor, VEGF, and the extracellular matrix component, fibronectin, are important in potentiating the invasion of the tumor cells. Fibronectin is known to contain binding domains that interact with cell surface heparan sulfate proteoglycans to promote focal adhesions and stress fiber formation (43). Heparan sulfate is known to potentiate the binding of VEGF to its receptors (31). It may be that fibronectin, in conjunction with heparan sulfate proteoglycans, also leads to an increased interaction of VEGF with its receptor. Thus, fibronectin, in cooperation with VEGF, appears to provide the signaling that is required for cellular invasion, whereas VEGF alone is unable to stimulate this process.

To date, we have no indication that other cellular functions might be stimulated in these cells, leading to increased tumorigenesis. There appeared to be little effect on cell survival or proliferation upon VEGF treatment of the T-47D cells (data not shown). Although phosphorylation of the Forkhead transcription factor is often connected with effects on the Fas ligand leading to cell survival (41), there may be other functions of this pathway. Another important question raised by these results is whether or not the endogenously secreted VEGF is sufficient to stimulate the effects that we have observed. As noted above, we and other investigators have shown that VEGF is secreted by the T-47D cells. An argument that could be made about the significance of the effect of VEGF on tumor cells is that because the tumor is secreting VEGF, there may be a higher local concentration of VEGF relative to other growth factors. Thus, *in vivo*, the effect of VEGF on the invasion of these cells may be much greater as compared with the effects of other growth factors that are present at subthreshold concentrations.

In summary, VEGF stimulated the increased invasion of T-47D cells through Matrigel/fibronectin-coated membranes. Northern analysis showed the expression of primarily the VEGF receptor, Flt-1, in a variety of breast cancer cell lines. However, binding of ^{125}I -labeled VEGF to T-47D cells indicated an affinity that was lower than that expected for the known VEGF receptors, suggesting the possibility of an as-yet unidentified VEGF receptor in these cells. VEGF stimulated signaling in T-47D breast cancer cells through the PI 3-kinase/Akt pathway and also through the ERK 1,2 pathway. This observation may indicate an effect of VEGF on tumorigenicity independent of its effects on the vasculature. Future studies will be aimed at characterizing the *in vivo* significance of VEGF signaling in the tumor cells as compared with its signaling in endothelial cells.

Materials and Methods

Materials. Antibodies used in immunological analysis were as follows: anti-phosphotyrosine antibody (PY99), phospho-ERK (E-4) antibody, anti-ERK 1 (K-23), anti-Flk-1 (N-931), and horseradish peroxidase-labeled secondary antibodies were from Santa Cruz Biotechnology (Santa Cruz, CA). Anti-Akt, and anti-phospho-Ser-473 Akt antibodies were from New England Biolabs (Beverly, MA). Anti-Flt-1, anti-phospho-Ser-253 FKH, and anti-phospho-Thr-32 FKH antibodies were from Upstate Biotechnology, Inc. (Lake Placid, NY).

LY294002 was from Sigma Chemical Co. (St. Louis, MO). VEGF-165 and heregulin were a generous gift of Genentech (San Francisco, CA). $\gamma^{32}\text{P}$ -ATP and $\alpha^{32}\text{P}$ -CTP were from New England Nuclear (Boston, MA). All other chemicals were from Fisher Scientific (Norcross, GA), unless otherwise noted.

Cell Culture. T-47D cells were an estrogen receptor-positive clone provided by Iafa Keydar, Tel Aviv University (Ramat Aviv, Israel). These cells were cultured in RPMI 1640 (Life Technologies, Inc., Bethesda, MD) supplemented with 7 $\mu\text{g}/\text{ml}$ insulin, 10% fetal bovine serum (Life Technologies, Inc.), and penicillin/streptomycin. MCF7 cells (American Type Culture Collection, Rockville, MD) were grown in MEM (Life Technologies, Inc.) supplemented with 1 mM sodium pyruvate, 0.1 mM nonessential amino acids, 10 $\mu\text{g}/\text{ml}$ insulin, 10% fetal bovine serum, and penicillin/streptomycin. MDA-MB-231 and MDA-MB-453 (American Type Culture Collection) were grown in DMEM supplemented with 10% fetal bovine serum, 0.2 mM glutamine, and penicillin/streptomycin. HUVECs were from Clonetics (San Diego, CA) and were cultured in EGM complete medium (Clonetics). HBL-100 (American Type Culture Collection) were cultured in McCoy's 5a medium supplemented with 10% fetal bovine serum and penicillin/streptomycin.

Iodination of VEGF-165. ^{125}I -labeled VEGF-165 was prepared using IODO-GEN, as described previously (31). The protein was separated from free iodine by heparin Sepharose affinity adsorption (Amersham-Pharmacia Biotech, Piscataway, NJ) and elution with 0.8 M NaCl. Specific activity of the ^{125}I -labeled VEGF-165 was $\sim 100,000$ cpm/ng protein.

Binding of VEGF-165 to Cells. For quantification of the binding of ^{125}I -labeled VEGF-165 to cells, the cells were detached briefly with trypsin/EDTA, washed in full medium, then suspended in binding buffer [20 mM MOPS (pH 7.4)/2 mM MgCl_2 /140 mM NaCl, and 0.2% gelatin/2 mg/ml glucose]. Cells were then incubated with a range of concentrations of VEGF-165 containing a fixed amount of ^{125}I -labeled VEGF-165 in binding buffer at a final concentration of 1×10^5 cells/ml on ice. Aliquots of 0.15 ml were pipetted onto a 0.9 cushion of fetal bovine serum. After centrifugation in a microcentrifuge (5 min; 7.5×1000 rpm), tubes were frozen on dry ice. The cell pellet was isolated by clipping the tip of the tube with a canine toenail clipper. Bound (pellet) and free (supernatant) counts were quantified in a Beckman gamma counter. K_d values and the number of binding sites/cell were calculated from Scatchard plots (44) by doing a least square fit of the data using the Microsoft Excel program.

Immunoprecipitations and Western Analysis. After growth factor stimulation, cells were lysed in 20 mM Tris-HCl (pH 7.4)/150 mM NaCl/1% NP-40/0.25% deoxycholate/1 mM Na_3VO_4 /1 mM EGTA and a cocktail of protease inhibitors (Complete, EDTA-free; Roche, Indianapolis, IN). Protein was normalized by Bio-Rad protein assay (Bio-Rad, Hercules, CA), and lysates were precipitated overnight with the addition of 1 μg of the specified antibody. The next day, protein G-Sepharose (Pierce, Rockford, IL) was added and the precipitates were washed 3 times with lysis buffer. Precipitates were treated with SDS-sample buffer and run on polyacrylamide gels, followed by transfer to nitrocellulose membranes

(Bio-Rad). Membranes were immunoblotted with primary antibodies as indicated in the figure legends, and with the appropriate horseradish peroxidase-linked secondary antibodies, before chemiluminescent development and exposure to X-ray film.

PI 3-kinase Assay. Assay of PI 3-kinase was carried out after growth factor stimulation of cells and precipitation of lysates by PY99 antibody/Protein G-Sepharose. Precipitates were subjected to an *in vitro* kinase reaction using $\gamma^{32}\text{P}$ -ATP and phosphatidylinositol (Sigma Chemical Co.) as substrates, according to Derman *et al.* (45). ^{32}P -labeled samples were applied to oxalate-coated cellulose/acetate plates and subjected to chromatographic separation (solvent, CHCl_3 :methanol: H_2O : NH_4OH [60:47:11.3:2]).

Northern Analysis. mRNAs were isolated from cellular extracts by oligo(dT) chromatography using a kit (Invitrogen, Carlsbad, CA) according to the manufacturer's directions. mRNAs were separated on an agarose gel and transferred to a Hybond N membrane (Amersham Pharmacia Biotech). The membrane was hybridized with probes to Flt-1, Flk-1/KDR, and Neuropilin-1 (a generous gift of Dr. Michael Klagsbrun, Children's Hospital, Boston, MA). Blots were prehybridized for 4 h at 42° in 50% formamide/5 \times SSC-10 \times Denhardt's/0.3% SDS/100 $\mu\text{g}/\text{ml}$ ssDNA/10 $\mu\text{g}/\text{ml}$ yeast tRNA. Specific ^{32}P -labeled probe DNA was added, and the incubation was continued for 4 h at 42° . The blots were washed twice in 2 \times SSC-1% SDS at room temperature, and then in 0.2 \times SSC-0.1% SDS at 42° followed by 0.2 \times SSC-0.1% SDS at 60° . After washing, the blots were then exposed to X-ray film. Blots were also stripped and reprobed for actin mRNA as a control.

Invasion Assay. Transwell membranes (8- μm pore size, 6.5-mm diameter; Corning Costar Corporation, Cambridge, MA) were coated with Matrigel (2.5 mg/ml) or Matrigel plus fibronectin (2.5 mg/ml), and dry coatings were reconstituted in DMEM for 1–2 h before cell passage. Cells were trypsinized, centrifuged, and resuspended at $\sim 10^7/\text{ml}$ in DMEM containing 0.2% BSA. Cells were seeded onto the upper wells of precoated transwells in the same medium alone [control or in medium supplemented with HRG (20 nM)] or VEGF-165 (100 ng/ml). Lower wells of the transwells contained 600 μl of DMEM and 0.2% BSA. After 24 h, membranes were swabbed with a Q-tip, fixed with methanol, and stained with crystal violet before counting under phase-contrast microscopy.

Acknowledgments

We thank Dr. Shalom Avraham for advice on this project. We also thank Dan Kelley for preparation of figures and Janet Delahanty for assistance with editing.

References

- Grunstein, J., Roberts, W. G., Mathieu-Costello, O., Hanahan, D., and Johnson, R. S. Tumor-derived expression of vascular endothelial growth factor is a critical factor in tumor expansion and vascular function. *Cancer Res.*, 59: 1592–1598, 1999.
- Risau, W. What, if anything, is an angiogenic factor? *Cancer Metastasis Rev.* 15: 149–151, 1996.
- Hanahan, D., and Folkman, J. Patterns and emerging mechanisms of the angiogenic switch during tumorigenesis. *Cell*, 86: 353–364, 1996.
- Klagsbrun, M., and D'Amore, P. A. Vascular endothelial growth factor and its receptors. *Cytokine Growth Factor Rev.*, 7: 259–270, 1996.
- Neufeld, G., Cohen, T., Gengrinovitch, S., and Poltorak, Z. Vascular endothelial growth factor (VEGF) and its receptors. *FASEB J.*, 13: 9–22, 1999.
- Obermair, A., Kucera, E., Mayerhofer, K., Speiser, P., Seifert, M., Czerwenka, K., Kaider, A., Leodolter, S., Kainz, C., and Zeillinger, R. Vascular endothelial growth factor (VEGF) in human breast cancer: correlation with disease-free survival. *Int. J. Cancer*, 74: 455–458, 1997.
- Gasparini, G., Toi, M., Gion, M., Verderio, P., Dittadi, R., Hanatani, M., Matsubara, I., Vinante, O., Bonoldi, E., Boracchi, P., Gatti, C., Suzuki, H., and Tominaga, T. Prognostic significance of vascular endothelial growth factor protein in node-negative breast carcinoma. *J. Natl. Cancer Inst.*, 89: 139–147, 1997.
- Linderholm, B., Tavelin, B., Grankvist, K., and Henriksson, R. Vascular endothelial growth factor is of high prognostic value in node-negative breast carcinoma. *J. Clin. Oncol.*, 16: 3121–3128, 1998.
- Heffelfinger, S. C., Miller, M. A., Yassin, R., and Gear, R. Angiogenic growth factors in preinvasive breast disease. *Clin. Cancer Res.*, 5: 2867–2876, 1999.
- Salven, P., Perhoniemi, V., Tykka, H., Maenpaa, H., and Joensuu, H. Serum VEGF levels in women with a benign breast tumor or breast cancer. *Breast Cancer Res. Treat.*, 53: 161–166, 1999.
- Leung, D. W., Cachianes, G., Kuang, W. J., Goeddel, D. V., and Ferrara, N. Vascular endothelial growth factor is a secreted angiogenic mitogen. *Science (Washington DC)*, 246: 1306–1309, 1989.
- Houck, K. A., Ferrara, N., Winer, J., Cachianes, G., Li, B., and Leung, D. W. The vascular endothelial growth factor family: identification of a fourth molecular species and characterization of alternative splicing of RNA. *Mol. Endocrinol.*, 5: 1806–1814, 1991.
- Tischer, E., Gospodarowicz, D., Mitchell, R., Silva, M., Schilling, J., Lau, K., Crisp, T., Fiddes, J. C., and Abraham, J. A. Vascular endothelial growth factor: a new member of the platelet-derived growth factor gene family. *Biochem. Biophys. Res. Commun.*, 165: 1198–1206, 1989.
- Poltorak, Z., Cohen, T., Sivan, R., Kandelis, Y., Spira, G., Vlodavsky, I., Keshet, E., and Neufeld, G. VEGF145, a secreted vascular endothelial growth factor isoform that binds to extracellular matrix. *J. Biol. Chem.*, 272: 7151–7158, 1997.
- Keyt, B. A., Berleau, L. T., Nguyen, H. V., Chen, H., Heinsohn, H., Vandlen, R., and Ferrara, N. The carboxyl-terminal domain (111–165) of vascular endothelial growth factor is critical for its mitogenic potency. *J. Biol. Chem.*, 271: 7788–7795, 1996.
- Soker, S., Gollamudi-Payne, S., Fidler, H., Charnahelli, H., and Klagsbrun, M. Inhibition of vascular endothelial growth factor (VEGF)-induced endothelial cell proliferation by a peptide corresponding to the exon 7- encoded domain of VEGF165. *J. Biol. Chem.*, 272: 31582–31588, 1997.
- Shibuya, M., Yamaguchi, S., Yamane, A., Ikeda, T., Tojo, A., Matsushime, H., and Sato, M. Nucleotide sequence and expression of a novel human receptor-type tyrosine kinase gene (*flt*) closely related to the *fms* family. *Oncogene*, 5: 519–524, 1990.
- de Vries, C., Escobedo, J. A., Ueno, H., Houck, K., Ferrara, N., and Williams, L. T. The *fms*-like tyrosine kinase, a receptor for vascular endothelial growth factor. *Science (Washington DC)*, 255: 989–991, 1992.
- Terman, B. I., Dougher-Vermazen, M., Carrion, M. E., Dimitrov, D., Armellino, D. C., Gospodarowicz, D., and Bohnen, P. Identification of the KDR tyrosine kinase as a receptor for vascular endothelial cell growth factor. *Biochem. Biophys. Res. Commun.*, 187: 1579–1586, 1992.
- Waltenberger, J., Claesson-Welsh, L., Siegbahn, A., Shibuya, M., and Heldin, C. H. Different signal transduction properties of KDR and Flt1, two receptors for vascular endothelial growth factor. *J. Biol. Chem.*, 269: 26988–26995, 1994.
- Soker, S., Fidler, H., Neufeld, G., and Klagsbrun, M. Characterization of novel vascular endothelial growth factor (VEGF) receptors on tumor cells that bind VEGF165 via its exon 7-encoded domain. *J. Biol. Chem.*, 271: 5761–5767, 1996.
- Soker, S., Takashima, S., Miao, H. Q., Neufeld, G., and Klagsbrun, M. Neuropilin-1 is expressed by endothelial and tumor cells as an isoform-

- specific receptor for vascular endothelial growth factor. *Cell*, 92: 735–745, 1998.
23. Yoshida, A., Anand-Apte, B., and Zetter, B. R. Differential endothelial migration and proliferation to basic fibroblast growth factor and vascular endothelial growth factor. *Growth Factors*, 13: 57–64, 1996.
 24. Yoshiji, H., Gomez, D. E., Shibuya, M., and Thorgeirsson, U. P. Expression of vascular endothelial growth factor, its receptor, and other angiogenic factors in human breast cancer. *Cancer Res.*, 56: 2013–2016, 1996.
 25. Kranz, A., Mattfeldt, T., and Waltenberger, J. Molecular mediators of tumor angiogenesis: enhanced expression and activation of vascular endothelial growth factor receptor KDR in primary breast cancer. *Int. J. Cancer*, 84: 293–298, 1999.
 26. Yoshiji, H., Harris, S. R., and Thorgeirsson, U. P. Vascular endothelial growth factor is essential for initial but not continued *in vivo* growth of human breast carcinoma cells. *Cancer Res.*, 57: 3924–3928, 1997.
 27. O'Reilly, M. S., Holmgren, L., Shing, Y., Chen, C., Rosenthal, R. A., Moses, M., Lane, W. S., Cao, Y., Sage, E. H., and Folkman, J. Angiostatin: a novel angiogenesis inhibitor that mediates the suppression of metastases by a Lewis lung carcinoma. *Cell*, 79: 315–328, 1994.
 28. Boehm, T., Folkman, J., Browder, T., and O'Reilly, M. S. Antiangiogenic therapy of experimental cancer does not induce acquired drug resistance. *Nature (Lond.)*, 390: 404–407, 1997.
 29. O'Reilly, M. S., Boehm, T., Shing, Y., Fukai, N., Vasios, G., Lane, W. S., Flynn, E., Birkhead, J. R., Olsen, B. R., and Folkman, J. Endostatin: an endogenous inhibitor of angiogenesis and tumor growth. *Cell*, 88: 277–285, 1997.
 30. Bergers, G., Javaherian, K., Lo, K. M., Folkman, J., and Hanahan, D. Effects of angiogenesis inhibitors on multistage carcinogenesis in mice. *Science (Washington DC)*, 284: 808–812, 1999.
 31. Cohen, T., Gitay-Goren, H., Sharon, R., Shibuya, M., Halaban, R., Levi, B. Z., and Neufeld, G. VEGF121, a vascular endothelial growth factor (VEGF) isoform lacking heparin binding ability, requires cell-surface heparin sulfates for efficient binding to the VEGF receptors of human melanoma cells. *J. Biol. Chem.*, 270: 11322–11326, 1995.
 32. Liu, B., Earl, H. M., Baban, D., Shoaibi, M., Fabra, A., Kerr, D. J., and Seymour, L. W. Melanoma cell lines express VEGF receptor KDR and respond to exogenously added VEGF. *Biochem. Biophys. Res. Commun.*, 217: 721–727, 1995.
 33. Defoy, I., Guy, I., Aprikian, A. G., and Chevalier, S. Vascular endothelial growth factor (VEGF) in human prostate cancer: more than angiogenesis. *Proc. Am. Assoc. Cancer Res.*, 40: 608, 1999.
 34. Hashimoto, M., Ohsawa, M., Ohnishi, A., Naka, N., Hirota, S., Kitamura, Y., and Aozasa, K. Expression of vascular endothelial growth factor and its receptor mRNA in angiosarcoma. *Lab. Invest.*, 73: 859–863, 1995.
 35. De Jong, J. S., van Diest, P. J., van der Valk, P., and Baak, J. P. Expression of growth factors, growth inhibiting factors, and their receptors in invasive breast cancer. I: An inventory in search of autocrine and paracrine loops. *J. Pathol.*, 184: 44–52, 1998.
 36. Adam, L., Vadlamudi, R., Kondapaka, S. B., Chernoff, J., Mendelsohn, J., and Kumar, R. Heregulin regulates cytoskeletal reorganization and cell migration through the p21-activated kinase-1 via phosphatidylinositol-3 kinase. *J. Biol. Chem.*, 273: 28238–28246, 1998.
 37. Thakker, G. D., Hajjar, D. P., Muller, W. A., and Rosengart, T. K. The role of phosphatidylinositol 3-kinase in vascular endothelial growth factor signaling. *J. Biol. Chem.*, 274: 10002–10007, 1999.
 38. Datta, S. R., Brunet, A., and Greenberg, M. E. Cellular survival: a play in three Akts. *Genes Dev.*, 13: 2905–2927, 1999.
 39. Hillion, J., Le Coniat, M., Jonveaux, P., Berger, R., and Bernard, O. A. AF6q21, a novel partner of the *MLL* gene in t(6;11)(q21;q23), defines a forkhead transcriptional factor subfamily. *Blood*, 90: 3714–3719, 1997.
 40. Anderson, M. J., Viars, C. S., Czekay, S., Cavenee, W. K., and Arden, K. C. Cloning and characterization of three human forkhead genes that comprise an FKHR-like gene subfamily. *Genomics*, 47: 187–199, 1998.
 41. Brunet, A., Bonni, A., Zigmond, M. J., Lin, M. Z., Juo, P., Hu, L. S., Anderson, M. J., Arden, K. C., Blenis, J., and Greenberg, M. E. Akt promotes cell survival by phosphorylating and inhibiting a Forkhead transcription factor. *Cell*, 96: 857–868, 1999.
 42. Speirs, V., and Atkin, S. L. Production of VEGF and expression of the VEGF receptors Flt-1 and KDR in primary cultures of epithelial and stromal cells derived from breast tumours. *Br. J. Cancer*, 80: 898–903, 1999.
 43. Woods, A., McCarthy, J. B., Furcht, L. T., and Couchman, J. R. A synthetic peptide from the COOH-terminal heparin-binding domain of fibronectin promotes focal adhesion formation. *Mol. Biol. Cell*, 4: 605–613, 1993.
 44. Dahlquist, F. W. The meaning of Scatchard and Hill plots. In: C. W. H. Hirs and S. N. Timasheff (eds.), *Methods in Enzymology*, Vol. 48, pp. 270–299. New York: Academic Press, 1978.
 45. Derman, M. P., Chen, J. Y., Spokes, K. C., Songyang, Z., and Cantley, L. G. An 11-amino acid sequence from c-met initiates epithelial chemotaxis via phosphatidylinositol 3-kinase and phospholipase C. *J. Biol. Chem.*, 271: 4251–4255, 1996.



VEGF₁₆₅ requires extracellular matrix components to induce mitogenic effects and migratory response in breast cancer cells

Tiho Miralem¹, Robert Steinberg¹, Dan Price¹ and Hava Avraham^{*,1}

¹Division of Experimental Medicine, Beth Israel-Deaconess Medical Center, Harvard Institutes of Medicine, 4 Blackfan Circle, Boston, Massachusetts, MA 02115, USA

The expression of VEGF and the relapse-free survival rate of breast cancer patients are inversely related. While VEGF induces the proliferation and migration of vascular endothelial cells, its function in breast cancer cells is not well studied. We reported previously that fibronectin increased VEGF-dependent migration in breast cancer cells. Since VEGF has an extracellular matrix (ECM)-binding domain and possesses binding affinity for heparin, we sought to determine the effects of VEGF in breast cancer cells and the role of heparin and/or fibronectin in VEGF-induced signaling. Cells grown on plastic were compared to those grown on fibronectin or to those grown on plastic in the presence of heparin, and analysed for intracellular signaling, proliferation and migration in response to VEGF₁₆₅. Both heparin and fibronectin enhanced the binding of VEGF to T47D cells. After treatment with VEGF, [³H]thymidine incorporation, *c-fos* induction, and the number of migrating cells were significantly higher (~twofold) in cells grown on fibronectin or in cells grown on plastic in the presence of heparin when compared to those grown on plastic only. Likewise, tyrosine phosphorylation of VEGF receptors, MAPK activity and PI3-kinase activity were all several-fold higher in cells seeded on fibronectin or in the presence of heparin as compared to cells exposed to VEGF alone. VEGF-dependent *c-fos* induction was found to be regulated through a MAPK-dependent, but PI3-kinase-independent pathway. In contrast, the migration of T47D cells in response to VEGF, in the presence of ECM, was regulated through PI3-kinase. Therefore, VEGF requires ECM components to induce a mitogenic response and cell migration in T47D breast cancer cells. *Oncogene* (2001) 20, 5511–5524.

Keywords: VEGF; breast cancer; cell signaling; mitogenic response; cell migration

Introduction

Vascular endothelial growth factor (VEGF) is angiogenic *in vitro* (Pepper *et al.*, 1992) and *in vivo* (Plouet *et al.*, 1989) by inducing the proliferation (Yu and Sato, 1999) and migration (Radisavljevic *et al.*, 2000) of vascular endothelial cells. VEGF is produced in numerous cell types such as tumor cells, smooth muscle cells, mesangial cells, macrophages, and osteoblasts (Klagsbrun and D'Amore, 1996). It is a homodimer (Gospodarowicz *et al.*, 1989) that occurs in five isoforms, specifically: VEGF₁₂₁, VEGF₁₄₅, VEGF₁₆₅, VEGF₁₈₉ and VEGF₂₀₆, as a result of alternative splicing from a single gene (Houck *et al.*, 1991). Of these, VEGF₁₂₁ and VEGF₁₆₅ are the most abundant and potent isoforms (Bacic *et al.*, 1995). While VEGF₁₂₁ lacks an ECM-binding domain and is secreted only in medium, VEGF₁₆₅ is found to be both cell-associated and secreted in medium (Park *et al.*, 1993).

Flt-1, Flk-1/KDR and Flt-4 belong to the family of VEGF receptors (Shibuya *et al.*, 1999). All three receptors have an extracellular domain containing seven immunoglobulin-like loops and an intracellular domain characterized by split tyrosine kinase motifs (Shibuya *et al.*, 1999). Upon activation, the phosphorylated tyrosines act as docking sites for adaptor-signaling molecules and non-receptor kinases (Dougher-Vermazen *et al.*, 1994), thereby generating signaling cascades such as MAPK (Malarkey *et al.*, 1995) and PI3K/Akt (Guo *et al.*, 1995).

VEGF and the fibroblast growth factor (FGF) group of growth factors are characterized by their binding affinity for heparin (Folkman and Klagsbrun, 1987; Tischer *et al.*, 1989). Such binding affinity was shown to have a biological effect, enabling a productive interaction between the growth factor and its cell-surface receptors (Taga *et al.*, 1989; Yayon *et al.*, 1991). Heparinase treatment of endothelial cells inhibited endothelial cell proliferation and *in vivo* neovascularization (Sasisekharan *et al.*, 1994), emphasizing the role of heparin-like molecules in angiogenesis. In some cell types, the presence of heparin-like molecules is essential for the binding of b-FGF to its receptors (Rapraeger *et al.*, 1991; Yayon *et al.*, 1991), thereby protecting b-FGF from heat and acidic inactivation (Gospodarowicz and Cheng, 1986). The

*Correspondence: H Avraham;

E-mail: havraham@caregroup.harvard.edu

Received 19 March 2001; revised 19 June 2001; accepted 26 June 2001

interaction of VEGF with heparin is more modest as compared to that of b-FGF (Taga *et al.*, 1989; Yayon *et al.*, 1991), and is comparable to the modest affinity shown by PDGF, a member of the same group of growth factors (Hicks *et al.*, 1989). Although having a relatively weak interaction with VEGF, heparin and heparan sulfate proteoglycans (HSPGs) are able to enhance the interaction of VEGF with its receptors (Gengrinovitch *et al.*, 1999). The binding of VEGF to its cell-surface receptors was restored by the addition of heparin after the concentration of heparin-like molecules on the cell surface was reduced by heparinase treatment (Gengrinovitch *et al.*, 1999; Gitay-Goren *et al.*, 1992). However, the binding of VEGF₁₂₁, a truncated variant that lacks a heparin-binding domain, could not be restored by the addition of heparin-like molecules (Cohen *et al.*, 1995).

Breast cancer cells express both VEGF (Blancher *et al.*, 2000; Price *et al.*, 2001) and VEGF receptors (Price *et al.*, 2001; Soker *et al.*, 1996). Heparin/HSPGs were shown to enhance and stabilize the binding of VEGF to its receptors in endothelial and breast cancer cells (Gitay-Goren *et al.*, 1992; Soker *et al.*, 1996). However, none of the previous studies have shown whether the enhanced binding of VEGF to its receptors is associated with functional responses in breast cancer cells. Only cells passaged on a membrane coat containing fibronectin responded to VEGF by increased migration (Price *et al.*, 2001). Fibronectin (Ruoslahti, 1991) and heparin (Halper, 1990) bind to the cell surface through receptors and high affinity sites, respectively. VEGF (Cardin and Weintraub, 1989), VEGF-receptors (Dougher *et al.*, 1997), and fibronectin (Ruoslahti *et al.*, 1981) possess a highly basic region that confers strong affinity for heparin. Furthermore, heparin and HSPGs enhance the binding of VEGF to its receptors (Gitay-Goren *et al.*, 1992) and are necessary for the biological actions of b-FGF (Rapraeger *et al.*, 1991; Yayon *et al.*, 1991). Therefore, we hypothesize that T47D cell responsiveness to VEGF might require the involvement of extracellular matrix components. This study was undertaken to examine the effects of ECM components, fibronectin and heparin, on the biological responsiveness of T47D breast cancer cells to VEGF₁₆₅.

Results

Effect of fibronectin and heparin on T47D cell migration

We reported recently the increased migration of breast cancer cells upon their stimulation with VEGF₁₆₅, in the presence of fibronectin (Price *et al.*, 2001). This observation was further confirmed in the present study, where VEGF increased T47D cell migration from 35 ± 14 cells on Matrigel to 88 ± 2 cells in the presence of fibronectin (Figure 1a). Because VEGF₁₆₅ is characterized by an extracellular matrix-binding domain and by its binding affinity for heparin, we wanted

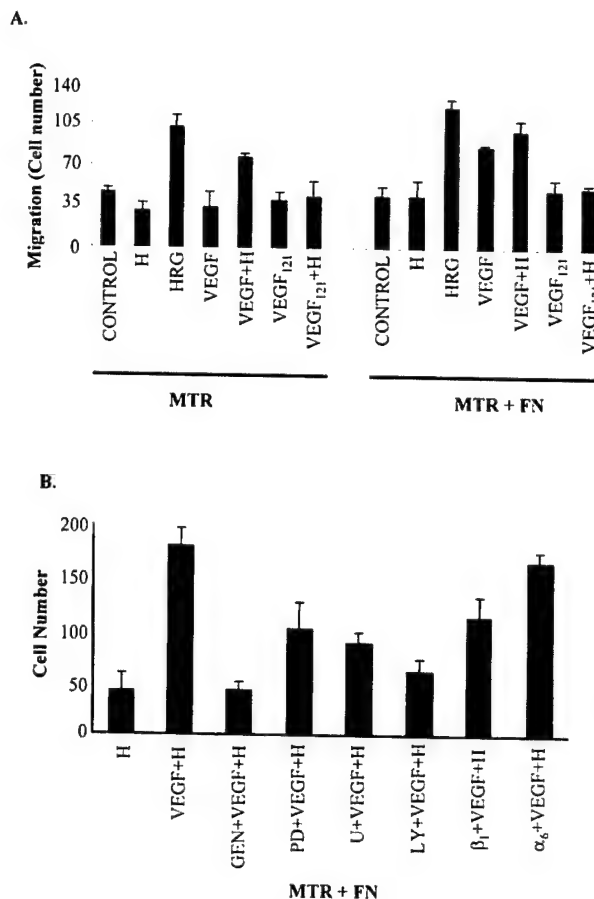


Figure 1 Heparin and fibronectin affect the VEGF-induced migration of T47D cells. Cells were suspended in DMEM containing 0.2% BSA and seeded onto transwell membranes precoated either with matrigel (MTR) or with a mix of matrigel and fibronectin (MTR + FN), as indicated in Materials and methods. (a) In the moment of passage, the cell suspension contained only BSA (control), heparin (H), HRG, VEGF₁₆₅ (VEGF), VEGF + H, VEGF₁₂₁ or VEGF₁₂₁ + H. The number of migrating cells was counted under a phase-contrast microscope after swabbing the membrane coat and staining the remaining cells with crystal violet. (b) Cells were pretreated for 30 min with kinase inhibitors such as genistein (GEN), PD98059 (PD), U0126 (U), or LY294002 (LY) prior to cell detachment or plus blocking anti- β_1 integrin or anti- α_6 integrin antibodies, in the presence of heparin (H) and VEGF. The effect of the inhibitors on the cells was compared to that of cells treated only with heparin (H) or with VEGF in the presence of heparin (VEGF + H). Values represent the means \pm s.d. of triplicate wells from three independent experiments

to extend this study and test whether this polyanion would also affect the VEGF₁₆₅-induced migration of breast cancer cells.

Migration of T47D cells was tested in 24-well plates containing transwell membranes coated with matrigel or matrigel + fibronectin. Approximately 30 to 40 cells migrated onto transwell membranes in the control wells or in wells treated with heparin alone (Figure 1a,b). When cells were treated with heregulin, a known stimulator of breast cancer cell migration, 104 ± 11 cells migrated onto the transwell membrane. Upon stimulation with VEGF, cells seeded on matrigel alone

migrated in approximately the same numbers as cells in control wells (Figure 1a). The migration rate of VEGF-stimulated cells was significantly increased to 78 ± 4 by the addition of heparin in the moment of cell passage (Figure 1a). Addition of fibronectin to the matrigel coat further increased the number of migrating cells after treatment with heregulin, VEGF or VEGF plus heparin to 122 ± 8 , 88 ± 2 and 101 ± 10 , respectively (Figure 1a). As we showed previously, the addition of fibronectin did not affect the migration of nontreated cells or cells treated with heparin alone. The number of migrating cells was not increased either upon treatment with VEGF₁₂₁ alone or VEGF₁₂₁ in the presence of heparin (1 μ g/ml) on both protein coatings (Figure 1a), suggesting the requirement for an ECM-binding domain of this growth factor. To elucidate the mechanism and signaling pathway that regulates this migration in T47D cells, cells were pretreated with genistein, PD98059, U0126, or LY294002 prior to detachment, or with blocking anti- β_1 or blocking anti- α_6 integrin antibodies prior to treatment with VEGF in the presence of heparin (Figure 1b). In the presence of heparin and VEGF, 178 ± 18 cells migrated to the membrane. This migration was decreased by approximately 50% after pretreatment with PD98059, U0126, or with blocking anti- β_1 integrin antibody, while blocking anti- α_6 integrin did not have a significant effect (Figure 1b), indicating a partial involvement of β_1 integrin in this process. When cells were pretreated with genistein or LY294002, the VEGF-induced migratory response was totally abolished (being 49 ± 11 and 67 ± 9 , respectively, Figure 1b), suggesting its dependence on both tyrosine kinase and PI3K.

Heparin and fibronectin affect VEGF binding to T47D breast cancer cells

Heparin has been shown to enhance the binding and to stabilize the complex between VEGF and its receptors in endothelial cells and MDA-MB-231 breast cancer cells (Gitay-Goren *et al.*, 1992; Soker *et al.*, 1996). To test whether heparin and/or fibronectin would affect VEGF binding to T47D cells, we radiolabeled VEGF with [¹²⁵I]. The [¹²⁵I]-VEGF was then added to the T47D cells and processed for [¹²⁵I] recovery either after cross-linking (Figure 2a) or binding (Figure 2b) to these cells. In the presence of heparin (1 μ g/ml), enhanced binding and cross-linking of [¹²⁵I]-VEGF to T47D cells was observed as compared to cells treated with [¹²⁵I]-VEGF alone (824 ± 69 c.p.m. VEGF vs 1306 ± 92 c.p.m. VEGF + heparin (H), $P < 0.01$, Figure 2a and 2b). When cells were seeded on fibronectin, an increase in [¹²⁵I]-VEGF binding was observed (1473 ± 102 c.p.m., VEGF on FN vs 824 ± 69 c.p.m., VEGF on PL). The highest recovery of [¹²⁵I] was found when heparin was present together with fibronectin, suggesting a stronger effect of heparin in this process (1794 ± 98 c.p.m.). The binding of [¹²⁵I]-VEGF to T47D cells was specific because the addition of a 20-fold excess of nonlabeled VEGF almost completely inhibited formation of the labeled complex on both surfaces (302 ± 37 c.p.m.,

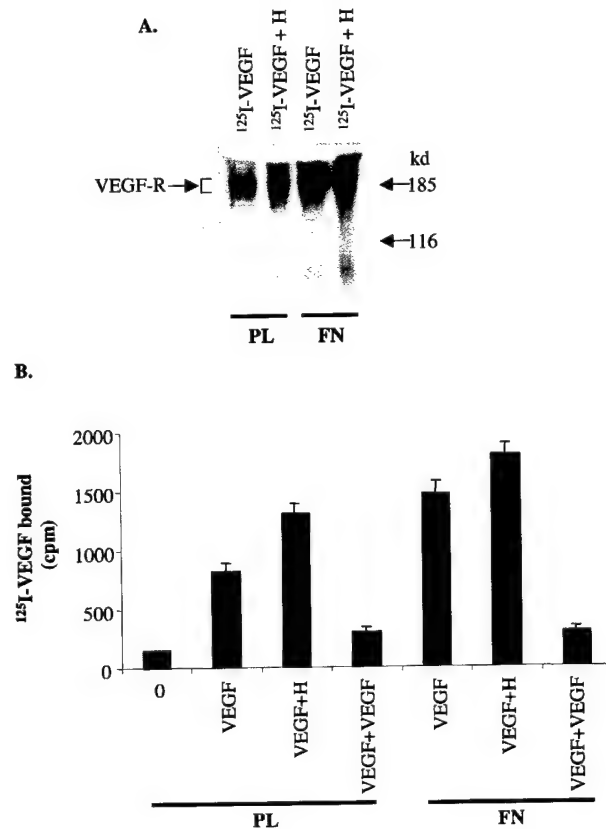


Figure 2 Heparin and fibronectin enhance binding of VEGF to T47D cells. T47D cells were grown to confluency either in 6-cm plates (a) or in 24-well plates (b), washed with PBS and treated with [¹²⁵I]-VEGF for 4 h in an ice-cold environment. (a) Cells seeded on plastic (lanes 1 and 2) or on fibronectin (lanes 3 and 4) were treated with [¹²⁵I]-VEGF alone (lanes 1 and 3) or with [¹²⁵I]-VEGF in the presence of heparin (H, lanes 2 and 4, 1 μ g/ml). After cross-linking the bound [¹²⁵I]-VEGF, cells were scraped as described in Materials and methods and subjected to SDS-PAGE followed by autoradiography. Molecular weight markers are indicated to the right. (b) Cells seeded on plastic (PL) or fibronectin (FN) were treated with [¹²⁵I]-VEGF alone, with [¹²⁵I]-VEGF in the presence of heparin (VEGF + H), or in the presence of 20-times excess of unlabeled VEGF (VEGF + VEGF). Cells were then washed with ice-cold PBS and processed for recovery of bound [¹²⁵I] radioactivity as described in Materials and methods. '0' indicates background radioactivity recovered from non-treated cells. Autoradiograph and values represent the mean \pm s.d. of two independent experiments

VEGF + VEGF on PL; 296 ± 45 c.p.m., VEGF + VEGF on FN, Figure 2b).

Effect of ECM on the VEGF-dependent mitogenic response in T47D cells

Since fibronectin and/or heparin increased T47D cell migration in response to VEGF and enhanced the binding of VEGF to T47D cells, we analysed the effect of ECM components on cell proliferation. To study the effect of substratum on mitogenic response, the incorporation of [³H]thymidine into DNA was measured during a 1 h labeling period following the release of cells from quiescence. Serum-starved T47D cells

become synchronized and begin to proliferate uniformly when fed with FBS or growth factors (Kodali *et al.*, 1994). Heregulin is a potent mitogen for breast cancer cells (Lupu *et al.*, 1995; Normanno *et al.*, 1994), and it was used in addition to FBS and EGF throughout this study for comparison analysis to VEGF. Untreated T47D cells showed very low [3 H]thymidine incorporation (3204 ± 480 c.p.m.), representing the basal level of DNA synthesis that is marked as 100% (Figure 3a). After treatment with heregulin (20 nM), cells grown on plastic slowly increased their incorporation of [3 H]thymidine, which peaked between 16 and 20 h ($18 \text{ h} = 243 \pm 19\%$) indicative of the progression through S phase. Cells grown on fibronectin did not significantly affect heregulin-induced DNA synthesis. When cells grown on plastic were treated with VEGF, no change in DNA synthesis was observed as compared to that of untreated cells during the course of 24 h ($100 \pm 12\%$; $t=0$ vs $117 \pm 22\%$; $t=18 \text{ h}$, N.S.). However, cells seeded on fibronectin responded to VEGF by a 2.5-fold increase of

[3 H]thymidine uptake, over quiescent cells, at the peak of DNA synthesis ($242 \pm 11\%$; $t=18$ vs $100 \pm 26\%$, $t=0$; $P<0.01$, Figure 3a).

To address the specificity of the fibronectin effect on the mitogenic response, cells were seeded on several other ECM components. At peak incorporation (18 h), the effect of matrigel, collagen types I and IV and poly-L-lysine, was tested and compared to those cells grown on plastic or fibronectin. A significantly low mitogenic response was observed in cells grown on collagen type IV or poly-L-lysine, which was similar to the cells grown on plastic or to untreated (control) cells (Figure 3b). Cells seeded on matrigel or collagen type I had a comparable increase in VEGF-dependent [3 H]thymidine incorporation, which was approximately two-times higher than in the control cells (203 ± 9 and $206 \pm 13\%$, respectively). However, fibronectin caused the most prominent increase in mitogenic response ($257 \pm 10\%$, Figure 3b) relative to the other matrices. Therefore, we have chosen to elucidate the role of fibronectin in VEGF-dependent signaling in breast cancer cells, as described below.

The heparin homologue of HSPGs stabilizes the complex between VEGF and its receptors and increases their binding due to several basic residues on both the ligand (Templeton, 1992) and receptor (Dougher *et al.*, 1997). Thus, this polyanion was used to test whether it would affect VEGF-dependent mitogenic response in T47D cells. FBS strongly increased [3 H]thymidine incorporation at the peak of DNA synthesis (7669 ± 920 c.p.m. for FBS vs 3349 ± 335 c.p.m. for control which is taken as 100%, $P<0.01$). An additional two-fold increase in DNA synthesis was observed upon FBS treatment of cells that were grown on fibronectin ($461 \pm 21\%$, FBS on FN; vs $229 \pm 12\%$, FBS on plastic; $P<0.01$, Table 1). In the presence of heparin, VEGF was able to increase DNA synthesis 2–3 times that in the control cells ($225 \pm 13\%$, VEGF + H vs $110 \pm 9\%$, VEGF alone, vs $100 \pm 10\%$, untreated cells), even though cells were seeded on plastic (Table 1). A similar increase in DNA synthesis was observed in cells grown on fibronectin after treatment with VEGF. Furthermore, heparin's presence further increased VEGF-dependent [3 H]thymidine incorporation ($298 \pm 12\%$, FN + VEGF + H vs $246 \pm 11\%$, FN + VEGF) in T47D cells seeded on fibronectin (Table 1), suggesting a stronger effect of heparin. Fibronectin or heparin alone or their combination did not dramatically affect DNA synthesis over the course of 18 h ($100 \pm 20\%$, $95 \pm 11\%$, and $93 \pm 9\%$, respectively). Therefore, the apparent effects of heparin and fibronectin on VEGF-dependent cell migration in the matrigel invasion assay may be attributed to their demonstrated effects on cell proliferation.

To address the mechanism by which fibronectin and heparin cause the increased VEGF-dependent mitogenic response, T47D cells were treated with VEGF₁₂₁ or EGF. We observed that VEGF₁₂₁, a shorter form of the VEGF protein which lacks an ECM-binding domain, was fully active and was able to induce DNA synthesis in endothelial cells (data not shown). However,

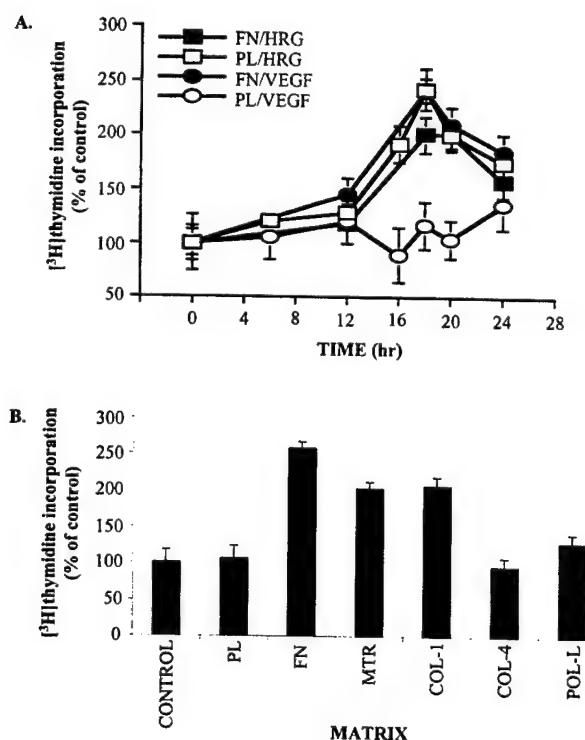


Figure 3 Fibronectin and heparin affect VEGF-dependent DNA synthesis in T47D cells. T47D cells seeded onto plastic (PL) or fibronectin (FN)-coated 24-well plates were starved and treated either with VEGF, heregulin (HRG) or FBS (10%). Cells were then processed for determination of incorporated radioactivity as described in Materials and methods. (a) Cells seeded on PL (○, □) or on FN (●, ■) were treated with VEGF (○, ●) or HRG (□, ■) for the indicated times. Values are expressed as the means (\pm s.d.) of control, non-treated cells (taken as 100%), from quadruplicate wells of three separate experiments. (b) Cells were seeded on plastic (PL), fibronectin (FN), Matrigel (MTR), collagen types I and IV (COL-1, COL-4) and poly-L lysine (POL-L), treated with VEGF (100 ng/ml), and processed for determination of the incorporated radioactivity at peak value (18 h, see Figure 3a) and compared to non treated cells (control)

Table 1 Heparin and fibronectin affect VEGF-dependent mitogenic response in T47D cells

Matrix	Treatment	[³ H]thymidine incorporation per cent of control (%)	P	n
Plastic	0	100 ± 10	—	20
	Heparin	95 ± 11	NS	12
	FBS	229 ± 12	<0.01	12
	VEGF ₁₆₅	110 ± 10	NS	20
	VEGF ₁₆₅ + Heparin	225 ± 13	<0.01	20
	VEGF ₁₆₅ + Heparin + mAb	98 ± 8	NS	8
	VEGF ₁₂₁	107 ± 9	NS	12
	VEGF ₁₂₁ + Heparin	108 ± 16	NS	12
	EGF	295 ± 10	<0.01	12
	EGF + Heparin	288 ± 9	<0.001	12
Fibronectin	0	100 ± 20	—	20
	Heparin	93 ± 9	NS	12
	FBS	461 ± 21	<0.01	12
	VEGF ₁₆₅	246 ± 11	<0.01	20
	VEGF ₁₆₅ + mAb	103 ± 9	NS	8
	VEGF ₁₆₅ + Heparin	298 ± 12	<0.01	20
	VEGF ₁₂₁	105 ± 11	NS	12
	VEGF ₁₂₁ + Heparin	102 ± 12	NS	12
	VEGF ₁₆₅ + β ₁	175 ± 7	<0.01	12
	VEGF ₁₆₅ + α ₆	228 ± 16	<0.01	12
	EGF	268 ± 8	<0.01	12
	EGF + Heparin	290 ± 16	<0.01	12

T47D cells were seeded either on plastic or on fibronectin-coated 24-well plates and rendered quiescent. Cells were then stimulated either with VEGF₁₆₅ (100 ng/ml), VEGF₁₂₁ (100 ng/ml) or EGF (10 ng/ml), in the presence or absence of heparin (1 μg/ml), or with FBS (10%) or left untreated '0'. Some cells were treated with blocking anti-β₁ integrin or with blocking anti-α₆ integrin antibodies prior to the treatment with VEGF₁₆₅, and some cells were treated with heparin (1 μg/ml) alone. Cells were then processed in the same way as described in Figure 3b to measure the incorporated [³H]thymidine. Values are expressed as the per cent of untreated cells ('0', taken as 100%) ± s.d. from the number (n) of wells (in quadruplicates) per experiment. The P values are calculated by the unpaired Student's *t*-test for comparison of treated versus the untreated T47D cells. To address the specificity of VEGF stimulation, monoclonal anti-VEGF antibodies (mAb, 10 μg/ml) were used. NS, not significant

stimulation with VEGF₁₂₁ on either plastic or fibronectin had no effect on the [³H]thymidine incorporation of T47D breast cancer cells in the presence or absence of heparin (Table 1), suggesting that the ECM binding domain of VEGF was required for this mitogenic response. Interestingly, EGF elicited a strong increase in [³H]thymidine uptake, which was not significantly affected by the presence of either fibronectin or heparin (Table 1). Several extracellular matrix proteins, such as fibronectin or collagens, utilize β₁ integrin to attach to and regulate cellular functions. To elucidate the role of β₁ integrin in our system, we pretreated cells with blocking anti-β₁ or anti-α₆ integrin antibodies prior to stimulation with VEGF. While VEGF-dependent DNA synthesis was not affected by the α₆ integrin antibody (228 ± 16%, VEGF₁₆₅ + α₆ vs 246 ± 11%, VEGF₁₆₅, both on fibronectin, Table 1), pretreatment with blocking anti-β₁ integrin antibody inhibited [³H]thymidine incorporation by approximately 50% (calculated from basal level, 175 ± 7% VEGF₁₆₅ + β₁ vs 246 ± 1% VEGF₁₆₅, both on fibronectin, Table 1).

Table 2 T47D cell attachment on different surfaces

Method	Plastic attached cells (%)	Fibronectin attached cells (%)	n
Recovered radioactivity	85 ± 12	83 ± 9	24
Cell number	83 ± 15	93 ± 8	24

T47D cells were either labeled with ³H-thymidine or left unlabeled and passed into 12-well plates noncoated or coated with fibronectin as described in Materials and methods. After allowing cells to attach for 60 min, unattached cells were removed and attached cells were released by trypsin/EDTA. The percentage of attached cells was measured by both direct counting of the attached and unattached cells using a Coulter counter and by scintillation counting of the radiolabeled cells. The values ± s.d. are calculated by the formula indicated in Materials and methods from the number (n) of wells from two separate experiments

The increased mitogenic response could be a consequence of more cells initially attaching to fibronectin. To address this possibility, nonlabeled cells or cells labeled with ³H-thymidine were passaged onto either fibronectin or plastic, allowed to attach for 1 h and then the number of adherent cells or radioactivity was counted. Two separate experiments showed no difference in the attachment of T47D cells to either plastic or fibronectin (Table 2). Therefore, the increased [³H]thymidine incorporation after treatment with VEGF (following a 48-h starvation period) is not due to initial greater adhesion, but rather to an increase of cell mitogenic response in the presence of fibronectin.

Effect of heparin and fibronectin on VEGF-dependent *c-fos* induction

Induction of the protooncogene *c-fos* is an early indicator of cell entry into the cell cycle. *c-fos* mRNA levels were reported to be maximal 30–60 min after the stimulation of quiescent breast cancer cells with heregulin (Sepp-Lorenzino *et al.*, 1996). Similar amounts of total RNA were loaded in all blots as indicated in the lower panels after probing with an 18S cDNA probe. Cells grown on plastic showed a transient increase in *c-fos* mRNA level in response to VEGF, although it was a much lower response as compared to cells treated with heregulin (Figure 4a,c). In the presence of heparin, a significant increase in VEGF-dependent *c-fos* mRNA level was observed, supporting the results showing a mitogenic response (Figure 4b). In additional experiments, we further compared *c-fos* mRNA levels 30 min after stimulation with VEGF in cells plated on plastic in the presence of chondroitin sulfate or dextran sulfate or in cells plated on fibronectin in the presence of heparin (Figure 4b). Dextran sulfate, an unrelated polyanion, increased VEGF-induced *c-fos* transcription similar to heparin, while chondroitin sulfate, a glycosaminoglycan control, did not significantly affect this induction. Because the *c-fos* mRNA level, in response to dextran sulfate alone, was almost as high as with VEGF and dextran sulfate together, it suggests that heparin possesses a VEGF-

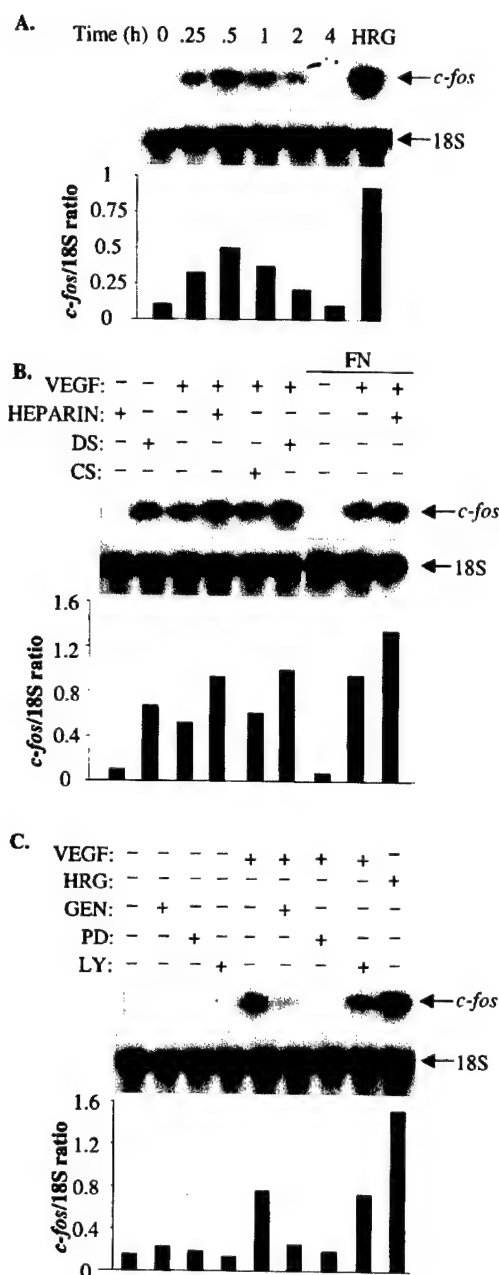


Figure 4 Heparin and fibronectin enhance VEGF-dependent *c-fos* induction in T47D cells. Quiescent T47D cells seeded on plastic or FN-coated plates were stimulated at time 0 with VEGF or with heregulin (HRG). (a) Cells were treated with VEGF over the indicated time or with HRG as a control, and total RNA was collected and subjected to Northern blotting. (b) Total RNA was collected immediately or after 30 min of treatment with VEGF in the presence or absence of heparin, dextran sulfate (DS), or chondroitin sulfate (CS), or (c) kinase inhibitors such as genistein (GEN, 50 μ M), PD98059 (PD, 50 μ M) and LY294002 (LY, 10 μ M). Blots shown in a, b and c were probed with cDNAs to *c-fos* (upper panels) and to 18S rRNA (lower panels). Histograms show the ratio of the *c-fos* signal relative to the intensity of the hybridized 18S probe as determined by densitometry. Results are representative of three independent experiments

specific mechanism of enhancing the signaling of this growth factor. Cells seeded on fibronectin-coated plates responded to VEGF with an elevated level of *c-fos* mRNA (Figure 4b) that was further increased when heparin was present in the medium. This enhancing effect of heparin is similar to that observed when the mitogenic response was tested (Table 1).

We next examined a series of kinase inhibitors to characterize the pathway by which *c-fos* is induced in T47D cells in response to VEGF. Cells were pretreated with genistein, PD98059 or LY294002 before the addition of VEGF and then tested for the level of *c-fos* mRNA (Figure 4c). While genistein inhibited tyrosine kinases and downstream pathways including MAPK and PI3K, PD98059 inhibited only MEK/ MAPK-dependent signaling (Dudley *et al.*, 1995) and LY294002 inhibited only the PI3K/Akt pathway (Vlahos *et al.*, 1994). None of the inhibitors affected a basal level of *c-fos* mRNA. Genistein and PD98059 abolished the VEGF-dependent increase in *c-fos* mRNA level while LY294002 had a modest suppressive effect (Figure 4c), suggesting the MAPK dependence of *c-fos* induction in these cells.

Heparin and fibronectin affect VEGF-dependent MAPK activation

Several pathways are known to be involved in *c-fos* induction, with one acting through the Erk family of MAPK (Treisman, 1992). Recently, we showed that T47D cells responded to VEGF with a modest MAPK activation which had maximal activity at 15 min (Price *et al.*, 2001). Thus, at 15 min, we tested the effects of heparin and fibronectin on VEGF-dependent MAPK activation. Phosphorylation as well as activation of MAPK were analysed by using phospho-specific antibody and an *in vitro* kinase assay, respectively. Quiescent cells on plastic, fibronectin, a collagen type IV, or cells treated with heparin alone showed very low levels of either MAPK phosphorylation or activity (Figure 5). When cells were treated with VEGF, a strong increase in the phosphorylation (Figure 5b) and activity (Figure 5a) of Erk occurred. However, this activity was still several times lower than that elicited by heregulin. This VEGF-induced increase was sensitive to pretreatment with the MAPK kinase (MEK1/2) inhibitor, PD98059, suggesting a MAPK-dependent process. The response to VEGF was greatly enhanced by the presence of heparin and dextran sulfate, whereas chondroitin sulfate was without effect (Figure 5a,b). Heparin also slightly increased the level of MAPK phosphorylation in cells seeded on fibronectin in response to VEGF, which otherwise was similar to the cells grown on plastic (Figure 5b). Consistent with the mitogenic response, MAPK activity was also low on collagen type IV when compared to that on fibronectin (Figure 5a). The total amount of MAPK protein detected by Western blotting was the same in cells grown on fibronectin or plastic as indicated (lower panels, Figure 5a,b).

Effect of fibronectin and heparin on VEGF receptor tyrosine phosphorylation

VEGF activates the Ras pathway through protein tyrosine kinase receptors (Dougher-Vermazen *et al.*, 1994; Sawano *et al.*, 1996), and subsequently activates MAPK through the dual specificity MEK. To determine whether fibronectin and heparin affect

VEGF receptor tyrosine phosphorylation, T47D cells were stimulated with VEGF and total cell lysates were immunoprecipitated with anti-Flt-1, anti-Flk-1 or anti-Flt-4 antibodies and subjected to immunoblotting with an anti-phosphotyrosine antibody. As indicated in Figure 6, the tyrosine phosphorylation was increased upon cell stimulation with VEGF on plastic. When cells were seeded on fibronectin, a greater increase in tyrosine phosphorylation was observed in response to VEGF in the presence of heparin. Although Flk-1 and Flt-4 showed a slight increase in tyrosine phosphorylation in the presence of heparin and fibronectin as compared to cells seeded on plastic, a significant increase in tyrosine phosphorylation, upon VEGF treatment, was observed with the Flt-1 receptor (Figure 6a). This suggests that the Flt-1 receptor could be responsible for the signaling observed in the T47D cells, although it is not the only receptor expressed on these cells.

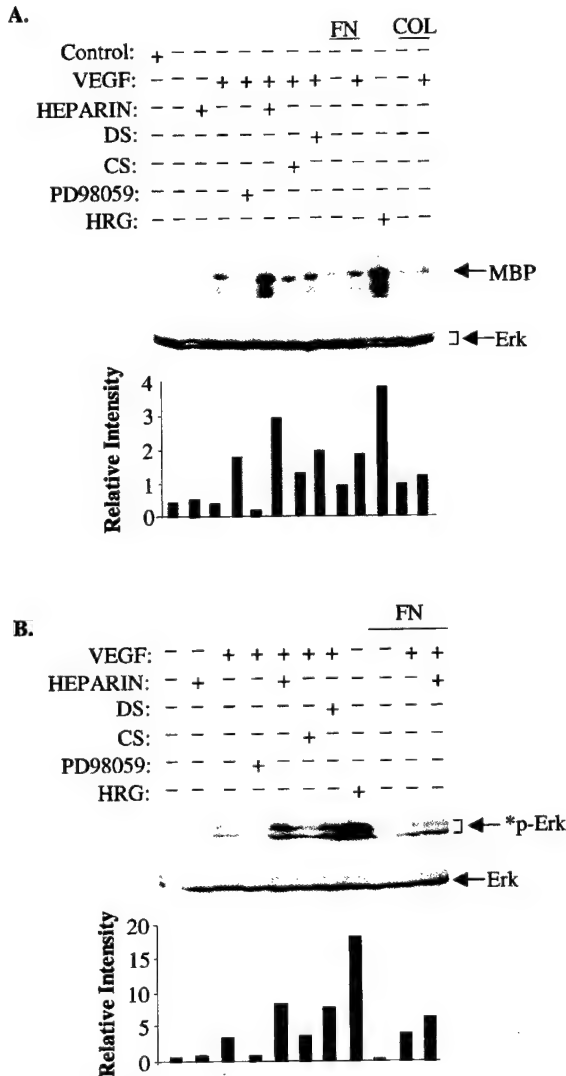


Figure 5 Effect of heparin and fibronectin on VEGF-induced MAPK phosphorylation and activation in T47D cells. T47D cells were seeded onto PL, collagen type IV (COL) or on FN-coated plates and starved as indicated in Figure 3. (a) Cell treatment was followed by immunoprecipitation with anti-Erk-2 antibody, and immunoprecipitates were used in an *in vitro* kinase assay with myelin basic protein (MBP) as a substrate. Control indicates the kinase activity of the sample containing lysate from cells treated with VEGF mixed with protein-G agarose without anti-Erk-2 antibody. The lower panel represents immunoblots of immunoprecipitates probed with anti-Erk-2 antibody. (b) Blots of total cell lysates were probed with anti-phospho-Erk-2 antibodies (*p-Erk, upper panel), and then were stripped and reprobed with anti-Erk-2 antibody as a control for total Erk protein (lower panel). Histograms show signal intensity after correction for loading. Blots are representative of two independent experiments

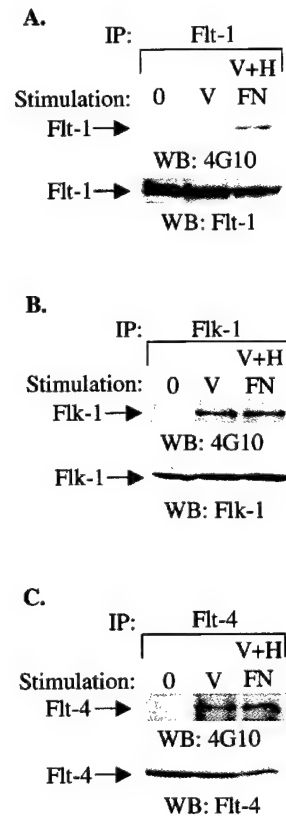


Figure 6 Effect of fibronectin and heparin on the tyrosine phosphorylation of VEGF receptors. T47D cells were seeded on plastic or on fibronectin (FN)-coated petri dishes. After 48 h starvation, cells were treated with VEGF₁₆₅ (V) alone or with VEGF₁₆₅ in the presence of heparin (1 µg/ml, V+H) for 15 min, and cell lysates were then immunoprecipitated with anti-Flt-1, anti-Flk-1 or with anti-Flt-4 antibodies. The immunoprecipitates were subjected to electrophoresis. The separated proteins were blotted to the membrane, and blots were probed with 4G10 (anti-phosphotyrosine antibody, upper panels), or after stripping, with anti-Flt-1, anti-Flk-1 or anti-Flt-4, antibodies (lower panels). The experiment was repeated twice with the same results

VEGF-induced PI3K activity is affected by heparin and fibronectin

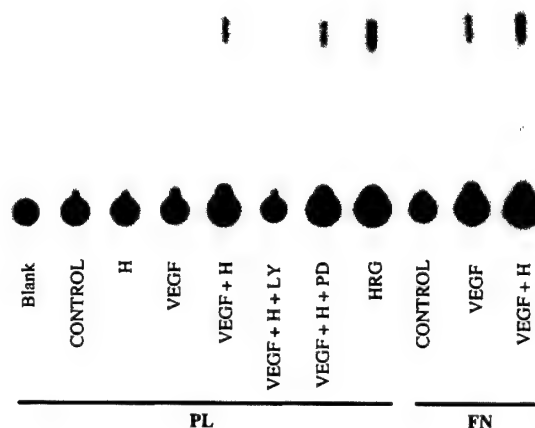
Tyrosine phosphorylation of receptors can activate PI3K, which in turn phosphorylates and consequently activates the serine/threonine kinase AKT (Carpenter and Cantley, 1996). AKT is activated by its PI3K-dependent recruitment to the plasma membrane that is followed by its phosphorylation at Thr-308 and Ser-473 residues (Downward, 1998). Therefore, measurement of Ser-473 phosphorylated AKT can be an indication of PI3K/AKT pathway activation (Altioek *et al.*, 1999; Downward, 1998). Stimulation of T47D cells by VEGF modestly increased PI3K activity over the basal level, as indicated by the phosphorylation of phospholipids (Figure 7a) and by AKT phosphorylation (*p-Akt, Figure 7b). This modest increase in PI3K activity was weaker than in cells stimulated with heregulin (Figure 7a,b). A significant increase in PI3-kinase activation was observed when heparin was present with VEGF in the T47D cells grown on plastic. A slightly higher intensity of VEGF-induced PI3-kinase activity was observed in T47D cells grown on fibronectin (Figure 7a,b). Similar to heparin, dextran sulfate enhanced Akt phosphorylation in the presence of VEGF, while chondroitin sulfate was without effect (Figure 7b). The increase in VEGF-dependent PI3K activity was completely blocked by pretreatment of cells with the inhibitor LY294002, while PD98059 had no effect. Neither heparin (for both methods), nor dextran sulfate (for the *p-Akt assay, data not shown), alone affected the low basal level of AKT phosphorylation of the quiescent T47D cells. Equal amounts of AKT proteins were observed in all samples (Figure 7b, lower panel).

Discussion

Our recent study (Price *et al.*, 2001), as well as investigations by others (Blancher *et al.*, 2000; de Jong *et al.*, 1998b; Speirs and Atkin, 1999; Yoshiji *et al.*, 1996), have demonstrated that breast cancer cells express both VEGF and VEGF receptors. However, VEGF alone was not able to induce either a proliferative or migratory response in T47D cells (Price *et al.*, 2001). Only cells that were seeded onto fibronectin-coated membranes migrated in significantly higher numbers than cells seeded on matrigel. Given that VEGF and its receptors possess regions rich in basic amino acids that confer binding to the ECM (Cardin and Weintraub, 1989; Dougher *et al.*, 1997; Templeton, 1992), and that VEGF binds to VEGF receptors in breast cancer cells via its exon 7-encoded ECM-binding region (which is not present in VEGF₁₂₁) (Soker *et al.*, 1996), it was reasonable to postulate that VEGF-induced signaling in T47D cells depends on an ECM component. Thus, the effects of heparin and fibronectin on these cells were considered.

In endothelial cells, VEGF binds with high-affinity to its receptors (Cohen *et al.*, 1995; Gitay-Goren *et al.*,

A.



B.

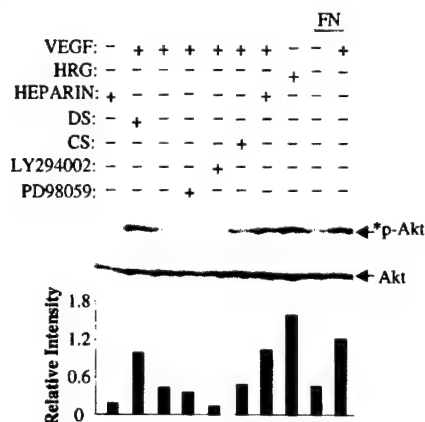


Figure 7 Effect of heparin and fibronectin on VEGF-dependent PI3K activity. Cells were seeded on PL or FN as described in Materials and methods. After 15-min treatment with VEGF, VEGF in the presence of heparin (VEGF + H), chondroitin sulfate (CS), or dextran sulfate (DS), or after treatment with heregulin (HRG), or with heparin alone, total cell lysates were subjected to either *in vitro* PI3K assay (a) or to immunoblotting (b). Untreated cells (control) or cells pretreated with either PD98059 (50 μ M, PD) or LY294002 (10 μ M, LY) were subjected to treatment with VEGF in the presence of heparin (H). (a) Immunoprecipitates with anti-phosphotyrosine antibodies were tested for their ability to phosphorylate lipids in the presence of γ [³²P]ATP in an *in vitro* PI3K assay. The phosphorylated lipids were then extracted from the reaction mixture by CHCl₃:CH₃OH [1:1] and were spotted onto TLC plates. Phosphorylated phospholipids were then separated in developing solution containing CHCl₃:CH₃OH:NH₄OH:H₂O [60:47:11.3:2] followed by autoradiography. 'Blank' represents the sample containing the reaction mixture of cells treated with heregulin that was precipitated with Protein-G sepharose without anti-phosphotyrosine antibody. The autoradiograph is representative of two separate experiments. (b) Immunoblots were probed with anti-p-Ser⁴⁷³ AKT antibody (*p-AKT, upper panel) or with anti-AKT antibodies (lower panel). The histogram was generated exactly as in Figure 5b. The blots are representative of two separate experiments

1992). In spite of its high-affinity binding, heparin (Cohen *et al.*, 1995; Dougher *et al.*, 1997; Gitay-Goren *et al.*, 1992) and HSPGs (Gengrinovitch *et al.*, 1999)

enhanced this binding and stabilized the complex between VEGF and its receptors. Therefore, it is expected that heparin would support VEGF-induced binding and signaling in T47D cells. Several pieces of information support our hypothesis indicating that an ECM component is required for VEGF-induced mitogenic and migratory response in these cells: (i) cells seeded onto plastic showed no significant increase in [³H]thymidine incorporation and no increase in the number of migrating cells after treatment with VEGF on matrigel. Accordingly, T47D cells in response to VEGF on plastic showed very modest increases in overall tyrosine phosphorylation, *c-fos* induction, MAPK activity and PI3K activation as opposed to quiescent cells. The degree of activation was several times lower than that observed in heregulin-treated cells; (ii) heparin presence and/or attachment to fibronectin-coated plates was sufficient to establish the mitogenic response and increase migration of these breast cancer cells in response to VEGF similar to the response elicited by heregulin, a potent breast cancer cell mitogen; (iii) signaling pathways that lead to proliferation such as MAPK and *c-fos* or that stimulate cell migration, such as PI3K, were significantly increased in response to VEGF when cells were exposed to heparin and/or seeded onto fibronectin-coated dishes; (iv) as suggested by Soker *et al.* (1996), heparin/HSPGs enhance binding of VEGF to its receptors, and finally, (v) VEGF₁₂₁, which does not possess an ECM binding domain, had no effect on DNA synthesis in the presence or absence of heparin and/or fibronectin, while EGF strongly induced DNA synthesis which was not affected by the presence of either fibronectin or heparin. Thus, in order to stimulate signaling in T47D cells, the binding of VEGF to its receptors needs to be stabilized by the presence of ECM components such as heparin and fibronectin.

Although the binding of both VEGF and its receptors to heparin has been suggested by several authors (Cohen *et al.*, 1995; Dougher *et al.*, 1997; Gitay-Goren *et al.*, 1992), their binding to fibronectin and its stabilizing role in the VEGF-VEGF receptor complex have not been reported to date. Cells primarily interact with fibronectin through β_1 integrins (Clark and Brugge, 1995), while cooperative signaling from transmembrane HSPGs results in assembly of focal adhesions and actin stress fibers (Saoncella *et al.*, 1999). Fibronectin contains several binding domains including those for fibrin, collagen, heparin and cell-surface receptors (Paoletta *et al.*, 1988), and it has been shown to augment cell migration (Clark *et al.*, 1988). Its two heparin-binding domains, one of low affinity and the other of high affinity, are located at its N- and C-termini, respectively (Paoletta *et al.*, 1988). The binding of the heparin-binding domain of fibronectin to cell surface HSPGs promotes activation of PKC (Woods *et al.*, 1993). This result could be duplicated in our system, as cells seeded on fibronectin showed the increased tyrosine phosphorylation of a protein migrating at ~120 kDa (Miralem and Avraham, unpublished observation). Although the nature of that

band was not further investigated, its molecular weight and the fact that it is more phosphorylated in cells grown on fibronectin suggest that this band could be FAK. Activated PKC and FAK could lead to MAPK activation, which induces *c-fos* transcription such as that observed in our present work. The effect of fibronectin also could be attributed to the specific peptide PHSRN contained in its molecule, that was recently reported to accelerate wound healing by increasing cell invasiveness (Livant *et al.*, 2000).

The suppressive effect of poly-L-lysine on DNA synthesis suggests the involvement of integrins, which may mediate signaling from matrices containing fibronectin, matrigel or collagens type I and IV. However, a partial inhibition of VEGF-dependent migration (Figure 1b) and DNA synthesis (Table 1) by blocking anti- β_1 -integrin antibodies indicates that this mechanism is not the sole process. Integrins might also play a role in inducing the inhibitory effect of collagen type IV. Collagen type IV was shown to inhibit proliferation of melanoma cells (Han *et al.*, 1997) and breast cancer cells (Shahan *et al.*, 1999a) by up to 67%. This inhibition was attributed to the Serine-N-Serine sequence of the $\alpha 3(\text{IV})$ collagen chain. Integrin $\alpha_v\beta_3$ and integrin-associated protein CD47 were also responsible for this effect (Shahan *et al.*, 1999b). Although collagen type IV peptides were added to the growth medium (Shahan *et al.*, 1999b), it is conceivable that in our experiments (where cells were seeded onto a collagen type IV coat) cells were also exposed to the $\alpha 3(\text{IV})$ chain, which exerted its anti-proliferative effect.

Breast cancer cells express VEGF receptors. Speirs and Atkin (1999) reported the presence of Flt-1 and Flk-1/KDR in breast cancer epithelial cells, while de Jong *et al.* (1998a) found significant expression of these molecules in 50% of breast tumor epithelial cells. Consistent with these findings, we recently reported the expression of Flt-1 and Flk-1 in several cell lines including T47D breast cancer cells (Price *et al.*, 2001). The results presented here suggest the presence of the Flt-4 receptor in addition to the Flt-1 and Flk-1 receptors in T47D cells. However, the increased signal from the Flt-1 receptor in the presence of fibronectin and heparin was the most prominent, followed by that from Flt-4 and Flk-1/KDR. The reason for the weak activation of the Flt-4 receptor could be attributed to its lack of responsiveness to VEGF₁₆₅. A shorter form of VEGF protein, VEGF-C, which has about 30% identity with VEGF₁₆₅ (Joukov *et al.*, 1996), has the highest affinity for the Flt-4 receptor. Heparin binding affinity has been identified for Flt-1 (Cohen *et al.*, 1995), and also for Flk-1/KDR (Dougher *et al.*, 1997). Both receptors are associated with heparan sulfates or heparin-like molecules on the cell surface (Cohen *et al.*, 1995). This may have implications for the binding of VEGF. Indeed, binding of VEGF to VEGF receptors was differentially regulated by heparin. For example, binding of VEGF to Flt-1 was inhibited whereas binding to Flk-1/KDR was stimulated (Terman *et al.*, 1994). Our results showed that the presence of heparin

and fibronectin increased the activity of all VEGF receptors. These results, reporting the most significant increase in activity and presumably binding of VEGF to Flt-1 in the presence of heparin and fibronectin, are different than those presented by Terman *et al.* (1994). These differences may represent the different experimental conditions and cell types used.

Signal transduction by tyrosine kinase receptors, such as VEGF, depends upon the binding of SH2-SH3 domain-containing proteins to tyrosine phosphorylation sites on the receptor (Shibuya *et al.*, 1999). Subsequent MAPK activation converges from several pathways, one emanating from the activation of PLC- γ through PKC and, another, through the Ras/MEK-dependent cascade (Guo *et al.*, 1995). Decreased MAPK activity, such as that observed in VEGF-treated T47D cells grown on plastic, is consistent with low mitogenic response and weak *c-fos* induction. Strong and sustained activity of MAPK is required for its translocation to the nucleus where the enzyme activates transcription factors (Traverse *et al.*, 1992). Likewise, as indicated in the present study, plating of T47D cells onto fibronectin, or onto plastic in the presence of heparin, significantly increased all the signaling components tested in response to VEGF, providing the additional requirements for cells to complete passage through the S phase. The phosphorylated VEGF receptor can also recruit the p85 subunit of PI3K (Cunningham *et al.*, 1995; Guo *et al.*, 1995), thereby activating the PI3K/AKT pathway. Activated PI3K/AKT may regulate cell survival (Downward, 1998), proliferation (Chung *et al.*, 1994; Thakker *et al.*, 1999), and migration (Fujikawa *et al.*, 1999). We have observed migration of T47D cells in response to VEGF only when heparin and/or fibronectin was present on the transwell membrane, suggesting that both the growth factor and the ECM components are important in potentiating the migration of tumor cells. In endothelial cells, the PI3K pathway was shown to be crucial in cell survival (Gerber *et al.*, 1998) and to play an important role in the regulation of cell migration (Fujikawa *et al.*, 1999; Radisavljevic *et al.*, 2000). Similarly, in our system, we found that PI3K is involved in the regulation of cell survival (Price *et al.*, 2001) as well as in the process of cell migration, because LY294002, a PI3K specific inhibitor, strongly inhibited the VEGF-dependent migratory response while PD98059 and U0126 specific MEK inhibitors, had a moderate effect. Our results are consistent with those of Adam *et al.* (1998), who reported that MCF-7 cells, another breast cancer cell line, migrated in response to heregulin through a PI3K-mediated process (Adam *et al.*, 1998).

Induction of *c-fos* by growth factors operates through initial tyrosine phosphorylation of activated receptors, leading to subsequent MAPK activation. This induction is sensitive to inhibition of either tyrosine phosphorylation or MEK. Activation of MAPK leads to phosphorylation of the transcription factor Elk, which drives transcription of *c-fos* through serum response elements in the *c-fos* promoter (Treis-

man, 1994). PI3K was also shown to contribute to the cell cycle by inducing the AKT-dependent phosphorylation of glycogen synthase kinase 3 (Cross *et al.*, 1995) and by activating protein-serine/threonine p70^{src} kinase (Chung *et al.*, 1994). However, our results strongly suggest that the PI3K-dependent pathway does not play a significant role in VEGF-induced *c-fos* transcription in T47D cells. First, the *c-fos* mRNA level was not markedly reduced by pretreatment with LY294002, whose specificity to PI3K has been demonstrated (Vlahos *et al.*, 1994). Additionally, the VEGF-dependent increase in the level of *c-fos* mRNA was abolished after cell pretreatment with PD98059. Finally, corroborating our results, it was recently reported in the HUVEC system that the PI3K and MAPK pathways do converge (Thakker *et al.*, 1999). However, PI3K was shown to be upstream of MAPK and to only affect induction of *c-fos* through the regulation of MAPK activity. The significant increase in *c-fos* transcription in response to VEGF could be attributed to the specific effect of heparin because dextran sulfate alone, an unrelated polyanion, caused a strong increase in *c-fos* induction. Chondroitin sulfate, a control for GAG chains, was without effect either on *c-fos* induction or MAPK or PI3K activation. The induction of *c-fos* transcription by dextran sulfate alone supports the notion that part of heparin's effect is through electrostatic stabilization of the binding complex. For example, the binding affinity of FGFs to heparin, which is a highly sulfated GAG, is greater than that to heparan-sulfate, a GAG that is less sulfated (Templeton, 1992). However, the high isoelectric point, by itself, is insufficient to explain the binding, because PDGF, with an isoelectric point similar to b-FGF, does not localize to anionic heparan sulfate sites on the basement membrane of the eye, whereas a-FGF and b-FGF do bind to the same sites (Jeanny *et al.*, 1987).

Extracellular matrix-induced oligomerization appears to be an important mechanism in regulating the biological activities of growth factors (Chirgadze *et al.*, 1999). Since breast cancer cells express Flt-1 and Flk-1/KDR receptors (de Jong *et al.*, 1998a; Price *et al.*, 2001; Speirs and Atkin, 1999) and secrete VEGF (Blancher *et al.*, 2000; Price *et al.*, 2001; Yoshiji *et al.*, 1996), this phenomenon may emphasize an autocrine mechanism by which VEGF increases the tumorigenicity of breast cancer cells. In the early stages of breast cancer development, there is an initial accumulation of ECM components in both the interstitial stroma (Christensen, 1992) and in the basement membrane (Ormerod *et al.*, 1985). Accumulated ECM, such as fibronectin and HSPGs, may increase the responsiveness of breast cancer cells to VEGF by maintaining the stability of the complex between the growth factor and its receptor resulting in receptor activation. This could increase tumorigenicity through the stimulation of cell proliferation, survival and invasiveness. However, this initial phase does not seem to last very long due to a general decrease in ECM components and in the level of sulfation of heparan sulfate, which has been

associated with the metastatic phenotype of cancer cells. This final stage of transformation can be ascribed to the upregulation of ECM-degrading matrix metalloproteinases (Sternlicht *et al.*, 2000).

In this report, we demonstrated that VEGF requires the presence of ECM components for the induction of mitogenic and migratory responses in T47D cells. As compared to T47D cells grown on plastic, cells seeded on fibronectin or cells grown on plastic in the presence of heparin had significantly higher [³H]thymidine incorporation and *c-fos* induction as well as a higher number of cells migrating to the transwell membranes. Likewise, intracellular signaling that supports mitogenic and migratory responses, such as tyrosine phosphorylation of VEGF receptors, MAPK activity, and PI3K activity, was much greater in cells seeded on fibronectin or seeded on plastic in the presence of heparin, as compared to cells grown on plastic. Heparin has been shown to enhance the binding of VEGF to its receptors in both breast cancer (Soker *et al.*, 1996) and endothelial cells (Gitay-Goren *et al.*, 1992), and fibronectin has been reported to enhance VEGF₁₆₅-dependent DNA synthesis in endothelial cells (Soldi *et al.*, 1999). However, to our knowledge, this is the first report associating ECM enhancement of VEGF binding to the induction of mitogenic and migratory responses in breast cancer cells.

Materials and methods

Materials

Antibodies used for immunological analysis were as follows: anti-phosphotyrosine antibody (4G10) was from Genentech (San Francisco, CA, USA). Phospho-Erk (E-4) antibody, anti-Erk-2 (C-154), anti-Flt-1 antibody, anti-Flt-4 antibody, anti-Flk-1 antibody and HRP-labeled secondary antibodies were from Santa Cruz Biotechnology (Santa Cruz, CA, USA). Anti-Akt, and anti-phospho-Ser-473 Akt antibodies were from New England-Biolabs (Beverly, MA, USA). Anti-phosphotyrosine antibody (PY20) was from Transduction Laboratories (Lexington, KY, USA). Genistein, LY294002, heparin, chondroitin sulfate A, and C, dextran sulfate, and phosphatidylinositol were from Sigma Chemical Co. (St. Louis, MO, USA). PD98059 and U0126 were from Calbiochem-Novobiochem Co. (La Jolla, CA, USA). VEGF₁₆₅ and heregulin were generous gifts from Genentech and VEGF₁₂₁ was from R&D Systems (Minneapolis, MN, USA). EGF was from Upstate Biotechnology (Lake Placid, NY, USA). γ [³²P]ATP, α [³²P]dCTP, [³H]thymidine and [¹²⁵I]Na were from New England Nuclear (Boston, MA, USA). Blocking anti- β_1 integrin antibody was from Hybridoma Bank (University of Iowa, Iowa City, IO, USA) and blocking anti- α_6 integrin antibody was a generous gift from Leslie Shaw (Beth Israel-Deaconess Medical Center, Boston, MA, USA). All other chemicals were from Fisher Scientific (Norcross, GA, USA), unless otherwise specified.

Cell culture

T47D cells were obtained from ATCC. These cells were cultured in RPMI-1640 medium (Gibco-BRL), supplemented

with 3.5 μ g/ml insulin, 10% fetal bovine serum (Gibco-BRL), and penicillin/streptomycin. To coat the plates: human plasma fibronectin (30 μ g/ml), collagen type IV (40 μ g/ml) and Matrigel (Engelberth-Holm-Swarm tumor basement membrane, 40 μ g/ml) (Becton-Dickinson, Bedford, MA, USA) were dissolved in sterile water, 0.05 M HCl, or in cold medium, respectively, spread on culture dishes (1.2 ml/10-cm petri dish, 70 μ l/well in 24-well plates), and allowed to dry in a sterile environment. Collagen type I solution (2.9 mg/ml) was purchased as Vitrogen-100 (Cohesion, Palo Alto, CA, USA) and was added to the wells of the tissue culture plates (0.25 ml/well in 24-well plates), then incubated for at least 60 min at 37°C to gel. Poly-L-lysine (40 μ g/ml, Sigma) was dissolved in water spread on culture dishes (70 μ l/ml in 24-well plates) and allowed to dry in a sterile environment. Quiescence was induced by replacing growth medium on cells at 60–80% confluence with medium containing 0.4% FBS, then followed by 48 h incubation. To study the initiation of signaling, cells were stimulated with heregulin (20 nM), or FBS (10%), VEGF (100 ng/ml), VEGF₁₂₁ (100 ng/ml), or EGF (10 ng/ml) alone or in the presence of heparin, chondroitin sulfate, or dextran sulfate (all at a concentration of 1 μ g/ml).

Cell attachment

Cell attachment was performed as described (Miralem *et al.*, 1996b). Briefly, labeled or unlabeled cells were released from petri dishes by trypsinization, resuspended in Dulbecco's modified Eagle's medium (DMEM) containing bovine serum albumin (BSA; 1 mg/ml) and then seeded in 12-well plates that were either uncoated or precoated with fibronectin (30 μ g/ml). After 60 min, the percentage of attached cells was measured by both the direct counting of attached and unattached cells using a Coulter counter or by scintillation counting of radiolabeled cells as described by Grinnell and Feld (1979). The per cent attachment was calculated as $100 \times [\text{attached}/(\text{attached} + \text{unattached})]$.

Radioiodination

The iodination of VEGF₁₆₅ was carried out using IODOGEN (Pierce, Rockford, IL, USA) as described previously (Soker *et al.*, 1996). ¹²⁵I-VEGF was then purified by heparin affinity chromatography in the presence of gelatin (10 μ g/ml). Aliquots of the iodinated VEGF were frozen on dry-ice and stored at –70°C until needed. The specific activity of ¹²⁵I-VEGF was approximately 5×10^4 c.p.m./ng protein.

Binding and cross-linking

T47D cells were grown in 24-well plates or in 60 mm petri dishes. After reaching confluency, they were transferred to an ice-cold environment and washed twice with ice-cold PBS. ¹²⁵I-VEGF (10 ng/ml) was added to F12 medium containing 25 mM HEPES (pH, 7.5) and 0.2% gelatin, and cells were then incubated for 4 h at 4°C. At the end of the incubation, cells were washed three times with ice-cold PBS supplemented with 0.1% BSA, lysed in buffer containing 1% Triton X-100 and 0.1% BSA, and counted in a γ counter for recovered radioactivity. For the cross-linking studies; following incubation for 4 h in 60 mm plates, cells were treated with PBS containing disuccinimidyl suberate (0.15 mM) and the reaction was stopped by the addition of 200 μ l of quenching buffer (10 mM Tris-HCl, pH 7.5, 200 mM glycine, and 2 mM EDTA). Cells were then washed with ice-cold PBS, scraped in PBS containing 1 mM PMSF and 1 mM EDTA and centri-

fused for 30 s prior to dissolving pellets in lysis buffer (10 mM Tris-HCl, pH 7.0, 0.5% Nonidet P-40, 0.5% Triton X-100, 0.1 mM EDTA, and 1 mM PMSF). The suspension was centrifuged and aliquots from the supernatant were analysed by SDS-PAGE followed by autoradiography.

Mitogenic response

Mitogenic response of T47D cells was performed as previously described (Miralem *et al.*, 1996b). Briefly, cells were passaged at 10^5 cells/well (24-well plate) and grown either on plastic, fibronectin, collagen type I or IV, Matrigel, and poly-L-lysine-coated plates and starved to arrest cell growth. A mitogenic response in the quiescent cells was induced with VEGF, VEGF₁₂₁, EGF, heregulin, or fetal bovine serum, and measured by [³H]thymidine (6.7 Ci/mM, 2 mCi/ml for 45 min) incorporation at different time points up to 24 h. After being labeled with [³H]thymidine, cells were washed three times with 5% trichloroacetic acid at 0°C, dissolved with 0.1 M NaOH, and radioactivity was measured by using scintillation counter.

RNA isolation and Northern blotting

Total RNA was isolated using an RNA kit from QIAGEN. The electrophoresis and blotting were done as described (Miralem *et al.*, 1996a). Briefly, equal amounts of RNA (~15 µg) were denatured, separated by electrophoresis on agarose-formaldehyde gels, and transferred to a Hybond-N nylon membrane (Amersham-Pharmacia Biotech). Membranes were hybridized with *c-fos* cDNA that was labeled with α -³²P-dCTP. Levels of mRNA were normalized to 18S rRNA after probing stripped blots with labeled cDNA to rat 18S rRNA. ³²P labeling of probes was carried out with a random primer DNA labeling kit from Boehringer-Mannheim (Indianapolis, IN, USA). The rat *c-fos* cDNA, cloned by T Curran (11), and the mouse 18S rRNA were obtained from DM Templeton (University of Toronto, Ontario, Canada).

MAPK activity

MAPK activity was determined by the ability of the immunoprecipitated enzyme to phosphorylate myelin basic protein (MBP) (Ahn *et al.*, 1990) in an *in vitro* kinase assay. Immunoprecipitates were mixed with assay buffer containing 20 mM HEPES (pH 7.4), 10 mM MgCl₂, 2 mM MnCl₂, 0.5 mM EGTA, 10 mM NaF, 0.5 mM Na₃VO₄, 1 mM dithiothreitol, 0.5 mg/ml MBP, 100 mM ATP, and 5 µCi of [³²P]ATP, and incubated at 30°C for 30 min. The reaction was stopped by the addition of sample buffer for electrophoresis according to Laemmli (1970), and the mixture was separated on 15% SDS-PAGE for silver staining and autoradiography.

PI3K activity

Cells were lysed in buffer A containing 137 mM NaCl, 20 mM Tris-HCl, pH 7.4, 1 mM CaCl₂, 1 mM MgCl₂, 1% NP-40, 1 mM PMSF and 0.1 mM Na₃VO₄, and then cytosolic extracts were immunoprecipitated with anti-phosphotyrosine antibody (PY20). Precipitates were subjected to an *in vitro* kinase assay using [³²P]ATP and phosphatidylinositol as substrates, according to Derman *et al.* (1996). Briefly, beads were washed and incubated for 10 min at room temperature in kinase buffer containing 0.5 mM ATP, 20 mM MgCl₂, 50 mM HEPES, pH 7.0, 0.25 mg/ml phosphatidylinositol and

30 µCi of [³²P]ATP (3000 Ci/mmol). Lipids were then extracted by CHCl₃:CH₃OH (1:1) mixture, separated on oxalate-coated thin-layer chromatography plates (EM Science, Gibbstown, NJ, USA) in developing solution containing CHCl₃:CH₃OH:H₂O:NH₄OH [60:47:11,3:2], followed by autoradiography.

Immunoblotting

Cells were lysed in the lysis buffer A, and lysates or immunoprecipitates were subjected to SDS-PAGE according to Laemmli (1970). Separated proteins were transferred to PVDF membranes in 25 mM Tris and 192 mM Glycine (pH 8.3) containing 15% methanol, and then blocked with 5% BSA and 5% Carnation milk in 30 mM Tris-HCl (pH 7.4) containing 137 mM NaCl, 2.6 mM KCl and 0.05% Tween 20. Membranes were then probed with either anti-Erk-2 antibody, polyclonal rabbit anti-phospho-Erk antibody, monoclonal mouse anti-phosphotyrosine antibody 4G10, monoclonal mouse anti-actin antibody, polyclonal rabbit anti-Akt, polyclonal rabbit anti-Flt-4 antibody, monoclonal mouse anti-Flk-1 antibody, polyclonal goat anti-Flt-1 antibody or polyclonal rabbit anti-phospho-Ser-473 Akt antibodies, and immunoreactive bands were detected with the NEN-Biolab (Boston, MA, USA) enhanced chemiluminescence system, followed by autoradiography.

Migration assay

Transwell membranes (Corning Costar Corporation, Cambridge, MA, USA) were coated with matrigel (MTR; 2.5 µg/ml) or MTR plus fibronectin (30 µg/ml), and dry coatings were exposed to DMEM for 1–2 h prior to cell passage. Cells were trypsinized, centrifuged and resuspended at approximately 10^7 /ml in DMEM containing 0.2% BSA, and then seeded onto precoated transwells in the same medium alone (control) or in medium supplemented with heparin (1 µg/ml), HRG (20 nM), VEGF (100 ng/ml), VEGF + heparin, VEGF₁₂₁ (100 ng/ml) or VEGF₁₂₁ + heparin. Some cells were pretreated for 30 min either with genistein (10 µM), PD98059 (50 µM), U0126 (10 µM), or LY294002 (10 µM) prior to cell detachment, or with blocking anti-β₁ integrin (10 µg/ml) or blocking anti-α₆ integrin (10 µg/ml) antibodies prior to treatment with VEGF in the presence of heparin. The bottom wells of the transwell contained 600 µl of the same medium as the upper wells but without the cells. After 24 h, the membranes were swabbed with Q-tips and exposed to methanol, followed by treatment with crystal violet prior to counting cell number under a phase-contrast microscope.

Abbreviations

VEGF, vascular endothelial growth factor; HRG, heregulin; MTR, matrigel; ECM, extracellular matrix; GAG, glycosaminoglycan; PI3K, phosphatidylinositol 3-kinase; ERK, extracellular regulated kinase; MAPK, mitogen-activated protein kinase; PDGF, platelet-derived growth factor; FBS, fetal bovine serum; SDS-PAGE, sodium dodecyl sulfate-polyacrylamide gel electrophoresis; HSPG, heparin sulfate proteoglycan; FN, fibronectin; MEK, mitogen-activated kinase-kinase; AKT, Akt kinase; a-, b-FGF, acidic-, basic-fibroblast growth factor.

Note added in proof

Unless otherwise stated, all notation of VEGF refers to the VEGF₁₆₅ isoform.

Acknowledgments

We are grateful to Jamal Misleh for technical assistance, Dan Kelley and Sarah Evans for preparation of figures and Janet Delahanty for editing this manuscript. This paper is supported by NIH grants HL 55445 (H Avrahan), CA 76226 (H Avrahan), and Department of

the Army DAMD 17-00-1-0152 (T Miralem), DAMD 17-98-8032 (H Avrahan), and DAMD 17-99-9078 (H Avrahan), NCI/NCI AR21 CA 87290-01 (H Avrahan). This work was done during the terms of an established investigatorship from the American Heart Association (H Avrahan).

References

- Adam L, Vadlamudi R, Kondapaka SB, Chernoff J, Mendelsohn J and Kumar R. (1998). *J. Biol. Chem.*, **273**, 28238–28246.
- Ahn NG, Weiel JE, Chan CP and Krebs EG. (1990). *J. Biol. Chem.*, **265**, 11487–11494.
- Altiok S, Batt D, Altiok N, Papautsky A, Downward J, Roberts TM and Avrahan H. (1999). *J. Biol. Chem.*, **274**, 32274–32278.
- Bacic M, Edwards NA and Merrill MJ. (1995). *Growth Factors*, **12**, 11–15.
- Blancher C, Moore JW, Talks KL, Houlbrook S and Harris AL. (2000). *Cancer Res.*, **60**, 7106–7113.
- Cardin AD and Weintraub HJ. (1989). *Arteriosclerosis*, **9**, 21–32.
- Carpenter CL and Cantley LC. (1996). *Curr. Opin. Cell Biol.*, **8**, 153–158.
- Chirgadze DY, Hepple JP, Zhou H, Byrd RA, Blundell TL and Gherardi E. (1999). *Nat. Struct. Biol.*, **6**, 72–79.
- Christensen L. (1992). *AMPIS Suppl.*, **26**, 1–39.
- Chung J, Grammer TC, Lemon KP, Kazlauskas A and Blenis J. (1994). *Nature*, **370**, 71–75.
- Clark EA and Brugge JS. (1995). *Science*, **268**, 233–239.
- Clark RA, Wikner NE, Doherty DE and Norris DA. (1988). *J. Biol. Chem.*, **263**, 12115–12123.
- Cohen T, Gitay-Goren H, Sharon R, Shibuya M, Halaban R, Levi BZ and Neufeld G. (1995). *J. Biol. Chem.*, **270**, 11322–11326.
- Cross DA, Alessi DR, Cohen P, Andjelkovich M and Hemmings BA. (1995). *Nature*, **378**, 785–789.
- Cunningham SA, Waxham MN, Arrate PM and Brock TA. (1995). *J. Biol. Chem.*, **270**, 20254–20257.
- de Jong JS, van Diest PJ, van der Valk P and Baak JP. (1998a). *J. Pathol.*, **184**, 44–52.
- de Jong JS, van Diest PJ, van der Valk P and Baak JP. (1998b). *J. Pathol.*, **184**, 53–57.
- Derman MP, Chen JY, Spokes KC, Songyang Z and Cantley LG. (1996). *J. Biol. Chem.*, **271**, 4251–4255.
- Dougher AM, Wasserstrom H, Torley L, Shridaran L, Westdock P, Hileman RE, Fromm JR, Anderberg R, Lyman S, Linhardt RJ, Kaplan J and Terman BI. (1997). *Growth Factors*, **14**, 257–268.
- Dougher-Vermazen M, Hulmes JD, Bohlen P and Terman BI. (1994). *Biochem. Biophys. Res. Commun.*, **205**, 728–738.
- Downward J. (1998). *Science*, **279**, 673–674.
- Dudley DT, Pang L, Decker SJ, Bridges AJ and Saltiel AR. (1995). *Proc. Natl. Acad. Sci. USA*, **92**, 7686–7689.
- Folkman J and Klagsbrun M. (1987). *Science*, **235**, 442–447.
- Fujikawa K, de Aros Scherpenseel I, Jain SK, Presman E, Christensen RA and Varticovski L. (1999). *Exp. Cell Res.*, **253**, 663–672.
- Gengrinovitch S, Berman B, David G, Witte L, Neufeld G and Ron D. (1999). *J. Biol. Chem.*, **274**, 10816–10822.
- Gerber HP, McMurtrey A, Kowalski J, Yan M, Keyt BA, Dixit V and Ferrara N. (1998). *J. Biol. Chem.*, **273**, 30336–30343.
- Gitay-Goren H, Soker S, Vlodavsky I and Neufeld G. (1992). *J. Biol. Chem.*, **267**, 6093–6098.
- Gospodarowicz D, Abraham JA and Schilling J. (1989). *Proc. Natl. Acad. Sci. USA*, **86**, 7311–7315.
- Gospodarowicz D and Cheng J. (1986). *J. Cell. Physiol.*, **128**, 475–484.
- Grinnell F and Feld MK. (1979). *Cell*, **17**, 117–129.
- Guo D, Jia Q, Song HY, Warren RS and Donner DB. (1995). *J. Biol. Chem.*, **270**, 6729–6733.
- Halper J. (1990). *Exp. Cell Res.*, **187**, 324–327.
- Han J, Ohno N, Pasco S, Monboisse JC, Borel JP and Kefalides NA. (1997). *J. Biol. Chem.*, **272**, 20395–20401.
- Hicks K, Friedman B and Rosner MR. (1989). *Biochem. Biophys. Res. Commun.*, **164**, 1323–1330.
- Houck KA, Ferrara N, Winer J, Cachianes G, Li B and Leung DW. (1991). *Mol. Endocrinol.*, **5**, 1806–1814.
- Jeanny JC, Fayein N, Moenner M, Chevallier B, Barritault D and Courtois Y. (1987). *Exp. Cell Res.*, **171**, 63–75.
- Joukov V, Pajusola K, Kaipainen A, Chilov D, Lahtinen I, Kukk E, Saksela O, Kalkkinen N and Alitalo K. (1996). *EMBO J.*, **15**, 290–298.
- Klagsbrun M and D'Amore PA. (1996). *Cytokine Growth Factor Rev.*, **7**, 259–270.
- Kodali S, Burkley M, Nag K, Taylor RC and Moudgil VK. (1994). *Biochem. Biophys. Res. Commun.*, **202**, 1413–1419.
- Laemmli UK. (1970). *Nature*, **227**, 680–685.
- Livnat DL, Brabec RK, Kurachi K, Allen DL, Wu Y, Haaseth R, Andrews P, Ethier SP and Markwart S. (2000). *J. Clin. Invest.*, **105**, 1537–1545.
- Lupu R, Cardillo M, Harris L, Hijazi M and Rosenberg K. (1995). *Semin. Cancer Biol.*, **6**, 135–145.
- Malarkey K, Belham CM, Paul A, Graham A, McLees A, Scott PH and Plevin R. (1995). *Biochem. J.*, **309**, 361–375.
- Miralem T, Wang A, Whiteside CI and Templeton DM. (1996a). *J. Biol. Chem.*, **271**, 17100–17106.
- Miralem T, Whiteside CI and Templeton DM. (1996b). *Am. J. Physiol.*, **270**, F960–F970.
- Normanno N, Ciardiello F, Brandt R and Salomon DS. (1994). *Breast Cancer Res. Treat.*, **29**, 11–27.
- Ormerod EJ, Warburton MJ, Gusterson B, Hughes CM and Rudland PS. (1985). *Histochem. J.*, **17**, 1155–1166.
- Paoletta G, Henchcliffe C, Sebastio G and Baralle FE. (1988). *Nucleic Acids Res.*, **16**, 3545–3557.
- Park JE, Keller GA and Ferrara N. (1993). *Mol. Biol. Cell*, **4**, 1317–1326.
- Pepper MS, Ferrara N, Orci L and Montesano R. (1992). *Biochem. Biophys. Res. Commun.*, **189**, 824–831.
- Plouet J, Schilling J and Gospodarowicz D. (1989). *EMBO J.*, **8**, 3801–3806.
- Price PJ, Miralem T, Jiang S, Steinberg R and Avraham H. (2001). *Cell Growth Diff.*, **12**, 129–135.
- Radisavljevic Z, Avraham H and Avraham S. (2000). *J. Biol. Chem.*, **275**, 20770–20774.
- Rapraeger AC, Krufka A and Olwin BB. (1991). *Science*, **252**, 1705–1708.

- Ruoslahti E. (1991). *J. Clin. Invest.*, **87**, 1–5.
- Ruoslahti E, Hayman EG, Engvall E, Cothran WC and Butler WT. (1981). *J. Biol. Chem.*, **256**, 7277–7281.
- Saoncella S, Echtermeyer F, Denhez F, Nowlen JK, Mosher DF, Robinson SD, Hynes RO and Goetinck PF. (1999). *Proc. Natl. Acad. Sci. USA*, **96**, 2805–2810.
- Sasisekharan R, Moses MA, Nugent MA, Cooney CL and Langer R. (1994). *Proc. Natl. Acad. Sci. USA*, **91**, 1524–1528.
- Sawano A, Takahashi T, Yamaguchi S, Aonuma M and Shibuya M. (1996). *Cell Growth Diff.*, **7**, 213–221.
- Sepp-Lorenzino L, Eberhard I, Ma Z, Cho C, Serve H, Liu F, Rosen N and Lupu R. (1996). *Oncogene*, **12**, 1679–1687.
- Shahan TA, Ohno N, Pasco S, Borel JP, Monboisse JC and Kefalides NA. (1999a). *Connect Tissue Res.*, **40**, 221–232.
- Shahan TA, Ziaie Z, Pasco S, Fawzi A, Bellon G, Monboisse JC and Kefalides NA. (1999b). *Cancer Res.*, **59**, 4584–4590.
- Shibuya M, Ito N and Claesson-Welsh L. (1999). In: *Current Topics in Microbiology and Immunology*. Claesson-Welsh L (ed). Springer: Berlin, New York, p. 237.
- Soker S, Fidler H, Neufeld G and Klagsbrun M. (1996). *J. Biol. Chem.*, **271**, 5761–5767.
- Soldi R, Mitola S, Strasly M, Defilippi P, Tarone G and Bussolino F. (1999). *EMBO J.*, **18**, 882–892.
- Speirs V and Atkin SL. (1999). *Br. J. Cancer*, **80**, 898–903.
- Sternlicht MD, Bissell MJ and Werb Z. (2000). *Oncogene*, **19**, 1102–1113.
- Taga T, Hibi M, Hirata Y, Yamasaki K, Yasukawa K, Matsuda T, Hirano T and Kishimoto T. (1989). *Cell*, **58**, 573–581.
- Templeton DM. (1992). *Crit. Rev. Clin. Lab. Sci.*, **29**, 141–184.
- Terman B, Khandke L, Dougher-Vermazan M, Maglione D, Lassam NJ, Gospodarowicz D, Persico MG, Bohlen P and Eisinger M. (1994). *Growth Factors*, **11**, 187–195.
- Thakker GD, Hajjar DP, Muller WA and Rosengart TK. (1999). *J. Biol. Chem.*, **274**, 10002–10007.
- Tischer E, Gospodarowicz D, Mitchell R, Silva M, Schilling J, Lau K, Crisp T, Fiddes JC and Abraham JA. (1989). *Biochem. Biophys. Res. Commun.*, **165**, 1198–1206.
- Traverse S, Gomez N, Paterson H, Marshall C and Cohen P. (1992). *Biochem. J.*, **288**, 351–355.
- Treisman R. (1992). *Trends. Biochem. Sci.*, **17**, 423–426.
- Treisman R. (1994). *Curr. Opin. Genet. Dev.*, **4**, 96–101.
- Vlahos CJ, Matter WF, Hui KY and Brown RF. (1994). *J. Biol. Chem.*, **269**, 5241–5248.
- Woods A, McCarthy JB, Furcht LT and Couchman JR. (1993). *Mol. Biol. Cell.*, **4**, 605–613.
- Yayon A, Klagsbrun M, Esko JD, Leder P and Ornitz DM. (1991). *Cell*, **64**, 841–848.
- Yoshiji H, Gomez DE, Shibuya M and Thorgeirsson UP. (1996). *Cancer Res.*, **56**, 2013–2016.
- Yu Y and Sato JD. (1999). *J. Cell. Physiol.*, **178**, 235–246.

Vascular Endothelial Growth Factor Modulates Neutrophil Transendothelial Migration via Up-regulation of Interleukin-8 in Human Brain Microvascular Endothelial Cells*

Received for publication, August 1, 2001, and in revised form, December 6, 2001
Published, JBC Papers in Press, January 9, 2002, DOI 10.1074/jbc.M107348200

Tae-Hee Lee[‡], Hava Avraham^{‡§}, Seung-Hoon Lee[¶], and Shalom Avraham^{‡||}

From the [‡]Division of Experimental Medicine, Beth Israel Deaconess Medical Center and Harvard Medical School, Boston, Massachusetts 02115 and the [¶]Neurooncology Clinic, National Cancer Center, Kyonggi, 411-351, Korea

Hypoxia, a strong inducer for vascular endothelial growth factor (VEGF)/vascular permeable factor (VPF) expression, regulates leukocyte infiltration through the up-regulation of adhesion molecules and chemokine release. To determine whether VEGF/VPF is directly involved in chemokine secretion, we analyzed its effects on chemokine expression in human brain microvascular endothelial cells (HBMECs) by using a human cytokine cDNA array kit. Cytokine array analysis revealed a significant increase in expression of monocyte chemoattractant protein-1 and the chemokine receptor CXCR4 in HBMECs, a result similar to that described previously in other endothelial cells. Interestingly, we also observed that VEGF/VPF induced interleukin-8 (IL-8) expression in HBMECs and that IL-8 mRNA was maximal after 1 h of VEGF/VPF treatment of the cells. Enzyme-linked immunosorbent assay data and immunoprecipitation analysis revealed that although VEGF/VPF induced IL-8 expression at the translational level in HBMECs, basic fibroblast growth factor failed to induce this protein expression within 12 h. VEGF/VPF increased IL-8 production in HBMECs through activation of nuclear factor- κ B via calcium and phosphatidylinositol 3-kinase pathways, whereas the ERK pathway was not involved in this process. Supernatants of the VEGF/VPF-treated HBMECs significantly increased neutrophil migration across the HBMEC monolayer compared with those of the untreated control. Furthermore, addition of anti-IL-8 antibody blocked this increased migration, indicating that VEGF/VPF induced the functional expression of IL-8 protein in HBMECs. Taken together, these data demonstrate for the first time that VEGF/VPF induces IL-8 expression in HBMECs and contributes to leukocyte infiltration through the expression of chemokines, such as IL-8, in endothelial cells.

Brain edema is a major life-threatening complication in a variety of brain injuries, including those caused by stroke and tumors. The common form of brain edema is defined by the disruption of the blood-brain barrier (BBB) (1). The BBB, which constitutes the endothelium and its surrounding cells, is an anatomic structure that is defined mainly by tight junctions between the brain endothelial cells. These junctions strictly regulate the flow of ions, nutrients, and cells into the brain.

Hypoxia is believed to be a precondition for edema development in the brain and mediates leukocyte infiltration through the up-regulation of adhesion molecules and chemokine release (2, 3). Hypoxia has been shown to contribute to the leakage of the BBB by inducing increases in vascular permeability (4, 5). Hypoxia is a strong inducer of vascular endothelial growth factor (VEGF), also known as vascular permeability factor (VPF) (6, 7).

VEGF/VPF has shown potent vascular permeable activity (8, 9) and significant mitotic activity specific to vascular endothelial cells (10). VEGF/VPF induces signaling mediated by its receptors, the Flt-1 and Flk-1/KDR tyrosine kinases, whose expressions are restricted almost exclusively to endothelial cells (11). Expression of VEGF/VPF has been identified in cells correlated with brain inflammation, including microglial cells and reactive astrocytes, suggesting its central role in inflammation of the central nervous system (12, 13). For example, enhanced expression of VEGF/VPF and its receptors was shown to be induced in the rat brain after focal cerebral ischemia (14–16) and to mediate brain injuries through leakage of the BBB in the ischemic brain (17). However, edema formation and brain damage after ischemia or stroke were reduced significantly by antagonism of VEGF/VPF or by inhibition of its signaling pathway (18, 19), indicating that VEGF/VPF is a key mediator in the pathogenesis of these disorders.

VEGF/VPF induces expression of the monocyte chemoattractant protein-1 (MCP-1) in bovine retinal endothelial cells (20) and of the SDF-1 receptor CXCR4 in human umbilical vein endothelial cells (21). These reports suggest that VEGF/VPF not only mediates brain injuries through the leakage of the BBB, but also may have a relevant role in the recruitment of leukocytes through the up-regulation of chemokines. However, its role in the regulation of chemokines is not well elucidated because of the redundancy of chemokines. Chemokines are a superfamily of small, cytokine-like proteins that induce the directional migration of various hematopoietic cells through their interaction with G protein-coupled receptors (22, 23). To date, 44 chemokines and 21 chemokine receptors have been described (23).

In this study, we examined the effects of VEGF/VPF on chemokine expression in human brain microvascular endothe-

* This work was supported in part by National Institutes of Health Grants NS39558 (to S. A.), HL51456 (to H. A.), DAMD17-98-1-8032 (to H. A.), DAMD17-99-1-9078 (to H. A.), and CA76226 (to H. A.), by a Diana Michelis fellowship in breast cancer research (to T.-H. L.), Experienced Breast Cancer Grant 3480057089, and a Massachusetts Department of Public Health grant. The costs of publication of this article were defrayed in part by the payment of page charges. This article must therefore be hereby marked "advertisement" in accordance with 18 U.S.C. Section 1734 solely to indicate this fact.

This paper is dedicated to Ronald Ansini for continuing friendship and support for our research program.

§ Recipient of an established investigatorship from the American Heart Association.

|| To whom correspondence should be addressed: Division of Experimental Medicine, Beth Israel Deaconess Medical Center, Harvard Institutes of Medicine, 4 Blackfan Circle, Boston, MA 02115. Tel.: 617-667-0063; Fax: 617-975-6373; E-mail: savraham@caregroup.harvard.edu.

lial cells (HBMECs) using a human cytokine cDNA array kit containing 34 chemokines and 14 chemokine receptors. We isolated total RNA from unstimulated and VEGF/VPF-stimulated HBMECs and analyzed the gene expression of both samples by hybridizing them with the cytokine cDNA array. Our results demonstrate that VEGF/VPF significantly increased MCP-1 and CXCR4 expression in HBMECs, similar to results reported in other endothelial cell types (20, 21). Interestingly, we also found that VEGF/VPF induced interleukin-8 (IL-8) expression in HBMECs. IL-8, which belongs to the CXC chemokine family, is a potent chemoattractant for neutrophils and T lymphocytes but not monocytes (22). In this report, we have characterized IL-8 expression and secretion upon VEGF stimulation of HBMECs and determined the role of IL-8 in modulating neutrophil transendothelial migration.

Based on these observations we suggest that, in addition to its angiogenic activity and vascular permeable property, VEGF/VPF has a role as an indirect leukocyte migrating factor through the up-regulation of chemokines including MCP-1 and IL-8.

EXPERIMENTAL PROCEDURES

Materials—VEGF/VPF, bFGF, the human cytokine cDNA array kit, IL-8, IL-8 antibody, the IL-8 enzyme-linked immunosorbent assay (ELISA) kit, quantitative IL-8 mRNA kits, and the SDF-1 α ELISA kit were purchased from R&D Systems (Minneapolis). TMB-8, PD98059, LY294002, chelerythrine chloride, cycloheximide, L-NAME, and SU-1498 were purchased from Calbiochem. Fibronectin was purchased from Roche Molecular Biochemicals. Von Willebrand factor was purchased from Dako (Carpinteria, CA). Matrigel and PDTC were purchased from Sigma. Acetylated low density lipoprotein (AcLDL) was purchased from Biomedical Technologies, Inc. (Stoughton, MA).

Cell Culture—HBMECs were purchased from Cell Systems, Inc. (Kirkland, WA). The cells were seeded onto attachment factor-coated culture plates and maintained in CSC-complete medium according to the protocol of the manufacturer.

Cytokine cDNA Array—HBMECs were grown subconfluently onto attachment factor-coated 100-mm dishes. The cells were starved in 0.5% FBS containing serum-free CSC medium for 4 h and then stimulated with 30 ng/ml VEGF for 5 h. Total RNA preparation and hybridization procedures were performed according to the manufacturer's protocol. Briefly, equal amounts (2 μ g) of total RNA from unstimulated or VEGF-stimulated HBMECs were used for the cytokine cDNA array analysis, with a commercially available membrane (R&D Systems). The membranes were prehybridized at 68 °C for 2 h in a hybrid solution (R&D Systems) containing 100 μ g/ml freshly boiled salmon sperm DNA, after which the cDNA probes were hybridized onto the membranes at 68 °C for 18 h. The membranes were washed three times in low stringency washing buffer (2 \times SSC and 1% SDS) and three times in high stringency washing buffer (0.1 \times SSC and 0.5% SDS) at 68 °C for 20 min each. The membranes were exposed on a PhosphorImager (Molecular Dynamics, Sunnyvale, CA) and analyzed using ArrayVision[®] software (Imaging Research Inc., Ontario, Canada).

Measurement of IL-8 mRNA—The amount of IL-8 mRNA was measured using quantitative IL-8 mRNA kits as directed by the manufacturer. Briefly, HBMECs were grown subconfluently in CSC-complete medium in gelatin-coated 60-mm dishes. The medium was replaced by serum-free CSC medium containing 0.5% FBS, and the cells were starved for 4 h. After incubation with VEGF/VPF for the indicated times, total RNA was isolated, and equal amounts (2 μ g) were evaluated for IL-8 content using quantitative IL-8 mRNA kits.

Measurement of IL-8 or SDF-1 α by ELISA—Chemokine release was quantitated by ELISA as directed by the manufacturer. Briefly, HBMECs were grown subconfluently in CSC-complete medium in gelatin-coated 24-well plates. The medium was replaced by serum-free CSC medium containing 0.5% FBS, and the cells were starved for 4 h. Synthetic inhibitors were added to the cells for 1 h before the assay was initiated. After incubation for the indicated times, the culture supernatant was removed and evaluated for IL-8 content using the ELISA kit.

Immunoprecipitation and Western Blot Analysis of IL-8—HBMECs were grown subconfluently onto attachment factor-coated 100-mm dishes. The cells were starved in 5 ml of 0.5% FBS containing serum-free CSC medium for 4 h and then stimulated with 30 ng/ml VEGF or 30 ng/ml bFGF for 12 h. After incubation, 5 ml of supernatant from

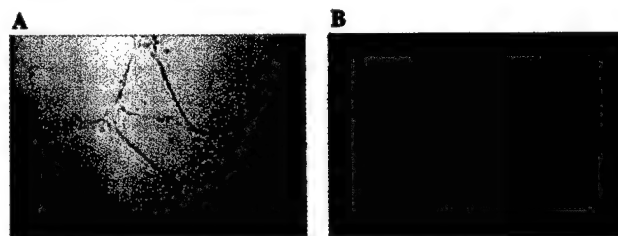


Fig. 1. Characterization of HBMECs. 50,000 HBMECs were cultured onto 24-well plates coated with 150 μ l of Matrigel for 12 h, and then 50 μ g of AcLDL was added to the wells. After 2 h, the cells were washed and fixed by 3.7% formaldehyde. Tubular-like networks (panel A) and AcLDL uptake (panel B) were observed under an inverted fluorescent microscope equipped with a light ramp.

HBMECs was harvested and incubated with 5 μ g of human IL-8-specific goat IgG at 4 °C. After overnight incubation, protein G-Sepharose at 1:100 was added to the reaction mixture and incubated for 6 h. The immune complexes were precipitated with the Sepharose beads, washed, and resuspended in SDS-PAGE sample buffer with reducing agent. The samples were separated by 15% SDS-PAGE and transferred onto nitrocellulose membrane (Millipore, Boston, MA). The membranes were blocked with 5% nonfat dried milk in phosphate-buffered saline and subsequently incubated with goat anti-human IL-8 antibody for 2 h at room temperature. Bound antibodies were detected by horseradish peroxidase-conjugated anti-goat IgG and enhanced chemiluminescence (Amersham Biosciences, Inc.).

Adenoviral Infection of HBMECs—An adenoviral construct encoding a constitutively active form of Akt (Ad-myrAkt) was constructed as described previously (24). HBMECs were grown subconfluently in CSC-complete medium in gelatin-coated six-well plates. The medium was replaced by serum-free CSC medium containing 0.5% FBS, and the cells were starved for 4 h. HBMECs were infected with Ad-myrAkt at a multiplicity of infection of 100. A synthetic inhibitor of nuclear factor- κ B (NF- κ B), PDTC (20 μ M), was added to the cells for 1 h before infection. After incubation for 24 h, the culture supernatant was removed and evaluated for IL-8 content using the ELISA kit. Alternatively, the cells were lysed, and 50 μ g of total protein was resolved by 12% SDS-PAGE and subjected to Western blot analysis by using rabbit anti-human phospho-Akt antibody (New England Biolabs, Beverly, MA). To verify the amount of loaded proteins, blots were reprobed with rabbit anti-human C-terminal SRC kinase antibody.

Isolation of Neutrophils—Human neutrophils were purified from normal donors by dextran sedimentation and Ficoll gradient centrifugation followed by hypotonic lysis of erythrocytes (25). Neutrophils were then resuspended in serum-free CSC medium containing 0.5% FBS. The purity of neutrophils prepared in this way was >95% as judged by the morphology of stained cytocentrifuged preparations, and the viability was >98% as judged by trypan blue exclusion.

Transendothelial Migration Assay—HBMECs were grown confluent onto gelatin-coated 100-mm dishes. The cells were starved in 5 ml of 0.5% FBS containing serum-free CSC medium for 4 h and then stimulated with 30 ng/ml VEGF for 12 h. After incubation, 5 ml of supernatant from HBMECs was harvested and stored frozen at -20 °C before use. Transendothelial migration of neutrophils was performed using Transculture chambers with pore size of 3 μ m (Costar Corp., Corning, NY). Approximately 100,000 HBMECs were added to fibronectin-coated 24-well Transculture chambers and grown for 4 days in 5% CO₂ at 37 °C. The medium was replaced every day with fresh medium. 0.6 ml of medium from untreated or VEGF/VPF-treated HBMECs was added to the lower compartment. Media that were not exposed to cells were used as the control. 20 μ g/ml human IL-8-specific goat antibody or 20 μ g/ml normal goat antibody was added to the VEGF/VPF-treated supernatant for 1 h before the assay was initiated, as indicated. In the upper compartment, 1 \times 10⁶ neutrophils in 0.1 ml of 0.5% FBS containing serum-free CSC medium were added onto the HBMEC monolayer. The chambers were incubated for 2 h at 37 °C in 5% CO₂. The cells in the lower compartments were counted on a hemocytometer. The results are presented as the means \pm S.D. of three separate experiments and are expressed as the increase in the number of cells migrating toward the lower compartment.

RESULTS

Characterization of HBMECs—The HBMECs formed tubular-like networks on Matrigel (Fig. 1A) and had the ability to

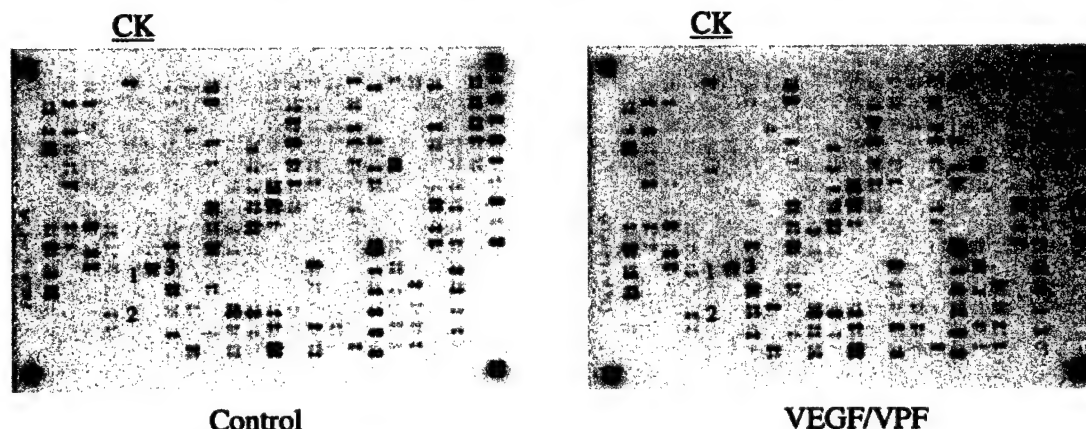


FIG. 2. Cytokine cDNA array of HBMECs. HBMECs were grown subconfluently onto attachment factor-coated 100-mm dishes. The cells were starved in 0.5% FBS containing serum-free CSC medium for 4 h and then stimulated with 30 ng/ml VEGF for 5 h. Total RNA preparation and hybridization were performed as described under "Experimental Procedures." The hybridized membranes were exposed on a PhosphorImager and analyzed by using ArrayVision[®] software. CK indicates the region containing cDNA spots corresponding to the chemokines and their receptors. The numbers indicate spots that were increased significantly in the VEGF/VPF-treated HBMECs. 1, IL-8; 2, MCP-1; 3, CXCR4.

uptake AcLDL (Fig. 1B), indicating that these cells maintained the general properties of endothelial cells. The cells also produced von Willebrand factor (data not shown), an endothelium-specific marker. During the course of the experiment, the cells were used until passages 4 to 10 and checked repeatedly for expression of von Willebrand factor.

VEGF/VPF Predominantly Up-regulates IL-8, MCP-1, and CXCR4 mRNA Expression.—To examine whether VEGF/VPF induces chemokines or their receptors in HBMECs, we used a cytokine cDNA array containing 34 chemokines and 14 chemokine receptors. We isolated total RNA from unstimulated and VEGF/VPF-stimulated HBMECs (5-h stimulation). The cytokine cDNA membranes were hybridized and exposed on a PhosphorImager and then analyzed using ArrayVision[®] software. The results showed that VEGF/VPF predominantly up-regulated IL-8, MCP-1, and CXCR4 mRNA expression in HBMECs (Fig. 2 and Table I). Our data are consistent with previous studies showing that VEGF/VPF induces expression of MCP-1 and CXCR4 in other endothelial cells (20, 21). Interestingly, we also found that VEGF/VPF significantly increased IL-8 mRNA expression in HBMECs (Fig. 2 and Table I). To determine further whether VEGF/VPF regulates IL-8 expression at the mRNA level, HBMECs were exposed to VEGF/VPF for various times, and the amount of IL-8 mRNA was determined by using a quantitative IL-8 mRNA kit. The results showed that VEGF/VPF induced IL-8 mRNA expression. This expression reached a maximal level of transcription at 1 h (13-fold increase compared with control) and decreased to control levels at 12 h (Fig. 3). These data indicate that VEGF/VPF induced expression of IL-8 mRNA in a rapid and transient manner.

VEGF/VPF but Not bFGF Induces Rapid Secretion of IL-8 Protein in HBMECs.—Next, to determine whether IL-8 expression was regulated at the protein level, the supernatants of VEGF/VPF-treated HBMECs were collected and analyzed for IL-8 secretion by ELISA. When HBMECs were exposed to different concentrations (1, 10, 30, 100 ng/ml) of VEGF/VPF for 24 h, increased IL-8 production with a maximal level of translation at 30 ng/ml was observed (data not shown). At this concentration, VEGF/VPF increased IL-8 production by as early as 3 h, and this increase was sustained for up to 32 h (Fig. 4). We also determined whether the leukocyte chemoattractant SDF-1 α was induced by VEGF/VPF. When the supernatants of the 30 ng/ml VEGF/VPF-treated HBMECs were tested by specific SDF-1 α ELISA, we observed no increase in SDF-1 α protein in these supernatants compared with the untreated con-

trol (data not shown). These results are in agreement with the results of the cytokine cDNA array shown in Fig. 2 and Table I.

In addition, we examined whether bFGF, known as a potent mitogen to endothelial cells, increased IL-8 or SDF-1 α production in HBMECs. Within 12 h of 30 ng/ml bFGF treatment, we observed no increase in IL-8 protein in the samples compared with the untreated controls. However, after 12 h of bFGF treatment, the amount of IL-8 in the samples was greater than that in the untreated controls, although it was much smaller than in the VEGF/VPF-treated samples (Fig. 4). On the other hand, we observed no increase in SDF-1 α protein in the supernatants of the bFGF-treated HBMECs compared with the untreated control (data not shown).

To confirm the molecular characterization of the VEGF/VPF-induced IL-8 protein expression, we performed immunoprecipitation and Western blot analysis. For these studies, supernatants from untreated, VEGF/VPF-, or bFGF-treated HBMECs were incubated with goat anti-human IL-8 antibody, and the immune complexes precipitated with protein G-Sepharose were then analyzed by Western blotting. As seen in Fig. 5, a significant increase in the band corresponding to a molecular mass of ~8 kDa was detected in the VEGF/VPF-treated conditioned medium. This VEGF/VPF-induced band migrated to a position similar to that of the human recombinant IL-8. These results support the molecular identity of the VEGF/VPF-induced IL-8 as being comparable with that of the recombinant IL-8. Therefore, VEGF/VPF stimulated the secretion of IL-8 protein in HBMECs.

Cycloheximide and SU-1498 Inhibit VEGF/VPF-induced IL-8 Production in HBMECs.—To confirm further that VEGF/VPF up-regulated IL-8 expression via new protein synthesis in HBMECs, the protein synthesis inhibitor cycloheximide was used to treat HBMECs for 12 h, and VEGF/VPF-induced IL-8 production was then evaluated by ELISA. As shown in Fig. 6, 10 μ M cycloheximide was enough to block VEGF/VPF-induced IL-8 production in HBMECs potentially. In addition, VEGF/VPF-induced IL-8 production was also inhibited significantly by 10 μ M SU-1498, an inhibitor of its receptor Flk-1/KDR (Fig. 6). These data demonstrate that VEGF/VPF increased IL-8 production at the translational level through its receptor in HBMECs.

NF- κ B Mediates VEGF/VPF-induced IL-8 Production in HBMECs.—VEGF/VPF has been shown to stimulate several molecules mediating intracellular signals, including mitogen-activated protein/extracellular signal-regulated kinase (ERK)

TABLE I
Expression of chemokines and their receptors in
VEGF/VPF-treated HBMECs

The cytokine cDNA membranes were hybridized with total RNA isolated from unstimulated and VEGF/VPF-stimulated HBMECs. The membranes were exposed on a PhosphorImager and analyzed using ArrayVision™ software. Bold lettering indicates expression (in untreated or VEGF/VPF-treated HBMECs) of chemokines and their receptors that have sVOL values over 2 and that are visualized as spots on the scanned images, as shown in Fig. 2. Asterisks indicate chemokine or chemokine receptor expression that is increased significantly in the VEGF/VPF-treated HBMECs. sVOL is the subtracted volume value derived by subtracting the background volume value from the volume value of the spot. Genomic DNAs represent the positive controls for the hybridizations. The results are presented as the means of two spots.

Chemokines and chemokine receptors	Control sVOL	VEGF sVOL	VEGF/control ratio (VOL)
Midkine	22.56	27.30	1.21
MIG	-0.12	0.82	-6.83
MIP-1 α	-0.32	0.58	-1.80
MIP-1 β	-0.12	0.98	-8.13
MIP-3 α	0.60	0.22	0.36
MIP-3 β	0.60	0.18	0.29
6Ckine	0.84	1.14	1.35
MIPF-1	2.00	1.34	0.67
BLC/BCA-1	0.60	0.46	0.76
PARC	0.68	0.86	1.26
IP-10	0.32	-0.82	-2.58
RANTES	0.40	0.30	0.74
ENA-78	0.36	1.30	3.60
SDF-1	3.12	3.66	1.17
Eotaxin	0.40	0.50	1.24
TARC	1.32	0.34	0.25
Eotaxin-2	1.08	0.86	0.79
TECK	0.60	-0.50	-0.84
Decorin	0.68	0.50	0.73
Fractalkine	1.24	-0.06	-0.05
GRO- α	1.12	0.22	0.19
GRO-β	2.52	0.90	0.36
GRO-γ	2.96	2.30	0.78
HCC-1	2.20	2.42	1.10
HCC-4	0.96	1.34	1.39
I-309	0.88	1.98	2.25

Chemokines and chemokine receptors	Control sVOL	VEGF sVOL	VEGF/control ratio (VOL)
IL-8*	1.20	4.74	3.95
LDGF	1.32	0.06	0.04
Lymphotactin	0.44	1.18	2.67
MCP-1*	4.72	8.54	1.81
MCP-2	2.96	1.86	0.63
MCP-3	1.04	0.46	0.44
MCP-4	0.08	-0.78	-9.80
MDC	0.12	-0.34	-2.87
CCR-1	1.68	-0.06	-0.04
CCR-2A	1.48	0.38	0.25
CCR-2B	-0.16	-0.38	2.40
CCR-3	1.64	0.38	0.23
CCR-4	1.32	-0.42	-0.32
CCR-5	1.16	0.58	0.50
CCR-6	-0.56	0.34	-0.60
CCR-7	1.72	0.10	0.06
CCR-9	1.36	0.46	0.34
CX3CR-1	1.99	0.30	0.15
CXCR-1	0.88	0.86	0.97
CXCR-2	2.60	1.54	0.59
CXCR-4*	25.44	36.78	1.45
CXCR-5	4.76	4.50	0.94
Genomic DNA	224.16	213.10	0.95
Genomic DNA	217.36	227.34	1.05
Genomic DNA	225.72	207.10	0.92
Genomic DNA	223.92	228.74	1.02

kinase (MEK), phosphatidylinositol 3-kinase (PI3-kinase), protein kinase C, and calcium in endothelial cells (26, 27). Because there are multiple VEGF/VPF signaling pathways, we examined which of these pathways were responsible for the increased IL-8 production in HBMECs. As shown in Fig. 7A, the intracellular calcium chelator TMB-8 (10 μ M) and PI3-kinase inhibitor

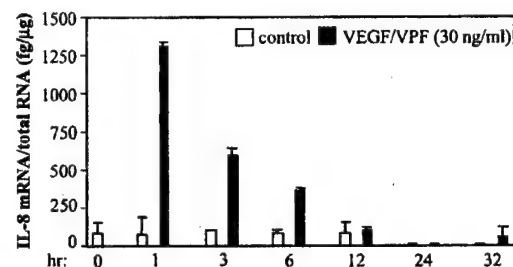


FIG. 3. Induction of IL-8 mRNA by VEGF/VPF in HBMECs. The amount of IL-8 mRNA was measured as described under "Experimental Procedures." Briefly, HBMECs were grown subconfluently in CSC-complete medium in gelatin-coated 60-mm dishes. The medium was replaced by serum-free CSC medium containing 0.5% FBS, and the cells were starved for 4 h. After incubation with VEGF/VPF for the indicated times, total RNA was isolated, and equal amounts (2 μ g) of total RNA were evaluated for IL-8 content using a quantitative IL-8 mRNA kit. One attomole of human IL-8 was considered to be 524 fg according to the protocol of the manufacturer. The results are presented as the means \pm S.D. of triplicate samples.

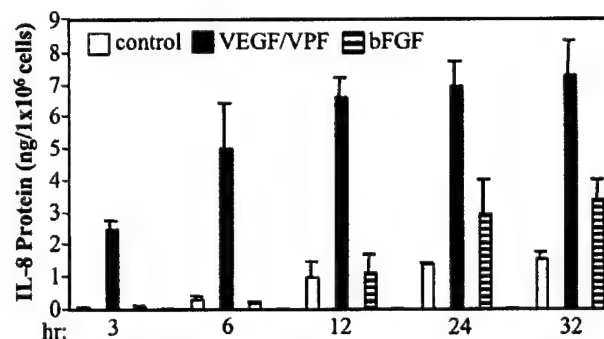


FIG. 4. VEGF/VPF but not bFGF induces rapid secretion of IL-8 protein in HBMECs. HBMECs were grown subconfluently in CSC-complete medium in gelatin-coated 24-well plates. The medium was replaced by serum-free CSC medium containing 0.5% FBS, and the cells were starved for 4 h. After incubation with VEGF/VPF or bFGF for the indicated times, the culture supernatants were removed and evaluated for IL-8 secretion using the ELISA kit. The results are presented as the means \pm S.D. of duplicate samples and are representative of three individual studies.

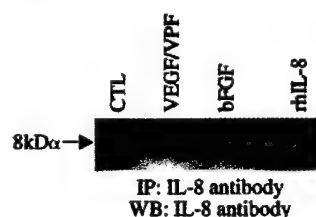


FIG. 5. Immunoprecipitation and Western blot analysis of VEGF/VPF-induced IL-8 expression in HBMECs. HBMECs were grown subconfluently onto attachment factor-coated 100-mm dishes. The cells were starved in 5 ml of 0.5% FBS containing serum-free CSC medium for 4 h and then stimulated with 30 ng/ml VEGF or 30 ng/ml bFGF for 12 h. After incubation, 5 ml of supernatant from the HBMECs was immunoprecipitated with anti-IL-8 antibody and applied to SDS-PAGE. CTL, control; rhIL-8, recombinant human IL-8 (20 ng); IP, immunoprecipitation; WB, Western blotting.

LY294002 (10 μ M) significantly blocked IL-8 production stimulated by VEGF/VPF, whereas the protein kinase C inhibitor chelerythrine chloride (2 μ M) and nitric oxide synthase inhibitor L-NAME (1 mM) moderately inhibited its production. However, the MEK inhibitor PD98059 (10 μ M) had no effect on IL-8 production in HBMECs stimulated by VEGF/VPF.

Next, we investigated the effect of PDTC, the inhibitor of NF- κ B, on VEGF/VPF-induced IL-8 production in HBMECs. The transcriptional factor NF- κ B has been shown to mediate

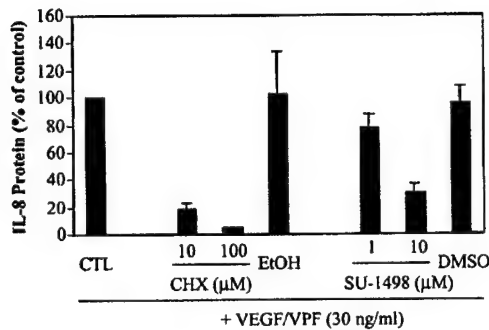


FIG. 6. Cycloheximide and SU-1498 inhibit VEGF/VPF-induced IL-8 production in HBMECs. HBMECs were grown subconfluently in CSC-complete medium in gelatin-coated 24-well plates. The medium was replaced by serum-free CSC medium containing 0.5% FBS, and the cells were starved for 4 h. Cycloheximide and SU-1498 were added to the cells for 1 h before the assay was initiated. After incubation with VEGF/VPF for 12 h, the culture supernatants were removed and evaluated for IL-8 content using the ELISA kit. The results are presented as the means \pm S.D. of triplicate samples and are representative of two individual studies. CTL, control; CHX, cycloheximide; DMSO, dimethyl sulfoxide.

IL-8 expression in endothelial cells upon treatment with various stimuli, such as tumor necrosis factor- α (28, 29), whereas the intracellular calcium chelator TMB-8 has been shown to inhibit the activation of NF- κ B (30, 31). As expected, the NF- κ B inhibitor PDTC (20 μ M) significantly blocked IL-8 production in HBMECs stimulated by VEGF/VPF (Fig. 7A). We further examined whether the PI3-kinase pathway mediates VEGF/VPF-induced IL-8 production in HBMECs through NF- κ B activation. To test this possibility, HBMECs were infected with Ad-myrAkt, which can express constitutively active Akt proteins that act downstream of PI3-kinase in the VEGF/VPF signaling pathway (24). As shown in Fig. 7B, infected Ad-myrAkt increased the expression of IL-8 proteins in HBMECs compared with the control adenovirus. However, the NF- κ B inhibitor PDTC (20 μ M) potently inhibited Ad-myrAkt-induced IL-8 production in HBMECs (Fig. 7B). Expression of phosphorylated Akt protein was confirmed by Western blotting (Fig. 7C).

These results indicate that VEGF/VPF induces IL-8 production in HBMECs through activation of the transcriptional factor NF- κ B via PI3-kinase and calcium signaling pathways.

VEGF/VPF-induced IL-8 Production Increased the Transendothelial Migration of Human Neutrophils. IL-8 is a potent chemoattractant for neutrophils. To determine whether VEGF/VPF induced the production of functional IL-8, the supernatants were harvested from HBMECs treated with VEGF/VPF for 12 h and added to the lower compartment as described under "Experimental Procedures." VEGF/VPF-treated supernatants significantly increased neutrophil migration across an HBMEC monolayer compared with untreated samples (Fig. 8A). To test specifically the role of IL-8 in migration, 20 μ g/ml human IL-8-specific goat antibody was added to the VEGF/VPF-treated supernatants for 1 h before the assay was initiated. The results demonstrated that anti-IL-8 antibody blocked the neutrophil migration across the HBMEC monolayer which was induced by the VEGF/VPF-treated supernatant, thereby indicating that VEGF/VPF induced functional IL-8 protein in HBMECs. In addition, we examined the amount of IL-8 in these VEGF/VPF-treated supernatants using ELISA and compared its functional activity with that of human recombinant IL-8. The sample contained \sim 3 ng/ml IL-8, and the transendothelial migration of neutrophils induced by this sample was comparable with that induced by human recombinant IL-8 (Fig. 8B). Thus, the secreted IL-8 in HBMECs treated with VEGF/VPF was functionally active.

DISCUSSION

In this study, we examined the role of VEGF/VPF in chemokine expression in HBMECs. We used a cytokine cDNA array containing 34 chemokines and 14 receptors. This array is an excellent tool to identify chemokines expressed differentially in response to external stimuli. By using the cytokine cDNA array, we observed that VEGF/VPF significantly increased MCP-1 and CXCR4 expression in HBMECs similar to that described in other endothelial cells (20, 21). Interestingly, VEGF/VPF also induced IL-8 production at the transcriptional level, and IL-8 mRNA expression was induced in a rapid and transient manner (Fig. 3). Furthermore, VEGF/VPF increased IL-8 protein production by as early as 3 h, and this increase was sustained for up to 32 h (Fig. 4). In addition, the protein synthesis inhibitor cycloheximide significantly inhibited IL-8 synthesis (Fig. 6), indicating that VEGF/VPF regulates IL-8 expression.

We also examined whether bFGF induces increased IL-8 production in HBMECs. bFGF has been shown to induce neovascularization like VEGF/VPF, but it does not induce vascular permeability (32). Within 12 h of bFGF treatment, we observed no increase in IL-8 protein expression in the samples compared with the untreated controls. However, after 12 h of bFGF treatment, the amount of IL-8 protein in these samples was greater than that in the untreated controls, although it was much smaller than in the VEGF/VPF-treated samples (Fig. 4). Thus, bFGF induced IL-8 production in the later time periods compared with VEGF/VPF. However, IL-8 has been shown to be secreted rapidly in endothelial cells upon treatment with various stimuli (33, 34). Therefore, bFGF might induce IL-8 production in HBMECs via another mechanism such as up-regulation of the IL-8 inducer. Based on our data and a previous report showing that bFGF induces VEGF/VPF expression in vascular endothelial cells through autocrine and paracrine mechanisms (35), we suggest that bFGF might induce IL-8 production in HBMECs via the up-regulation of VEGF/VPF.

VEGF/VPF is involved in intracellular signaling mediated by ERK, PI3-kinase, protein kinase C, calcium, and NF- κ B in endothelial cells. We observed that the intracellular calcium chelator TMB-8, the NF- κ B inhibitor PDTC, and the PI3-kinase inhibitor LY294002 significantly blocked IL-8 production in HBMECs stimulated by VEGF/VPF. The transcriptional factor NF- κ B has been shown to induce IL-8 expression in endothelial cells upon treatment with various stimuli, such as tumor necrosis factor- α (28, 29). Also, the intracellular calcium chelator TMB-8 has been shown to inhibit the activation of NF- κ B (30, 31). Therefore, it is possible that the PI3-kinase pathway may mediate VEGF/VPF-induced IL-8 production in HBMECs through NF- κ B activation. Indeed, when HBMECs were infected with an adenovirus encoding constitutively active Akt, the increased expression of IL-8 protein in HBMECs was observed, whereas the NF- κ B inhibitor PDTC potently blocked this IL-8 protein synthesis induced by activated Akt. These data indicate that VEGF/VPF induces IL-8 synthesis in HBMECs through activation of the transcriptional factor NF- κ B via PI3-kinase and calcium signaling pathways. However, the MEK inhibitor PD98059 had no effect on IL-8 production in HBMECs stimulated by VEGF/VPF. These results also indicate that the ERK pathway did not mediate IL-8 production in HBMECs and are comparable with the results for bFGF, a potent inducer of the ERK pathway in endothelial cells (32), which failed to induce IL-8 within 12 h of treatment.

IL-8 belongs to the CXC chemokine family and is a potent chemoattractant for neutrophils and T lymphocytes, but not monocytes. In humans, it was reported that intradermal injection of IL-8 induced the perivascular infiltration of neutrophils

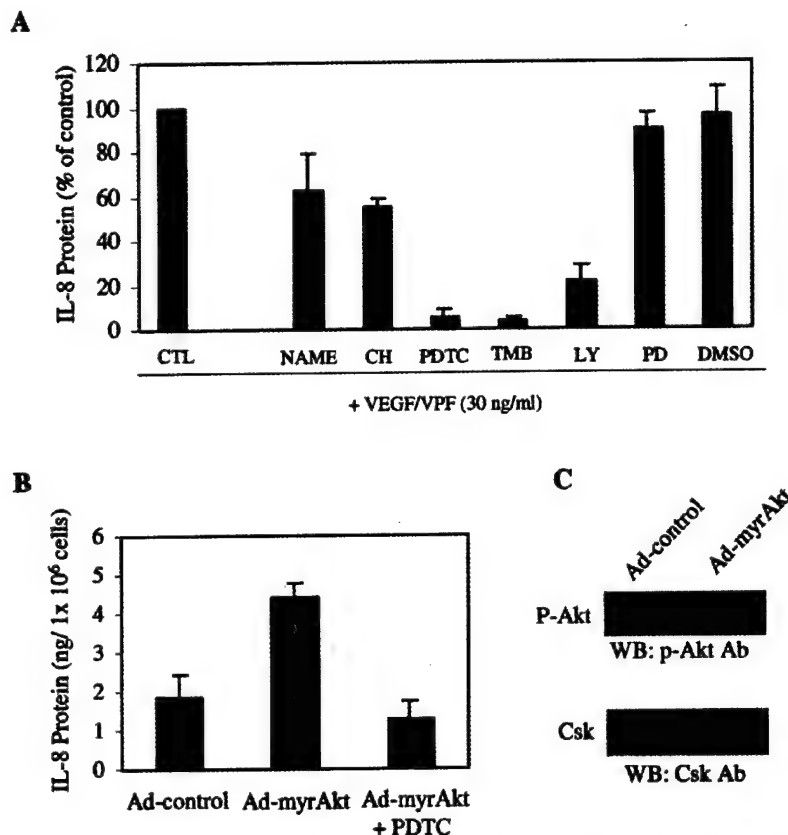


FIG. 7. VEGF/VPF increases IL-8 production in HBMECs through activation of NF- κ B. Panel A, HBMECs were grown subconfluently in CSC-complete medium in gelatin-coated 24-well plates. The medium was replaced by serum-free CSC medium containing 0.5% FBS, and the cells were starved for 4 h. Synthetic inhibitors against VEGF/VPF signal transduction were added to the cells for 1 h followed by the addition of 30 ng/ml VEGF/VPF for 12 h. The culture supernatants were collected and evaluated for IL-8 production using the ELISA kit. The results are presented as the means \pm S.D. of triplicate samples and are representative of two individual studies. CTL, control. Concentrations: L-NAME, 1 mM; chelerythrine chloride (CH), 2 μ M; PDTC, 20 μ M; TMB-8, 10 μ M; LY (LY294002), 10 μ M; PD (PD98059), 10 μ M. Panel B, HBMECs were grown subconfluently in CSC-complete medium in gelatin-coated six-well plates. The medium was replaced by serum-free CSC medium containing 0.5% FBS, and the cells were starved for 4 h. 20 μ M PDTC was added to the cells for 1 h followed by the addition of control (Ad-control) or Ad-myrAkt for 24 h. The culture supernatants were collected and evaluated for IL-8 production using the ELISA kit. The results are presented as the means \pm S.D. of duplicate samples and are representative of three individual studies. Panel C, after the culture, supernatants were collected, the cells were lysed, and 50 μ g of total protein was resolved by 12% SDS-PAGE and subjected to Western blot analysis by using rabbit anti-human phospho-Akt antibody. To verify the amount of loaded proteins, blots were reprobed with rabbit anti-human C-terminal SRC kinase (Csk) antibody. p-Akt, phosphorylated Akt.

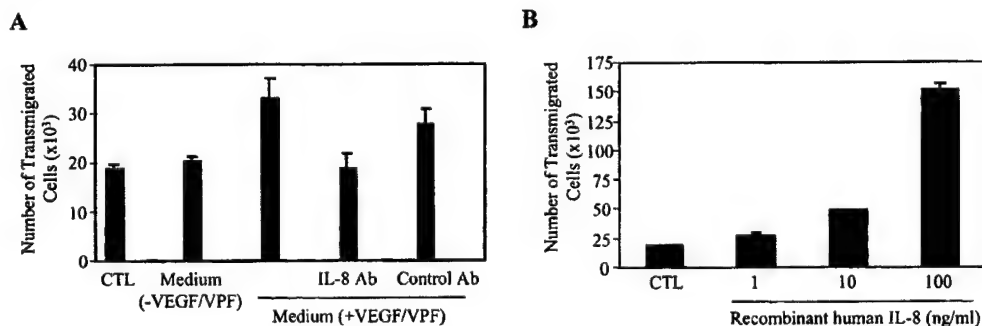


FIG. 8. VEGF/VPF-induced IL-8 production increased the transendothelial migration of human neutrophils. Panels A and B, HBMECs were grown confluent in CSC-complete medium in gelatin-coated 100-mm dishes. HBMECs were starved in 5 ml of 0.5% FBS containing serum-free CSC medium for 4 h and then stimulated with 30 ng/ml VEGF for 12 h. After incubation, 5 ml of supernatant from HBMECs was harvested, and 20 μ g/ml human IL-8-specific goat antibody or 20 μ g/ml normal goat antibody (control Ab) was added to the VEGF/VPF-treated supernatants for 1 h before the assay was initiated. 0.6 ml of the experimental supernatants was added to the lower compartment, and 1×10^6 neutrophils in 0.1 ml medium were added onto the HBMEC monolayer of the upper compartment. After 2 h, the cells in the lower compartment were counted on a hemocytometer. The results are presented as the means \pm S.D. of three separate experiments and are expressed as the increase in the number of cells migrating toward the lower compartment. CTL, control.

within 1 h, which was sustained for several hours (36). IL-8 has been shown to be produced in a variety of cell types including monocytes and endothelial cells by stimuli such as the inflam-

matory cytokines, tumor necrosis factor- α and interleukin-1 β (22, 33). In particular, activated endothelial cells are a source of a number of chemotactic molecules including IL-8. Enhanced

chemotactic molecules in the endothelium elicit the movement of leukocytes from blood into tissues, a characteristic feature of inflammation. Our data suggest that VEGF/VPF can mediate leukocyte infiltration in endothelial cells through the up-regulation of chemokines, including IL-8, because supernatants of VEGF/VPF-treated HBMECs significantly increased neutrophil migration across an HBMEC monolayer compared with the untreated control, and that anti-IL-8 antibody blocked this migration (Fig. 8A).

Hypoxia is a strong inducer of VEGF/VPF expression. Hypoxia, an important factor in the pathophysiology of vascular and inflammatory diseases, contributes to leukocyte infiltration through the up-regulation of adhesion molecules and chemokine release (2, 3). During systemic hypoxia *in vivo*, VEGF/VPF was shown to be expressed in glial cells as well as in neurons in the hippocampus and dentate gyrus (37). However, VEGF/VPF expression does not appear to be localized in endothelial cells, although marked receptor expression was noted, thus suggesting that a paracrine action is involved in this condition (37). Therefore, our data suggest that hypoxia might at least in part contribute to leukocyte infiltration through the up-regulation of VEGF/VPF, which in turn induces the secretion of chemokines such as IL-8 in endothelium through a paracrine mode.

Recently, we and others reported that VEGF/VPF up-regulated intercellular adhesion molecule-1 (ICAM-1), the receptor for neutrophil adhesion molecules CD11/CD18 (MAC-1), in rat brain microvascular endothelial cells (38) and in human umbilical vein endothelial cells (39). Taken together with these studies, we suggest that VEGF/VPF might be responsible for the accumulation of neutrophils within hypoxic areas through the simultaneous up-regulation of IL-8 and its receptor ICAM-1 in endothelium.

In conclusion, this is the first report that VEGF/VPF induces IL-8 expression in human brain microvascular endothelial cells. We therefore suggest that VEGF/VPF contributes to leukocyte infiltration through the up-regulation of chemokines in endothelial cells.

Acknowledgments—We thank Dr. Kenneth Walsh (Division of Cardiovascular Research, St. Elizabeth's Center of Boston and the Program in Cell, Molecular and Developmental Biology, Sackler School of Biomedical Studies, Tufts University School of Medicine, Boston) for providing the adenoviral construct encoding the constitutively active form of Akt and Dr. Ewa Matczak for preparing the blood samples. We also thank Dr. Tae Kim for valuable advice during this study, Janet Delahanty for editing, Daniel Kelley for preparation of the figures, and Mikyung Kim-Park for typing the manuscript.

REFERENCES

- Betz, A. L. (1997) pp. 156–159, *Vasogenic Brain Edema*, Academic Press, Orlando, FL.
- Stanimirovic, D., and Satoh, K. (2000) *Brain Pathol.* **10**, 113–126.
- Bona, E., Andersson, A. L., Blomgren, K., Gilland, E., Fuka-Sundvall, M., Gustafson, K., and Hagberg, H. (1999) *Pediatr. Res.* **45**, 500–509.
- Olesen, S. P. (1986) *Brain Res.* **368**, 24–29.
- Tanno, H., Nockels, R. P., Pitts, L. H., and Noble, L. J. (1992) *J. Neurotrauma* **9**, 335–347.
- Ikeda, E., Achen, M. G., Breier, G., and Risau, W. (1995) *J. Biol. Chem.* **270**, 19761–19766.
- Gleadle, J. M., Ebert, B. L., Firth, J. D., and Ratcliffe, P. J. (1995) *Am. J. Physiol.* **268**, C1362–C1368.
- Fischer, S., Clauss, M., Wiesnet, M., Renz, D., Schaper, W., and Karliczek, G. F. (1999) *Am. J. Physiol.* **276**, C812–C820.
- Mayhan, W. G. (1999) *Am. J. Physiol.* **276**, C1148–C1153.
- Ferrara, N., and Davis-Smyth, T. (1997) *Endocr. Rev.* **18**, 4–25.
- Plate, K. H., Beck, H., Danner, S., Allegrini, P. R., and Wiessner, C. (1999) *J. Neuropathol. Exp. Neurol.* **58**, 654–666.
- Proescholdt, M. A., Heiss, J. D., Walbridge, S., Muhlhauser, J., Capogrossi, M. C., Oldfield, E. H., and Merrill, M. J. (1999) *J. Neuropathol. Exp. Neurol.* **58**, 613–627.
- Neufeld, G., Cohen, T., Gengrinovitch, S., and Poltorak, Z. (1999) *FASEB J.* **13**, 9–22.
- Kovacs, Z., Ikezaki, K., Samoto, K., Inamura, T., and Fukui, M. (1996) *Stroke* **27**, 1865–1872.
- Hayashi, T., Abe, K., Suzuki, H., and Itoyama, Y. (1997) *Stroke* **28**, 2039–2044.
- Lennmyr, F., Ata, K. A., Funa, K., Olsson, Y., and Terent, A. (1998) *J. Neuropathol. Exp. Neurol.* **57**, 874–882.
- Zhang, Z. G., Zhang, L., Jiang, Q., Zhang, R., Davies, K., Powers, C., Bruggen, N. V., and Chopp, M. J. (2000) *J. Clin. Invest.* **106**, 829–838.
- van Bruggen, N., Thibodeaux, H., Palmer, J. T., Lee, W. P., Fu, L., Cairns, B., Tumas, D., Gerlai, R., Williams, S. P., van Lookeren Campagne, M., and Ferrara, N. (1999) *J. Clin. Invest.* **104**, 1613–1620.
- Paul, R., Zhang, Z. G., Eliceiri, B. P., Jiang, Q., Boccia, A. D., Zhang, R. L., Chopp, M., and Cheresch, D. A. (2001) *Nat. Med.* **7**, 222–227.
- Marumo, T., Schini-Kerth, V. B., and Busse, J. T. (1999) *Diabetes* **48**, 1131–1137.
- Salcedo, R., Wasserman, K., Young, H. A., Grimm, M. C., Howard, O. M., Anver, M. R., Kleinman, H. K., Murphy, W. J., and Oppenheim, J. J. (1999) *Am. J. Pathol.* **154**, 1125–1135.
- Rollins, B. J. (1997) *Blood* **90**, 909–928.
- Nelson, P. J., and Krensky, A. M. (2001) *Immunity* **14**, 377–386.
- Fujio, Y., and Walsh, K. (1999) *J. Biol. Chem.* **274**, 16349–16354.
- Taniguchi, N., and Gutteridge, J. M. (2000) pp. 40–41, *Experimental Protocols for Reactive Oxygen and Nitrogen Species*, Oxford University Press, London.
- Petrova, T. V., Makinen, T., and Alitalo, K. (1999) *Exp. Cell Res.* **263**, 117–130.
- Gerber, H. P., McMurtrey, A., Kowalski, J., Yan, M., Keyt, B. A., Dixit, V., and Ferrara, N. (1998) *J. Biol. Chem.* **273**, 30336–30343.
- Munoz, C., Pascual-Salcedo, D., Castellanos, M. C., Alfranca, A., Aragones, J., Vara, A., Redondo, M. J., and de Landazuri, M. O. (1996) *Blood* **88**, 3482–3490.
- Yoshida, S., Ono, M., Shono, T., Izumi, H., Ishibashi, T., Suzuki, H., and Kuwano, M. (1997) *Mol. Cell. Biol.* **17**, 4015–4023.
- Kurose, I., Saito, H., Miura, S., Ebinuma, H., Higuchi, H., Watanabe, N., Zeki, S., Nakamura, T., Takaishi, M., and Ishii, H. (1997) *J. Clin. Invest.* **99**, 867–878.
- Gong, G., Waris, G., Tanveer, R., and Siddiqui, A. (2001) *Proc. Natl. Acad. Sci. U. S. A.* **98**, 9599–9604.
- Friesel, R. E., and Maciag, T. (1995) *FASEB J.* **9**, 919–925.
- Strieter, R. M., Kunkel, S. L., Showell, H. J., Remick, D. G., Phan, S. H., Ward, P. A., and Marks, R. M. (1989) *Science* **243**, 1467–1469.
- Qi, J., Goralnick, S., and Kreutzer, D. L. (1997) *Blood* **90**, 3595–3602.
- Seghezzi, G., Patel, S., Ren, C. J., Gualandris, A., Pintucci, G., Robbins, E. S., Shapiro, R. L., Galloway, A. C., Rifkin, D. B., and Mignatti, P. (1998) *J. Cell Biol.* **141**, 1659–1673.
- Swenson, O., Schubert, C., Christophers, E., and Schroder, J. M. (1991) *J. Invest. Dermatol.* **96**, 682–689.
- Marti, H. H., and Risau, W. (1998) *Proc. Natl. Acad. Sci. U. S. A.* **95**, 15809–15814.
- Radisavljevic, Z., Avraham, H., and Avraham, S. (2000) *J. Biol. Chem.* **275**, 20770–20774.
- Kim, I., Moon, S. O., Kim, S. H., Kim, H. J., Koh, Y. S., and Koh, G. Y. (2001) *J. Biol. Chem.* **276**, 7614–7620.

The Invasive Phenotype in HMT-3522 Cells Requires Increased EGF Receptor Signaling Through Both PI 3-Kinase and ERK 1,2 Pathways

DANIEL J. PRICE, SHALOM AVRAHAM, JOSEPH FEUERSTEIN, YIGONG FU, and HAVA KARSENTY AVRAHAM
Division of Experimental Medicine, Beth Israel-Deaconess Medical Center, Harvard Institutes of Medicine, Boston, MA

We studied the invasion of HMT-3522 breast epithelial cells in response to epidermal growth factor (EGF), and the associated signaling pathways. HMT-3522 T4-2 cells were shown to invade Matrigel-coated Transwell membranes in response to EGF while HMT-3522 S-1 cells failed to invade when treated with EGF. Studies utilizing specific molecular inhibitors showed the importance of $\beta 1$ integrin, phosphatidylinositol 3 kinase (PI 3-kinase), p38, extracellular regulated kinase 1, 2 (Erk 1,2) MAP kinases, and metalloproteinases in invasion and motility. T4-2 cell invasion was shown to be time-dependent and also gene transcription-dependent as shown by inhibition with Actinomycin D. T4-2 cells exhibited an increased activation of MAP kinases Erk 1,2 (2-fold), EGF receptor (3-fold), and PI 3-kinase (3- to 4-fold) when compared to the S-1 cells. In response to EGF, T4-2 cells showed a 5-fold greater secretion of matrix metalloproteinase-9 (MMP-9) as compared to S-1 cells, and this increase was largely dependent on the activity of PI 3-kinase. These findings indicate that expression of the invasive phenotype in these breast epithelial cells requires increased EGF receptor signaling, involving both PI 3-kinase and Erk 1,2 activities, which leads to multiple downstream effects, including enhanced secretion of MMP-9 and transcription of invasion-related genes.

Keywords. EGF, breast cancer, PI 3-kinase, ERK 1,2, cellular invasion

INTRODUCTION

The action of epidermal growth factor (EGF) on its receptor is known to result in increased cell migration and invasiveness of a variety of cell types. Study of breast tumor cell lines such as MDA-MB-231 has shown that EGF treatment of these cells leads to increased invasiveness by a PI 3-kinase and phospholipase C (PLC)-dependent mechanism (29, 33). This phenomenon appears to be similar to the

EGF-dependent invasion that is observed in renal (39), prostate (18), pancreatic (15), and colon cancer cells (10), as well as in normal mammary epithelial cells (14). Interestingly, the action of EGF in the breast tumor cells does not appear to be related to proliferation (16, 33). As of yet, it is unclear how the increase in PI 3-kinase and PLC activities results in increased invasiveness of the breast tumor cells. In a related study, it was shown in MCF-7 breast cancer cells that heregulin (HRG) treatment

Received 17 September 2001; accepted 25 June 2002.

Address correspondence to: Hava Karsenty Avraham, Beth Israel-Deaconess Medical Center, Division of Experimental Medicine, Harvard Institutes of Medicine, 4 Blackfan Circle, Boston, MA 02115, USA; e-mail: havraham@caregroup.harvard.edu

led to increased cell migration that was mediated by PI 3-kinase and the down-stream component p21 activated kinase 1 (PAK1) (1). This action of heregulin led to actin cytoskeletal reorganization and filopodia/lamellopodia formation. Others have implicated the GTPases Rac1, Cdc42, and RhoA in the growth factor dependent PI 3-kinase mediated induction of cellular motility and invasion (5, 19).

The HMT-3522 series of breast epithelial cells was originally derived from a biopsy of a nonmalignant breast lesion (8, 9). Serial culturing led to cells that spontaneously developed tumorigenic properties (termed T4-2). These cells exhibited trisomy of chromosome 7p, mutation of p53, and amplification of the c-myc oncogene (8, 23, 25, 27). While these cells were shown to overexpress the EGF receptor, their growth in culture was independent of EGF. Another subline of these cells exhibited non tumorigenic properties (termed S-1). These cells had a normal karyotype, and their growth was EGF-dependent. Genetic studies have indicated that the T4-2 cells most likely resulted from the spontaneous mutational conversion of the S-1 cells (27, 28). Thus, these cell lines serve as a unique model for studying the effect of EGF on cellular migration and invasion. Recent studies by Weaver and colleagues (45) have shown that when the cells were grown in a three-dimensional culture, T4-2 cells formed disorganized colonies while S-1 cells formed tubule-like colonies. Treatment of the T4-2 cells with a neutralizing anti- β 1 integrin antibody led to their conversion to the organized tubule-like structure. Down-regulation of β 1 integrin by the anti- β 1 integrin antibody also appeared to result in down-regulation of the EGF receptor. Likewise, down-regulation of the EGF receptor led to the concurrent down-regulation of β 1 integrin (44). Moreover, when the EGF receptor was overexpressed in the S-1 cells, there was a similar increase in the β 1 integrin protein. This indicated that the reciprocal up-regulation of the EGF receptor and the β 1 integrin might be related to the tumorigenic phenotype that was observed in the three-dimensional cultures.

In the present study, we examined whether HMT-3522 cells might show differential abilities to migrate or invade in response to signaling through the EGF receptor. We have investigated the ability of T4-2 and S-1 cells to invade a Matrigel-coated membrane or to migrate across a plastic or Matrigel-coated plastic surface. We show the ability of the T4-2 cells to invade and migrate upon treatment with EGF, however, the S-1 cells fail to respond in this way when treated with EGF. We further show, by the use of specific inhibitors, the pathways that are likely to be critical to the motility of the T4-2 cells. We show that the increased activity of the EGF receptor in the T4-2 cells leads to increased signaling through both PI 3-kinase and MAP kinase Erk 1,2 pathways, and that multiple downstream effectors of these pathways are required for the invasive phenotype.

MATERIALS AND METHODS

Antibodies and reagents. The neutralizing anti- β 1 integrin monoclonal antibody AIIB2 was obtained from the Developmental Studies Hybridoma Bank (University of Iowa, Iowa City, IA). The anti- β 1 monoclonal antibody TS2/16 was a gift from Dr. Martin Hemler (Dana Farber Cancer Institute, Boston, MA). Anti-MMP-9 monoclonal antibody (IM09L) and MMP-9 standard were from Calbiochem (San Diego, CA). Anti-phosphotyrosine PY20 and PY99 were from Transduction Laboratories (Lexington, KY). Anti-phospho-Erk 1,2 polyclonal, anti-Erk 1,2 polyclonal, and anti-EGF receptor antibodies were from Santa Cruz Biotechnology (Santa Cruz, CA). Anti-phospho-p38, anti-p38, anti-phospho-Akt and anti-Akt polyclonal antibodies were from New England Biolabs (Beverly, MA). Anti-PAK1 polyclonal antibody (N-20) and anti- β -catenin monoclonal antibody (E-5) were from Santa Cruz Biotechnology. Another anti-PAK1 polyclonal antibody was a generous gift of Dr. Gary Bokoch (Salk Institute, La Jolla, CA). Anti-mouse FITC-labelled IgG (H+L) was from Vector Laboratories (Burlingame,

CA). Metalloproteinase inhibitor 5-phenyl-1,10-phenanthroline was from Sigma (St. Louis, MO). Inhibitors LY294002, PD98059, SB202190, and actinomycin D were from Calbiochem. γ^{32} P-ATP was from New England Nuclear (Boston, MA). All other reagents were from Fisher Scientific (Norcross, GA).

Cell Culture

HMT-3522 breast epithelial cells (T4-2 and S-1) were obtained from Dr. Mina Bissell (Lawrence Berkeley National Laboratory, Berkeley, CA). The cells were grown in monolayer culture in DMEM/F12 (GIBCO/BRL, St. Louis, MO) containing 250 ng/ml insulin (Sigma), 10 μ g/ml transferrin (Sigma), 2.6 ng/ml sodium selenite (GIBCO/BRL), 1×10^{-10} M estradiol (Sigma), 1.4×10^{-6} M hydrocortisone (Sigma), and 5 μ g/ml prolactin (Sigma). For further details, see the description of H14 medium by Blaschke and colleagues (7). For the growth of the S-1 cells, 10 ng/ml EGF (Becton Dickinson, Bedford, MA) was added to the medium. For passaging, the cells were trypsinized by addition of 0.25% trypsin/1 mM EDTA (GIBCO/BRL), and after detachment of the cells, 1.8 mg of soybean trypsin inhibitor was added per ml of trypsin/EDTA. The cells were then replated on tissue culture dishes at $\sim 2 \times 10^4$ cells per cm^2 .

Cell Invasion Assay

Transwell membranes (8 μ m pore size, 6.5 mm dia., Corning Costar Corp., Cambridge, MA) were coated with 40 μ l of 62.5 μ g/ml Matrigel (Becton Dickinson) and 30 μ g/ml fibronectin (Calbiochem) or with Matrigel alone. The membranes were dried in a tissue culture hood and then reconstituted in 40 μ l of DMEM/F12 medium. The cells were trypsinized as described above, centrifuged and suspended in DMEM/F12 containing 0.2% BSA (Sigma, 1X crystallized grade). The cells were counted, centrifuged, and suspended in DMEM/F12, 0.2% BSA. The cells were then centrifuged and suspended at a final con-

centration of 1×10^6 /ml in DMEM/F12, 0.2% BSA containing 2.6 ng/ml sodium selenite (Sigma), 1×10^{-10} M estradiol (Sigma), 1.4×10^{-6} M hydrocortisone (Sigma) (migration medium) containing growth factors and inhibitors as indicated in the figure legends. The cells (100 μ l) were then layered in the upper chamber of the coated Transwell chamber. In the lower chamber was added 600 μ l of the migration medium (including the growth factors and inhibitors as indicated in the figure legends). The Transwells were then incubated in a tissue culture incubator for various times as indicated in the text. After the incubation, the cells remaining in the upper chamber were removed by swabbing with a Q-tip[®]. The cells on the lower side of the membrane were fixed in methanol and then stained with Hema 3 stain (Fisher Scientific). Invading cells were counted in a Nikon Diaphot microscope.

Cell Scattering

For observation of cell scattering in response to growth factor, T4-2 or S-1 cells were grown to $\sim 30\%$ confluence on either Matrigel or uncoated tissue culture wells. Cells were washed 3X with PBS and then incubated with or without 100 ng/ml EGF in the presence or absence of the inhibitors as described in the figure legends. The medium used was DMEM/F12 supplemented with sodium selenite, estradiol, hydrocortisone, and penicillin/streptomycin at the concentrations indicated above. The cells were placed in a tissue culture incubator for 18 hours and viewed by phase contrast confocal microscopy.

Measurement of Metalloproteinase Activity

To measure the metalloproteinases secreted in the cell medium, confluent cells were washed briefly with DMEM/F12 medium and then incubated for 18 hours in the presence or absence of 100 ng/ml EGF and the inhibitors as indicated in the figure legends. The media were collected, centrifuged briefly to remove cellular debris, and then concentrated 100-fold by ultrafiltration (Millipore, Bedford, MA). The

samples were treated with nonreducing SDS sample buffer, heated at 42°C for 20 min and then subjected to gelatin zymography according to the method of Leber and others (21). Samples were run on SDS polyacrylamide gels (12% acrylamide) containing 0.1% gelatin as substrate. After the gel was electrophoresed, it was incubated in 2% Triton X-100 for one hour at room temperature with shaking. The gel was then incubated overnight with shaking at 37°C in 50 mM Tris-HCl, pH 7.4/0.2 M NaCl/5 mM CaCl_2 . The gel was then stained with coomassie blue for 30 min and destained in 10% acetic acid.

Immunoprecipitation and Western Immunoblotting

For cellular signaling experiments, cells were deprived of EGF, transferrin, and prolactin for 18 hours. The cells were then stimulated with 100 ng/ml EGF, washed with PBS, and lysed in 20 mM Tris-HCl, pH 7.4/150 mM NaCl/1% NP-40/0.25% deoxycholate/1 mM Na_3VO_4 /1 mM EGTA (Lysis Buffer) and a cocktail of protease inhibitors (Complete, Roche Bioscience, Palo Alto, CA). Extracts were centrifuged in a microfuge and total protein concentration was measured by Bradford assay (BioRad, Richmond, CA). Extracts were normalized for total protein and ~1 μg of antibody was added per precipitation. After overnight incubation at 5°C, Protein G sepharose (Pierce, Rockford, IL) was added. Precipitates were washed 3X with Lysis Buffer. The washed precipitates or total cell extracts in SDS sample buffer were run on SDS-PAGE and the proteins were transferred to a nitrocellulose membrane (BioRad). Transfers were blocked with 4% BSA (Roche) or 5% nonfat dry milk (Nestle, Basel, Switzerland) in PBS supplemented with 0.1% Tween 20 (PBST). The blots were incubated with the primary antibody in PBST plus the blocking protein. The blots were then washed 3X in PBST and incubated with the secondary horseradish peroxidase-linked antibody (Santa Cruz). The blots were washed 3X with PBST, treated with chemiluminescent reagent (New England Nuclear) and exposed to x-ray film. Densitometry was performed using an AlphaImager 2000

documentation and analysis system (AlphaInnotech Corp., San Leandro, CA).

Assay of PI 3-Kinase Activity

Assay of PI 3-kinase was carried out after growth factor stimulation of cells. Cells were lysed in 20 mM Tris-HCl, pH 7.4/150 mM NaCl/1% NP-40/1 mM Na_3VO_4 /1 mM EGTA, and a cocktail of protease inhibitors (Complete, Roche Bioscience). Centrifuged extracts were normalized for total protein as above and then precipitated with an anti-phosphotyrosine PY99 antibody and Protein G sepharose. Precipitates were washed and subjected to an *in vitro* kinase reaction using phosphatidylinositol and $\gamma^{32}\text{P}$ -ATP as substrates according to Derman and others (13). The ^{32}P samples were applied to oxalate-coated cellulose/acetate plates and subjected to chromatographic separation (solvent: CHCl_3 :Methanol: H_2O : NH_4OH [60:47:11.3:2]). The developed plate was then exposed to x-ray film.

RESULTS

T4-2 Breast Epithelial Cells Invade a Matrigel Layer in Response to EGF while S-1 Cells do not Invade

Our initial experiments showed the ability of T4-2 breast epithelial cells to invade into a Matrigel/fibronectin layer of a Transwell chamber in response to treatment with EGF (Figure 1). Results were expressed such that the maximum migration of T4-2 cells in the presence of EGF was taken as 100%. Similar results were seen even when fibronectin was not added to the Matrigel layer (data not shown). S-1 cells failed to show detectable invasion when treated with EGF under these conditions. Treatment of the T4-2 cells with heregulin or vascular endothelial growth factor (VEGF) showed a much smaller but detectable invasion, on the order of <5% of the invasion seen in response to EGF. Growth of T4-2 cells for four days in 10 ng/ml EGF failed to significantly affect their ability to invade in response to EGF (Figure 1B). This indicated that the difference

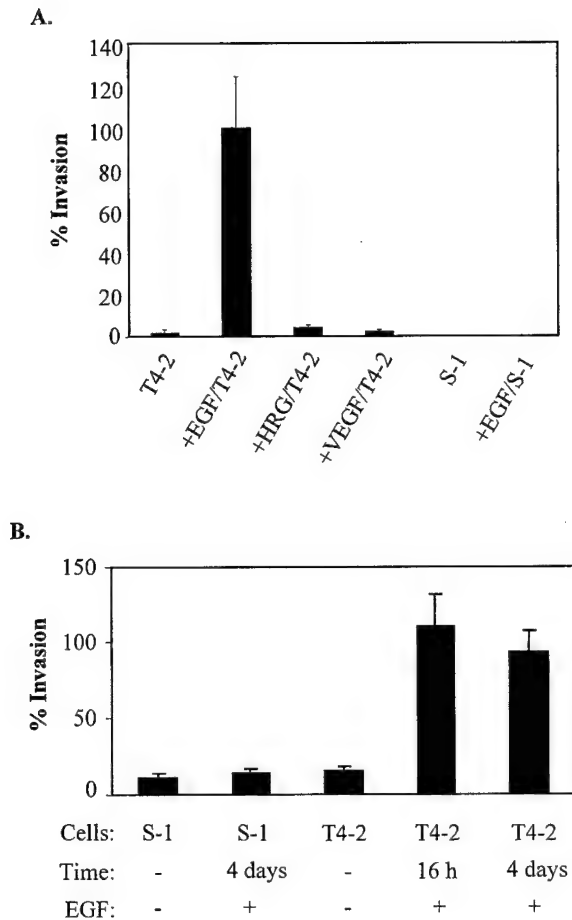


Figure 1. (A). Invasion of T4-2 and S-1 cells into Matrigel/fibronectin-coated Transwell membranes in response to growth factors. T4-2 and S-1 cells were applied to the upper wells of Transwell chambers, with the indicated growth factors present in the upper and lower chambers. Invasion of T4-2 cells in response to EGF is taken as 100%. (B). Effect of EGF on the invasion of cells. T4-2 and S-1 cells were grown either in the absence (-) or presence (+) of 10 ng/ml EGF. These cells were then analyzed for their invasion.

in the ability of the T4-2 and S-1 cells to invade was not due to the differences in the growth media of the two cell lines.

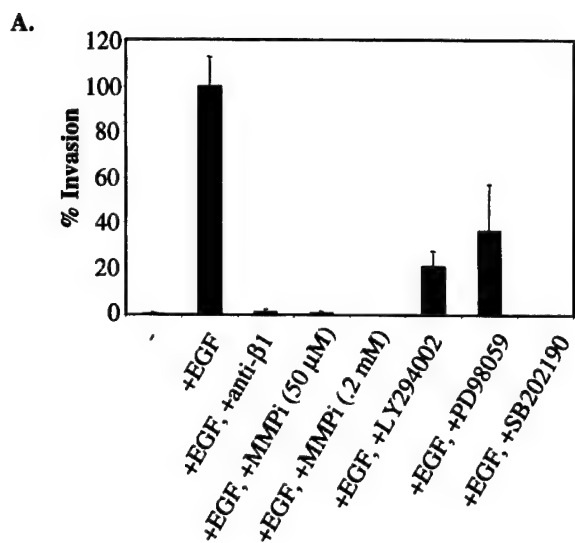
Invasion of T4-2 Breast Epithelial Cells is Blocked by Specific Inhibitors

To further characterize the signaling leading to T4-2 cell invasion, we tested a variety of inhibitors in the Transwell invasion assay. We first tested for the effect of the neutralizing anti- β 1

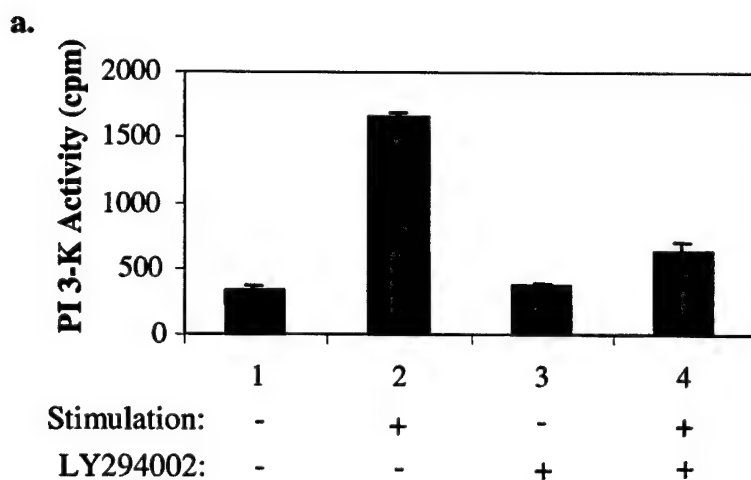
integrin antibody (AIIB2) on the T4-2 invasion. As can be seen in Figure 2, the anti- β 1 integrin antibody almost totally inhibited the ability of T4-2 cells to invade into the Matrigel/fibronectin layer. This was consistent with our finding (data not shown) and that of Weaver and others (45) that β 1 integrin was overexpressed in the T4-2 cells as compared to S-1 cells. We also tested the ability of the metalloproteinase inhibitor (MMPi), 5-phenyl-1,10-phenanthroline, to inhibit the invasion of the T4-2 cells. As is shown in Figure 2, this metalloproteinase inhibitor almost totally inhibited the invasion of the T4-2 cells at concentrations of 50 μ M or greater. Three other inhibitors were tested for their ability to block the invasion of the T4-2 cells. As can be seen in Figure 2, SB202190, a specific inhibitor of the p38 MAP kinase completely inhibited the invasion of the T4-2 cells. The Erk 1,2 pathway inhibitor, PD98059, partially inhibited T4-2 cell invasion to about 35% of the maximal migration in the absence of inhibitors. The PI 3-kinase inhibitor, LY294002, inhibited T4-2 invasion to about 20% of the maximal invasion in the absence of inhibitors. It should be noted that inhibitors were used at concentrations based on their specific I.C.₅₀'s for the target molecules, and these inhibitors were not toxic to the cells at these concentrations (data not shown). Control experiments showed the specific effects of these inhibitors: A PI 3-kinase assay of cells inhibited with LY294002 showed ~60% inhibition of the heregulin-stimulated PI 3-kinase signal (Figure 2Ba). Heregulin stimulation of Erk activation was significantly inhibited by PD98059 (Figure 2Bb). SB202190 inhibited heregulin-stimulated p38 activity as shown by Western blotting with a phospho-p38-specific antibody (Figure 2Bc). Specific action of the metalloproteinase inhibitor 5-phenyl-1,10-phenanthroline on MMP-9 is shown in Figure 7C.

Specific Inhibitors Also Affect the Scattering of T4-2 Cells in Response to EGF

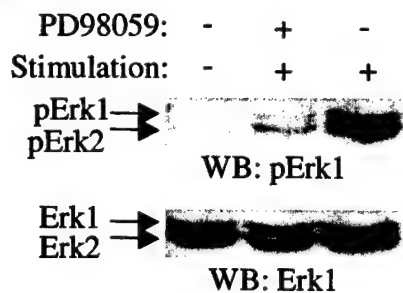
In order to distinguish between motility across a surface and penetration of the Matrigel layer, we



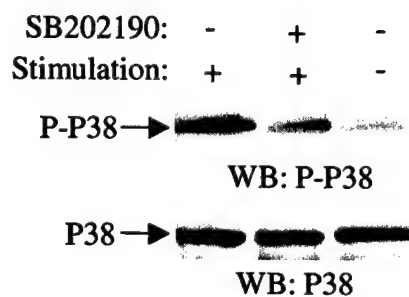
B.



b.



c.



conducted experiments to observe cell scattering on tissue culture plates in response to EGF treatment. Cells were grown to 30–50% confluence on Matrigel-coated polystyrene wells and then cultured in the presence or absence of EGF. As is shown in Figure 3A, T4-2 cells grown in the presence of EGF migrated into the open spaces. In the absence of EGF, the cells remained in distinct islands. In contrast, S-1 cells failed to scatter in response to EGF treatment (Figure 3F). When T4-2 cells were tested for scattering in the presence of various inhibitors, results similar to those of the Transwell assays were obtained. Treatment of T4-2 cells with 5-phenyl-1,10-phenanthroline (MMPi) and SB202190 resulted in the complete suppression of scattering (Figures 3B, E). Treatment of T4-2 cells with LY294002 and PD98059 resulted in significant, but not complete, suppression of the scattering (Figures 3C, D). Treatment of T4-2 cells with the anti- β 1 antibody, A11B2, resulted in a significant reduction in scattering, but numerous projections of the cells were observed, indicating that lamellipodia formation was not completely suppressed (data not shown). When the scattering of T4-2 cells was observed on non-Matrigel-coated polystyrene wells, results were indistinguishable from those on the Matrigel-coated wells (data not shown).

EGF-Dependent Invasion of T4-2 Cells is Time-Dependent and Also Dependent on Gene Transcription

When T4-2 cells were treated with EGF, and tested for their invasion via the Transwell assay, very little invasion was observed until about nine hours after

the addition of EGF (Figure 4, open squares). After this time, the rate of increase in the invasion rose dramatically. Actinomycin D at 10 μ M totally inhibited the time-dependent invasion (Figure 4, open triangles), indicating that the invasion was dependent on specific gene expression. This is a concentration that has been used by others to inhibit transcription in similar systems (24, 40).

EGF-Treated T4-2 and S-1 Cells Differ in Cellular Signaling Including Total Tyrosine Phosphorylation, Erk 1,2 Activation, EGFR Activation, and PI 3-Kinase Activity

In order to better understand the basis of the differences in invasion and motility seen in the T4-2 and S-1 cells, we studied the cellular signaling of the two cell lines in response to EGF. Initially, we treated growth factor-deprived T4-2 or S-1 cells with EGF and carried out anti-phosphotyrosine Western blotting of crude extracts. As shown in Figure 5A, a number of differences were seen in the intensities of the bands (indicated by arrows). The S-1 cells exhibited major EGF-stimulated bands of M.W. 50 and 65 kDa, however, these were of lesser intensity in the T4-2 cells. On the other hand, EGF-stimulated bands of 90, 85, 42, and 36 kDa were of greater intensity in the T4-2 cells. We tested whether one of these bands might be the 42–44 kDa MAP kinase Erk 1,2 by Western blotting of the crude extracts with anti-phospho Erk antibody. As shown in Figure 5B, there was an approximately two-fold increased level of Erk 1,2 activity in the T4-2 cells compared to the S-1 cells. The levels of total Erk 1,2 were only slightly greater in the T4-2 cells

Figure 2. (A). Effect of various inhibitors on the invasion of T4-2 cells into Matrigel/fibronectin-coated Transwell membranes. T4-2 cells were applied to the upper wells of Transwell chambers with EGF and the indicated inhibitors present in the upper and lower chambers. Invasion of T4-2 cells in response to EGF in the absence of inhibitors is taken as 100%. LY294002 was used at a concentration of 30 μ M. PD98059 and SB202190 were used at a concentration of 10 μ M. (B). Effects of inhibitors on enzyme activities in MCF-7 cells. Serum-starved MCF-7 cells were treated with or without heregulin for 10 minutes in the presence or absence of inhibitors. PI 3-kinase activity was measured for cells incubated in the presence or absence of LY294002 at 30 μ M final concentration (a). Erk activity was measured in these cells incubated in the presence or absence of PD98059 at 10 μ M (b) by Western blotting of extracts with phospho- and pan-Erk antibodies. P38 MAP kinase activity was observed in these cells incubated in the presence or absence of SB202190 at 10 μ M by Western blotting of extracts with phospho- and pan-P38 antibodies (c).

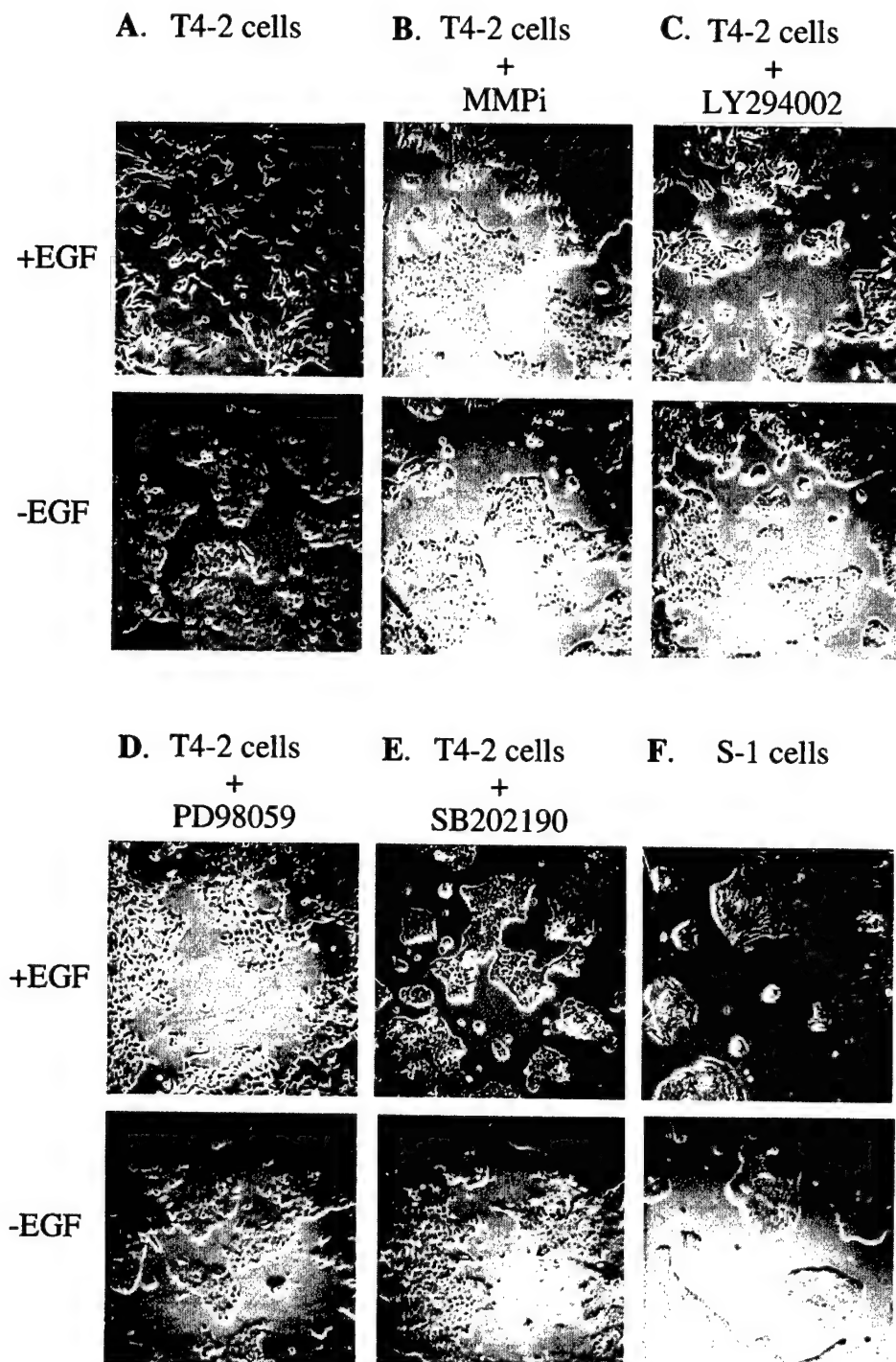


Figure 3. Scattering of T4-2 and S-1 cells on Matrigel-coated tissue culture wells in the presence and absence of EGF and in the presence of various inhibitors. Cells were grown to 30–50% confluence on Matrigel-coated polystyrene wells. Cells were then grown in the presence or absence of EGF and in the presence of the indicated inhibitors for 18 hours. Inhibitors were used at the concentrations indicated in Figure 2. Cells were viewed by phase contrast microscopy.

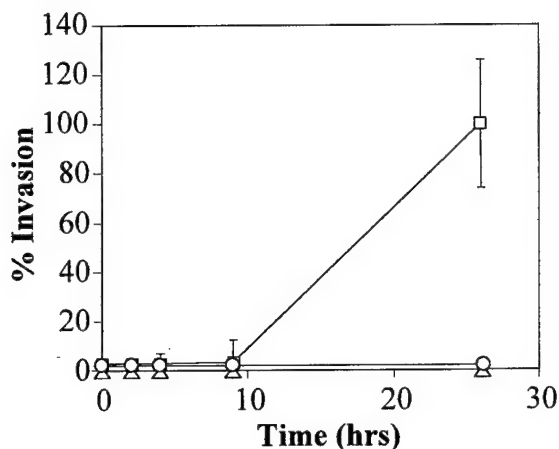


Figure 4. Invasion of T4-2 cells is time-dependent and gene transcription-dependent. Invasion of T4-2 cells was measured in the Transwell assay in the presence or absence of EGF. Treatments were initiated at time 0, and cells were fixed at the indicated times for quantification of invasion. \square - \square , +EGF; \circ - \circ , -EGF; \triangle - \triangle , +EGF + Actinomycin D ($10 \mu\text{M}$).

compared to the S-1 cells, indicating that we had correctly balanced the total proteins from the T4-2 and the S-1 extracts. We failed to see a change in the p38 MAP kinase activity by either *in vitro* kinase assay of specific immunoprecipitates or by blotting with anti-phospho-p38 antibodies. We also did not see a difference in the levels of p38 MAP kinase protein in the T4-2 and S-1 cells (data not shown). We also tested to determine whether the 200 kDa EGF receptor might be preferentially activated in the T4-2 cells compared to the S-1 cells. From lysates of the same experiment as that shown in Figure 5A, we immunoprecipitated the EGF receptor from T4-2 and S-1 cells with an anti-EGF receptor polyclonal antibody. We then blotted SDS-PAGE transfers of these immunoprecipitates with anti-phosphotyrosine antibodies. As is shown in Figure 5C, these blots showed that there was a 3-fold activation of the EGF receptor in the T4-2 cells as compared with the S-1 cells. Blotting of these same precipitates with anti-EGF receptor antibody showed that there were only slightly greater amounts of EGF receptor protein in the T4-2 cells compared to the S-1 cells. Thus, it was unlikely that the increased activation of EGF receptor in the T4-2 cells was due to changes in the amount of epidermal growth factor

receptor (EGFR). In the same experiment, we also measured the effect of EGF on the stimulation of PI 3-kinase activity in T4-2 and S-1 cells. As shown in Figure 5D, both cell lines showed an increase in PI 3-kinase activity in response to EGF, but the T4-2 cells showed an approximately 3- to 4-fold greater PI 3-kinase activity than was seen in the S-1 cells. We tested to see whether changes in PI 3-kinase might lead to differences in Akt activity. As shown in Figure 6A Western blotting of crude extracts with a phospho-Akt antibody failed to show differences in activation in the T4-2 and the S-1 cells treated with EGF. We also examined whether differences in PI 3-kinase activity might lead to differences in PAK1 kinase activity as has been shown by Adam and others (1, 2), Vadlamudi and colleagues (43), and Sells and others (38). We observed approximately two-fold EGF-dependent activation of PAK1 kinase activities in both T4-2 and S-1 cells, but saw no significant difference in PAK1 activation in the two cell lines (Figure 6B). Western blotting of PAK1 in cellular extracts indicated that the extracts contained equivalent amounts of PAK1 protein. Thus, neither Akt nor PAK1 activations appeared to explain the observed differences in motility seen in the two cell lines.

T4-2 Cells Secrete Greater Amounts of MMP-9 as Compared to S-1 Cells

Initial attempts to detect matrix metalloproteinases in the crude extracts of T4-2 and S-1 cells by Western immunoblotting led to no specific conclusions. We then attempted to measure metalloproteinases in the conditioned media of the cells using SDS-PAGE/ zymography (see Methods). Using this method, we found that there was a metalloproteinase secreted by the T4-2 cells that exhibited mobility similar to that of MMP-9 (Figure 7A). The activity of this protein in the T4-2 cells was increased approximately two-fold by EGF treatment. A significantly lesser amount of this metalloproteinase was seen in the S-1 cells (5-fold less as indicated by densitometry). Even at these lower levels, the S-1 cells responded to EGF by increasing MMP-9 activity by

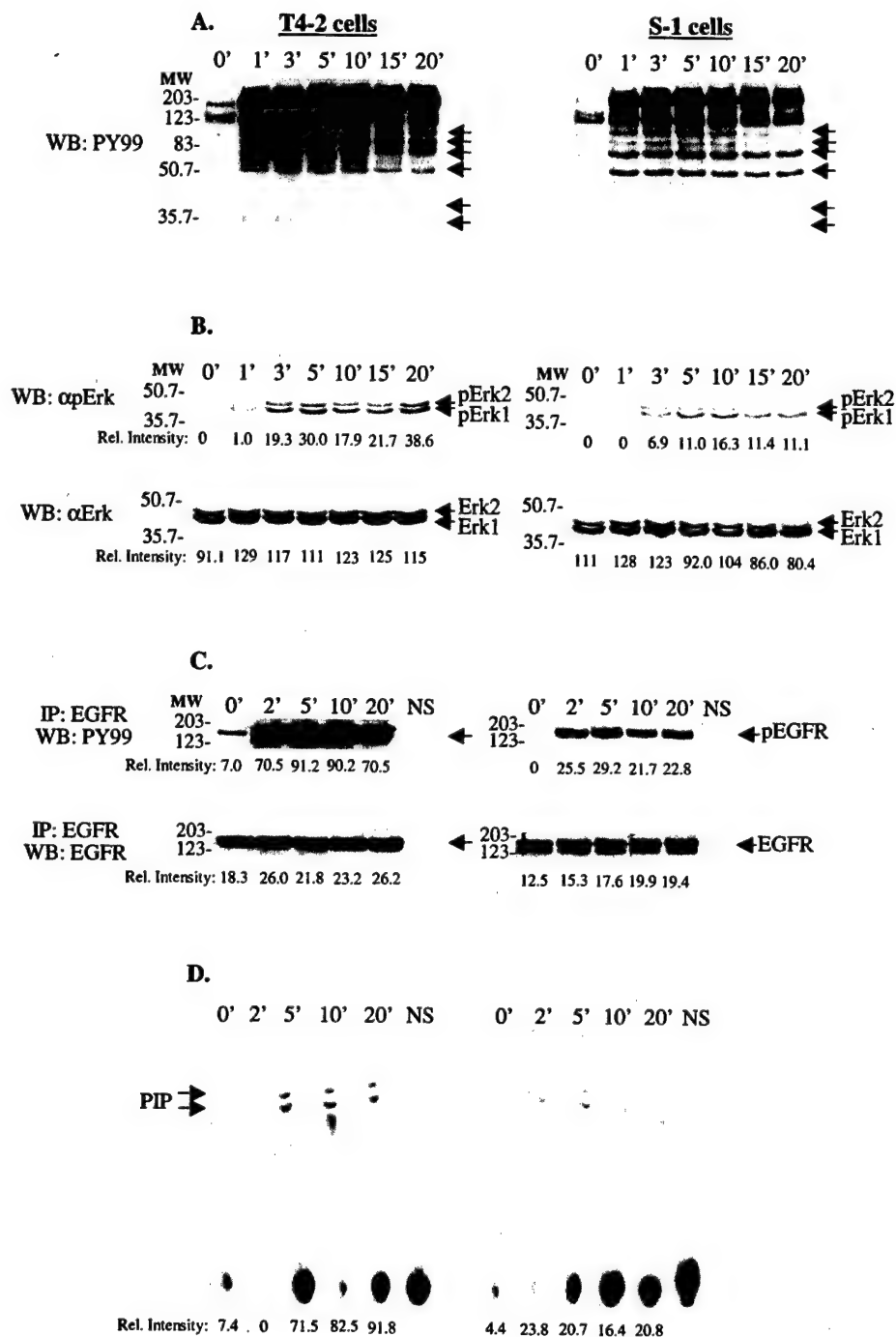


Figure 5. Comparison of EGF-mediated signaling in T4-2 and S-1 cells. (A). Total EGF-dependent tyrosine phosphorylation was shown by Western blotting (PY99 antibody) of crude extracts. (B). Activation of Erk 1,2 was shown by Western blotting of crude extracts with anti-phospho-Erk (pErk) antibody or anti-Erk 1,2 (Erk) antibody. (C). EGFR immunoprecipitates were visualized by Western blotting with PY99 antibody or anti-EGFR antibody. (D). PI 3-kinase activity was measured by *in vitro* kinase assay. Arrows indicate 32 P phosphatidylinositol 3-phosphate (PIP). The relative intensities of the bands were determined by densitometry as indicated below the respective lanes. NS indicates normal serum control immunoprecipitate at 10 minutes (C and D). Time points are in minutes as indicated (A–D).

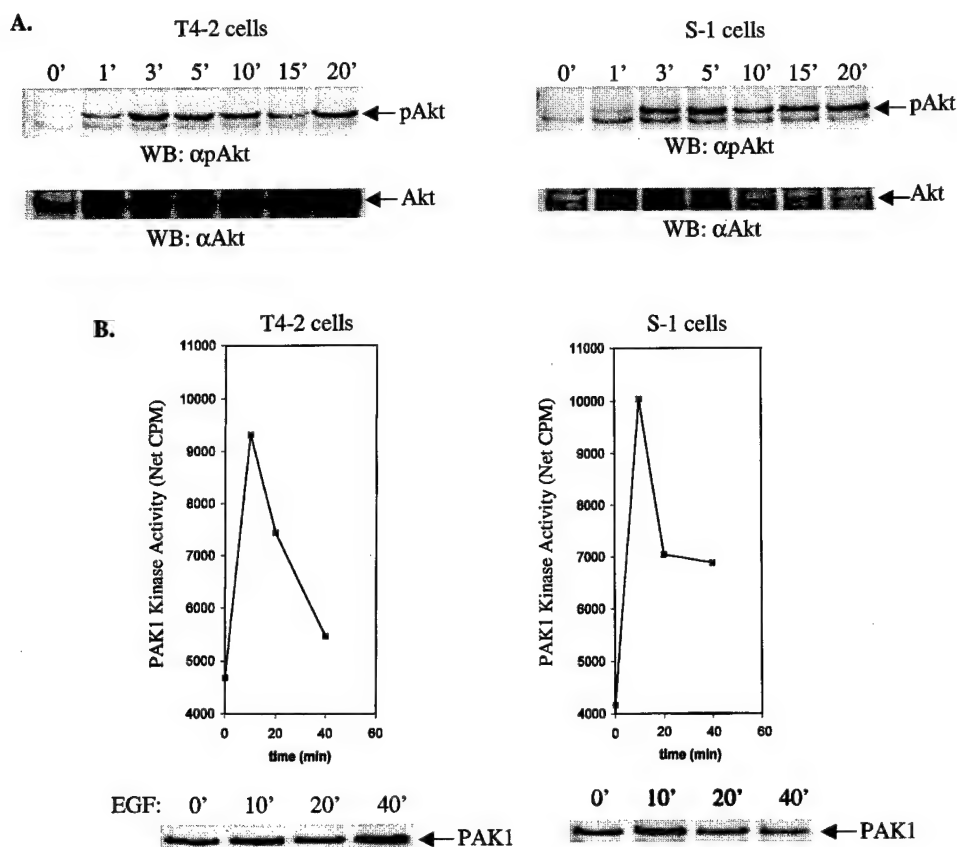


Figure 6. Comparison of EGF stimulated Akt and PAK1 activities in T4-2 and S-1 cells. (A). EGF-dependent activations of Akt in T4-2 or S-1 cells were shown by Western immunoblotting of crude extracts with an anti-phospho-Akt (pAkt) antibody or an anti-Akt (Akt) antibody. (B). PAK1 activities in T4-2 and S-1 cells were shown by *in vitro* kinase assay of PAK1 immunoprecipitates using myelin basic protein as substrate. Western immunoblotting of cellular extracts with anti-PAK1 indicated similar amounts of PAK1 total protein in the immunoprecipitations. Time points are in minutes as indicated (A and B).

two-fold (Figure 7A). Western blotting of these conditioned media with an anti-MMP-9 antibody revealed a 92 kDa band corresponding to the activity seen in the zymography (Figure 7B). This was a confirmation that the activity observed in the zymography was in fact MMP-9.

EGF-Dependent Secretion of MMP-9 is Dependent on the Increase in PI 3-Kinase Activity

In order to determine which cellular pathways were responsible for the secretion of MMP-9 in response to EGF, we treated T4-2 cells with EGF in the

presence and absence of various inhibitors. As can be seen in Figure 7C, incubation in the presence of either LY294002 or 5-phenyl-1,10-phenanthroline (MMPi) led to a reduction of metalloproteinase secretion to levels seen in the absence of EGF. This was an indication that MMP-9 secretion was PI 3-kinase-dependent. The inhibition by the metalloproteinase inhibitor probably represents a direct inhibition of the enzyme. Treatment with the $\beta 1$ integrin antibody, AIB2, resulted in a slight stimulation of MMP-9 secretion, for reasons that are not completely clear. Neither PD98059 nor SB202190 treatment resulted in a significant change in the secretion of MMP-9, indicating that the MAP kinases Erk 1,2 and p38 are probably not involved in the secretion of MMP-9.

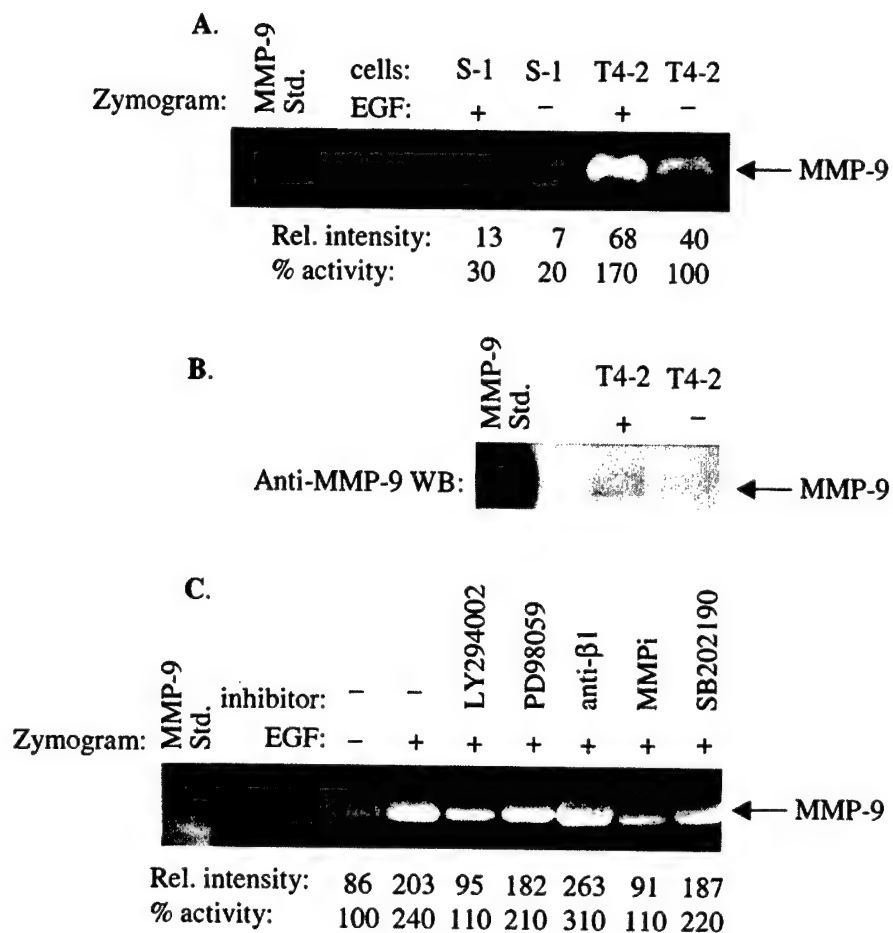


Figure 7. EGF-stimulated Matrix Metalloproteinase-9 (MMP-9) secretion by T4-2 and S-1 cells. (A). Zymography of conditioned media from T4-2 and S-1 cells +/- EGF. (B). Western blotting of T4-2 cell conditioned media +/- EGF with an anti-MMP-9 antibody. (C). Zymography of EGF-stimulated T4-2 cell conditioned media in the absence and presence of various inhibitors. The relative intensities of the bands were determined by densitometry as indicated below the respective bands.

DISCUSSION

We have used the HMT-3522 series of breast epithelial cells as a model for studying growth factor-dependent cellular invasiveness and migration. The initial finding of our work is that T4-2 breast epithelial cells were found to invade a Matrigel/fibronectin layer, and to migrate on a plastic culture dish in response to EGF. The related S-1 cells from this HMT-3522 series failed to invade or migrate under these conditions. We then investigated the differences in EGF signaling between the two cell lines that might account for the differences in the

invasion and motility. Our findings regarding the invasiveness and motility of the T4-2 cells in response to EGF represent a new approach to the observation of phenotypic differences between the T4-2 and S-1 cells. Our results regarding the invasiveness of these cells, under the conditions that we have developed, are consistent with the findings of Weaver and others (45) and Wang and others (44) in the three-dimensional culture in that the phenotypes are determined by up-regulation of $\beta 1$ integrin and the EGF receptor. However, in our system, the tumor properties of invasion and motility specifically occur in response to EGF, and we have shown that both

Erk 1,2 and PI 3-kinase pathways are required in order to produce the invasive phenotype.

There are two general points that can be made about the studies on inhibition of invasion and motility (Figures 2 and 3). Firstly, the studies involving inhibitors of invasion and motility point to a number of pathways that are essential for the processes to occur. These include requirements for Erk 1,2, PI 3-kinase, metalloproteinases, and $\beta 1$ integrin. The means by which these pathways might be operative in invasion and motility will be addressed below. Secondly, there appears to be little difference between the requirements for invasion and for scattering, based on the responses to the various inhibitors in the two assays. This does not necessarily mean that the mechanism of invasion is the same as that of motility across a surface. It may be that the way in which the invasion assay is set up, the penetration through the Matrigel, is not a major factor in cells reaching the other side of the membrane. Thus, movement across a surface may be a major factor in the motility, even in the Matrigel-coated membrane of the Transwell. It is of interest that both of the processes require the action of metalloproteinases. This is an indication that protease action is not only required for penetration of the Matrigel layer in the Transwell, but may also be important for such processes as the release of cellular adhesions of the advancing cell. The effects of inhibitors on cellular invasion suggest that some elements such as $\beta 1$ integrin, metalloproteinases, and p38 MAP kinase are absolutely required for the invasion and motility of T4-2 cells. Other components such as PI 3-kinase and Erk 1,2 appear to contribute significantly to invasion and motility, but may not be absolutely required based on the partial inhibitions of invasion (Figure 2) and motility (Figure 3).

Our finding that Erk 1,2 activation is important for invasiveness and motility is consistent with previous findings in the HMT-3522 series (44). Our results showing a transcriptional requirement for invasiveness indicate that Erk 1,2 may lead to increases in transcription. However, the fact that PD98059 inhibited invasion only by ~63%, while actinomycin D completely inhibited invasion, indicates that a

certain amount of EGF-dependent transcription is occurring through non- Erk 1,2 related pathways. Since a strong inhibition of invasion was seen with the p38 MAP kinase inhibitor SB202190, it is possible that this MAP kinase is also responsible for transcriptional regulation leading to migration. There are numerous reports of both Erk 1,2 and p38 MAP kinases being required for transcription (11), Ravanti and others (34), Ozanne and others (30). The fact that the p38 inhibitor completely inhibits the invasion may indicate that some of its targets are more essential for invasion compared to those of the Erk 1,2 inhibitor.

The differential ability to activate PI 3-kinase appears to be an important factor in determining the invasion and motility of the T4-2 and S-1 cells. PI 3-kinase activity has been shown to play a role in stimulating actin cytoskeletal rearrangement (35), cellular adhesion (6), and cell survival (12). Here, we show that MMP-9 secretion by T4-2 cells is dependent on PI 3-kinase activity (Figure 7C). Thus, LY294002 treatment (Figure 2) may have led to decreased invasiveness partly by decreasing MMP-9 secretion. As is noted in the Results, we found that changes in PAK1 and Akt kinases in response to EGF did not appear to be major factors in the cell motility, as they were similar in T4-2 and S-1 cells. This does not mean that these kinases do not play a role in cell motility and invasiveness. In fact, the PAK1 kinase has been shown by other workers to have a specific role in the directionality and persistence of cell motility (38). It has also been shown by Adam and others (1) that the PAK1 kinase regulates breast cancer invasiveness in a PI 3-kinase-dependent manner. However, in the case of the T4-2 and S-1 cells, it appears that PI 3-kinase is not a major determinant of PAK1 activity, as there is no differential activation when comparing the two cell lines. Since Akt has not been reported to be connected with motility, it is somewhat understandable that there would be no difference in its activation in T4-2 and S-1 cells. Another possible mode of action of PI 3-kinase leading to motility may be through the stimulation of the GTPases Rac1, Cdc42, and RhoA (19, 5). These GTPases

have been reported to activate the Wiscott Aldrich Associated Protein (WASP) and then the Arp2/3 complex leading to actin cytoskeletal rearrangement (17, 20, 26, 32, 35, 41). This is another area that needs to be investigated in the HMT-3522 system in terms of the effects of PI 3-kinase on motility.

As indicated by the effect of the anti- $\beta 1$ integrin antibody, $\beta 1$ integrin plays a significant role in migration and invasion. The requirement of the $\beta 1$ integrin might relate to the process of cellular adhesion independent of growth factor action. $\beta 1$ integrin in a heterodimeric complex with $\alpha 5$ and $\alpha 6$ integrins is known to play a role in the adhesion to extracellular matrix, predominantly fibronectin, in neuronal (42), neutrophilic (31), and tumor cells (3, 4). In our studies, there appeared to be little regulation of the level of $\beta 1$ integrin by EGF (data not shown). This, however, does not rule out the possible modulation of $\beta 1$ integrin binding affinity by EGF signaling. Numerous reports have shown the importance of PI 3-kinase leading to the activation of the small GTPases Rac1, Cdc42, and RhoA in connection with cell motility (5, 19, 37). The studies of Berrier and others (6) also indicate the importance of $\beta 1$ integrin signaling to GTPases via PI 3-kinase. While our studies do not indicate the mode of action of $\beta 1$ integrin, they clearly show that its interaction with the extracellular matrix via $\beta 1$ integrin is essential for cell motility and invasion.

In summary, our findings point to an increased activation of the EGF receptor in the invasive T4-2 cells compared to the noninvasive S-1 cells. This more highly activated EGF receptor leads to increased signaling through both PI 3-kinase and MAP kinase Erk 1,2 pathways. One of the major downstream effects of increased PI 3-kinase activity appears to be increased MMP-9 secretion. We have shown the importance of both PI 3-kinase and MMP-9 in the invasion process by the use of specific inhibitors. PI 3-kinase may also have other effects on actin cytoskeletal rearrangement important for cell motility. Erk 1,2 activation is important for invasion, and this may be related to the fact that specific EGF-dependent transcriptional activity is required for invasion. Genes important for the invasive phenotype

may include integrins such as integrin $\beta 1$, which we have shown to be important for adhesion and invasion. Two other serine/threonine kinases, PAK1 and Akt, are regulated by EGF, but show no significant differences in the T4-2 and S-1 cells, indicating that these activities are not sufficient in themselves to lead to motility. Nonetheless, they may still contribute to the motile phenotype. Taken together, increased EGFR signaling leading to higher PI 3-kinase and Erk 1,2 activities is important in determining the increased invasive and migratory abilities of HMT-3522 T4-2 cells as compared to the noninvasive/nonmigratory S-1 cells.

ACKNOWLEDGEMENTS

The authors wish to thank Dr. Tiho Miralem for advice on integrin engagement, Janet Delahanty for help with editing of the manuscript, and Dan Kelley for help in preparation of the figures. We also thank Dr. Mina Bissell for kindly providing the T4-2 and S-1 cells.

This paper is supported by NIH Grants CA 76226 and R21CA87290, DAMD 17-98-1-8032, and DAMD 17-99-1-9078, by Experienced Breast Cancer Research Grant 34080057089, by the Milheim Foundation, and by the Massachusetts Department of Public Health (to H.A.). This work was done during the tenure of an established investigatorship from the American Heart Association (H.A.).

REFERENCES

1. Adam L, Vadlamudi R, Kondapaka SB, Chernoff J, Mendelsohn J, Kumar R (1998). Heregulin regulates cytoskeletal reorganization and cell migration through the p21-activated kinase-1 via phosphatidylinositol-3 kinase. *J Biol Chem* 273: 28238-28246.
2. Adam L, Vadlamudi R, Mandal M, Chernoff J, Kumar R (2000). Regulation of microfilament reorganization and invasiveness of breast cancer cells by kinase dead p21-activated kinase-1. *J Biol Chem* 275: 12041-12050.
3. Adamsman MA, McCarthy JB, Shimizu Y (1999). Stimulation of beta1-integrin function by epidermal growth factor and heregulin-beta has distinct requirements for erbB2 but a similar dependence on phosphoinositide 3-OH kinase. *Mol Biol Cell* 10: 2861-2878.

4. Alford D, Pitha-Rowe P, Taylor-Papadimitriou J (1998). Adhesion molecules in breast cancer: Role of alpha 2 beta 1 integrin. *Biochem Soc Symp* 63: 245-259.
5. Banyard J, Anand-Apte B, Symons M, Zetter BR (2000). Motility and invasion are differentially modulated by Rho family GTPases. *Oncogene* 19: 580-591.
6. Berrier AL, Mastrangelo AM, Downward J, Ginsberg M, LaFlamme SE (2000). Activated R-ras, Rac1, PI 3-kinase and PKCepsilon can each restore cell spreading inhibited by isolated integrin beta1 cytoplasmic domains. *J Cell Biol* 151: 1549-1560.
7. Blaschke RJ, Howlett AR, Desprez PY, Petersen OW, Bissell MJ (1994). Cell differentiation by extracellular matrix components. *Methods Enzymol* 245: 535-556.
8. Briand P, Nielsen KV, Madsen MW, Petersen OW (1996). Trisomy 7p and malignant transformation of human breast epithelial cells following epidermal growth factor withdrawal. *Cancer Res* 56: 2039-2044.
9. Briand P, Petersen OW, Van Deurs B (1987). A new diploid nontumorigenic human breast epithelial cell line isolated and propagated in chemically defined medium. *In Vitro Cell Dev Biol* 23: 181-188.
10. Chakrabarty S, Rajagopal S, Huang S (1995). Expression of antisense epidermal growth factor receptor RNA downmodulates the malignant behavior of human colon cancer cells. *Clin Exp Metastasis* 13: 191-195.
11. Chen F, Ding M, Lu Y, Leonard SS, Vallyathan V, Castranova V, Shi X (2000). Participation of MAP kinase p38 and IkkappaB kinase in chromium (VI)-induced NF-kappaB and AP-1 activation. *J Environ Pathol Toxicol Oncol* 19: 231-238.
12. Datta SR, Brunet A, Greenberg ME (1999). Cellular survival: A play in three acts. *Genes Dev* 13: 2905-2927.
13. Derman MP, Tokar A, Hartwig JH, Spokes K, Falck JR, Chen CS, Cantley LC, Cantley LG (1997). The lipid products of phosphoinositide 3-kinase increase cell motility through protein kinase C. *J Biol Chem* 272: 6465-6470.
14. Di Cristofano A, Pesce B, Cordon-Cardo C, Pandolfi PP (1998). Pten is essential for embryonic development and tumour suppression. *Nat Genet* 19: 348-355.
15. Friess H, Guo XZ, Nan BC, Kleeff O, Buchler MW (1999). Growth factors and cytokines in pancreatic carcinogenesis. *Ann NY Acad Sci* 880: 110-121.
16. Gasparini G, Bevilacqua P, Pozza F, Meli S, Boracchi P, Marubini E, Sainsbury JR (1992). Value of epidermal growth factor receptor status compared with growth fraction and other factors for prognosis in early breast cancer. *Br J Cancer* 66: 970-976.
17. Jimenez C, Portela RA, Mellado M, Rodriguez-Frade JM, Collard J, Serrano A, Martinez AC, Avila J, Carrera AC (2000). Role of the PI3K regulatory subunit in the control of actin organization and cell migration. *J Cell Biol* 151: 249-262.
18. Kassisi J, Moellinger J, Lo H, Greenberg NM, Kim HG, Wells A (1999). A role for phospholipase C-gamma-mediated signaling in tumor cell invasion. *Clin Cancer Res* 5: 2251-2260.
19. Keely PJ, Westwick JK, Whitehead IP, Der CJ, Parise LV (1997). Cdc42 and Rac1 induce integrin-mediated cell motility and invasiveness through PI(3)K. *Nature* 390: 632-636.
20. Kim L, Kimmel AR (2000). GSK3, a master switch regulating cell-fate specification and tumorigenesis. *Curr Opin Gen & Devel* 10: 508-514.
21. Leber TM, Balkwill FR. (1997) Zymography: A single-step staining method for quantitation of proteolytic activity on substrate gels. *Anal Biochem* 249: 24-28.
22. Lewis S, Locker A, Todd JH, Bell JA, Nicholson R, Elston CW, Blamey RW, Ellis IO (1990). Expression of epidermal growth factor receptor in breast carcinoma. *J Clin Pathol* 43: 385-389.
23. Madsen MW, Lykkesfeldt AE, Laursen I, Nielsen KV, Briand P (1992). Altered gene expression of c-myc, epidermal growth factor receptor, transforming growth factor-alpha, and c-erb-B2 in an immortalized human breast epithelial cell line, HMT-3522, is associated with decreased growth factor requirements. *Cancer Res* 52: 1210-1217.
24. Mazumdar A, Adam L, Boyd D, Kumar R (2001). Heregulin regulation of urokinase plasminogen activator and its receptor: Human breast epithelial cell invasion. *Cancer Res* 61: 400-405.
25. Moyret C, Madsen MW, Cooke J, Briand P, Theillet C (1994). Gradual selection of a cellular clone presenting a mutation at codon 179 of the p53 gene during establishment of the immortalized human breast epithelial cell line HMT-3522. *Exp Cell Res* 215: 380-385.
26. Muller T, Choidas A, Reichmann E, Ullrich A (1999). Phosphorylation and free pool of beta-catenin are regulated by tyrosine kinases and tyrosine phosphatases during epithelial cell migration. *J Biol Chem* 274: 10173-10183.
27. Nielsen KV, Briand P (1989). Cytogenetic analysis of in vitro karyotype evolution in a cell line established from nonmalignant human mammary epithelium. *Cancer Genet Cytogenet* 39: 103-118.
28. Nielsen KV, Madsen MW, Briand P (1994). In vitro karyotype evolution and cytogenetic instability in the non-tumorigenic human breast epithelial cell line HMT-3522. *Cancer Genet Cytogenet* 78: 189-199.
29. Oehler MK, Rehn M, Kristen P, Sutterlin M, Caffier H (1997). Correlation of the EGF-receptor with cell kinetic and classical prognostic factors in breast cancer. *Anticancer Res* 17: 3137-3140.
30. Ozanne BW, McGarry L, Spence HJ, Johnston I, Winnie J, Meagher L, Stapleton G (2000). Transcriptional regulation of cell invasion: AP-1 regulation of a multigenic invasion programme. *Eur J Cancer* 36: 1640-1648.
31. Pierini LM, Lawson MA, Eddy RJ, Hendey B, Maxfield FR (2000). Oriented endocytic recycling of alpha5beta1 in motile neutrophils. *Blood* 95: 2471-2480.
32. Pollard TD, Blanchoin L, Mullins RD (2000). Molecular mechanisms controlling actin filament dynamics in nonmuscle cells. *Annu Rev Biophys Biomol Struct* 29: 545-576.
33. Price JT, Tiganis T, Agarwal A, Djakiew D, Thompson EW (1999). Epidermal growth factor promotes MDA-MB-231 breast cancer cell migration through a phosphatidylinositol 3'-kinase and phospholipase C-dependent mechanism. *Cancer Res* 59: 5475-5478.
34. Ravanti L, Heino J, Lopez-Otin C, Kahari VM (1999). Induction of collagenase-3 (MMP-13) expression in human skin fibroblasts by three-dimensional collagen is mediated by p38 mitogen-activated protein kinase. *J Biol Chem* 274: 2446-2455.
35. Rodriguez-Viciana P, Warne PH, Khwaja A, Marte BM, Pappin D, Das P, Waterfield MD, Ridley A, Downward J (1997). Role of phosphoinositide 3-OH kinase in cell transformation and control of the actin cytoskeleton by Ras. *Cell* 89: 457-467.
36. Sainsbury JR, Farndon JR, Needham GK, Malcolm AJ, Harris AL (1987). Epidermal-growth-factor receptor status as predictor of early recurrence of and death from breast cancer. *Lancet* 1: 1398-1402.
37. Sarner S, Kozma R, Ahmed S, Lim L (2000). Phosphatidylinositol 3-kinase, Cdc42, and Rac1 act downstream of Ras in integrin-dependent neurite outgrowth in N1E-115 neuroblastoma cells. *Mol Cell Biol* 20: 158-172.

38. Sells MA, Pfaff A, Chernoff J (2000). Temporal and spatial distribution of activated Pak1 in fibroblasts. *J Cell Biol* 151: 1449–1458.
39. Steck PA, Pershouse MA, Jasser SA, Yung WK, Lin H, Ligon AH, Langford LA, Baumgard ML, Hattier T, Davis T, Frye C, Hu R, Swedlund B, Teng DH, Tavtigian SV (1997). Identification of a candidate tumour suppressor gene, MMAC1, at chromosome 10q23.3 that is mutated in multiple advanced cancers. *Nat Genet* 15: 356–362.
40. Syrovets T, Jendrach M, Rohwedder A, Schule A, Simmet T (2001). Plasmin-induced expression of cytokines and tissue factor in human monocytes involves AP-1 and IKKbeta-mediated NF-kappaB activation. *Blood* 97: 3941–3950.
41. Thrasher AJ, Burns S, Lorenzi R, Jones GE (2000). The Wiskott-Aldrich syndrome: Disordered actin dynamics in haematopoietic cells. *Immunol Rev* 178: 118–128.
42. Tomaselli KJ, Doherty P, Emmett CJ, Damsky CH, Walsh FS, Reichardt LF (1993). Expression of beta 1 integrins in sensory neurons of the dorsal root ganglion and their functions in neurite outgrowth on two laminin isoforms. *J Neurosci* 13: 4880–4888.
43. Vadlamudi RK, Adam L, Wang RA, Mandal M, Nguyen D, Sahin A, Chernoff J, Hung MC, Kumar R (2000). Regulatable expression of p21-activated kinase-1 promotes anchorage-independent growth and abnormal organization of mitotic spindles in human epithelial breast cancer cells. *J Biol Chem* 275: 36238–36244.
44. Wang F, Weaver VM, Petersen OW, Larabell CA, Dedhar S, Briand P, Lupu R, Bissell MJ (1998). Reciprocal interactions between beta1-integrin and epidermal growth factor receptor in three-dimensional basement membrane breast cultures: A different perspective in epithelial biology. *Proc Natl Acad Sci USA* 95: 14821–14826.
45. Weaver VM, Petersen OW, Wang F, Larabell CA, Briand P, Damsky C, Bissell MJ (1997). Reversion of the malignant phenotype of human breast cells in three-dimensional culture and in vivo by integrin blocking antibodies. *J Cell Biol* 137: 231–245.

The Autocrine and Paracrine Role of Vascular Endothelial Growth Factor in Breast Cancer Metastasis

Tae-Hee Lee[†], Hava Avraham[†], Myeong-Jin Nam[§] and Shalom Avraham^{†*}

[†]Division of Experimental Medicine, Beth Israel Deaconess Medical Center and Harvard Medical School, 4 Blackfan Circle, Boston, MA 02115 and [§]Division of Cancer Research, Korean National Institute of Health, Eunpung-ku, Nokbun-dong 5, Seoul, Korea, 122-020

*All correspondence should be addressed to:

Dr. Shalom Avraham
Division of Experimental Medicine
Beth Israel Deaconess Medical Center
Harvard Institutes of Medicine
4 Blackfan Circle
Boston, MA 02115
Phone: (617) 667-0063; Fax: (617) 975-6373
E-mail: savraham@caregroup.harvard.edu

Running title: "VEGF/VPF in breast cancer metastasis"

Key words: VEGF/VPF, brain endothelial cells, blood-brain barrier, metastasis, breast cancer

ABSTRACT

Vascular endothelial growth factor (VEGF), also known as vascular permeability factor (VPF), has been shown to increase potently the permeability of endothelium and is highly expressed in breast cancer cells. In this study, we investigated the role of VEGF/VPF in breast cancer metastasis to the brain. To metastasize to the brain, malignant tumor cells must attach to microvessel endothelial cells and then invade the blood-brain barrier (BBB).

We observed that VEGF/VPF induced a retraction of the human brain microvascular endothelial cell (HBMEC) monolayer and increased significantly the adhesion and transendothelial migration of the highly metastatic MDA-MB-231 breast cancer cells onto this monolayer. These effects were inhibited by pre-treatment of HBMECs with the VEGF/VPF receptor inhibitor, SU-1498, and the calcium chelator BAPTA-AM. In addition, we observed inhibition of transendothelial migration in MDA-MB-231 clones stably transfected with antisense VEGF/VPF: AS-VEGF-C1 and AS-VEGF-C2. Furthermore, we found that down-regulation of VEGF/VPF expression resulted in apoptosis of these cells. Apoptosis gene array analysis revealed significant up-regulation of apoptosis-related genes such as TRAIL, Cox-2, caspase-7, and -8 in AS-VEGF-C1 and -C2 cell clones. Activation of PI3-kinase as well as phosphorylation of Akt were significantly increased in cells overexpressing VEGF/VPF, indicating that VEGF/VPF mediates autocrine survival signaling via the PI3-kinase/Akt pathway in MDA-MB-231 cells.

Taken together, these findings indicate that VEGF/VPF plays a role in breast cancer metastasis by enhancing the transendothelial migration of tumor cells through the down-

regulation of endothelial integrity in a paracrine mode and the promotion of tumor cell survival via the PI3-kinase/Akt pathway in an autocrine mode.

INTRODUCTION

Brain metastasis, which is an important cause of cancer morbidity and mortality, occurs in at least 30% of patients with breast cancer. A key event of brain metastasis is the migration of cancer cells through the blood-brain barrier (BBB), which constitutes the endothelium and the surrounding cells (1, 2). To metastasize to the brain, malignant tumor cells must enter into the circulatory system through the endothelium (intravasation), and then attach to microvessel endothelial cells to invade the BBB (extravasation)(1). The precise molecular mechanism of extravasation of tumor cells penetrating the BBB is poorly defined. A widely supported hypothesis is that tumor cell adhesion to endothelium induces the retraction of endothelial cells, which exposes their basement membrane to the tumor cells (3). Tumor cells recognize and bind to components in the vascular membrane, thereby initiating extravasation and the beginning of new growth at secondary organ sites (4). This suggests that the intact endothelium can serve as a "defensive barrier" to the extravasation of tumor cells.

Tumor bearing blood vessels, however, do not seem to be effective in acting as a defensive barrier for the prevention of tumor cell intravasation, since these blood vessels display high leakage and disrupted integrity (5, 6). Hypoxia is believed to contribute to the leakage of tumor blood vessels by inducing increased vascular permeability (7, 8). Hypoxia is also a strong inducer of vascular endothelial growth factor (VEGF), otherwise known as vascular permeability factor (VPF)(9, 10). VEGF/VPF has potent mitotic activity specific to vascular endothelial cells and significant vascular permeable activity (11, 12). VEGF/VPF binds to its cognate receptors, Flt-1, Flk-1/KDR and neuropilin-1. Among them, Flk-1/KDR is responsible for the initiation of signal transduction pathways

within the cells (11, 12). VEGF/VPF has an essential role in promoting new blood vessel formation (angiogenesis) during tumor development, and inhibition of its function effectively prevents tumor growth through incomplete blood vessel formation (13, 14). Indeed, VEGF/VPF expression has been reported in a number of cancer cell lines and in several clinical specimens derived from breast, brain, and ovarian cancers (15-18). Although the role of VEGF/VPF as an angiogenic factor in primary tumor growth and secondary tumor growth (metastatic tumors) is well studied, its role as a vascular permeability factor in metastatic processes is not well elucidated. Tumor cells may more easily penetrate a retracted endothelial monolayer caused by VEGF/VPF than a tightly arranged monolayer, suggesting that the vascular permeability activity of VEGF/VPF contributes an "offensive ability" to the tumor cells, allowing them to penetrate blood vessels. To examine this hypothesis, we constructed a Transwell culture system of the human brain endothelial monolayer as an in vitro model for the BBB. We then evaluated the inter-relationship between the integrity of the endothelial monolayer and the vascular permeability of VEGF/VPF and their effect on the transendothelial migration of the highly metastatic MDA-MB-231 breast cancer cells.

Importantly, the functions of VEGF/VPF do not seem to be restricted exclusively to endothelial cells, since some tumor cells have been reported to express VEGF/VPF receptors. In nearly 50% of the breast tumors, there was significant expression of Flt-1 and Flk-1/KDR in the tumor epithelial cells, correlating with the expression of VEGF/VPF by these cells (19). Furthermore, recent studies showed that VEGF/VPF acts as an autocrine growth and survival factor for VEGF/VPF receptor-expressing tumor cells, including breast cancer cells (20, 21). Our previous studies also demonstrated that

VEGF/VPF induces intracellular signaling-mediated proliferation and invasion in breast cancer cells (22, 23). Therefore, in this study, we also investigated whether the autocrine role of VEGF/VPF as a survival factor in MDA-MB-231 cells, which are known to express high amount of VEGF/VPF (20), contributes to their penetration of the endothelial monolayer.

EXPERIMENTAL PROCEDURES

Materials—Human recombinant VEGF₁₆₅/VPF and anti-human VEGF/VPF monoclonal antibody were obtained from Genentech Inc (San Francisco, CA). Human recombinant bFGF was purchased from R & D Systems, Inc. (Minneapolis, MN). Rhodamine-Phalloidin, DiI and BCECF-AM were from Molecular Probes, Inc (Eugene, OR), and PD98059, BAPTA-AM, Wortmannin, and SU-1498 were purchased from Calbiochem, Inc (San Diego, CA). Anti-human VE-cadherin monoclonal antibody was from Chemicon International, Inc (Temecula, CA). Anti-human phospho-Akt/PKB antibody was purchased from New England Biolabs (Beverly, MA). Anti-mouse phospho-ERK and anti-human Csk antibodies were from Santa Cruz Biotechnology (San Diego, CA). Anti-human p85 subunit specific PI3-kinase antibody was purchased from Upstate Biotechnology (Lake Placid, NY).

Cell Culture—Human brain microvascular endothelial cells (HBMECs) were purchased from Cell Systems Inc. (Kirkland, WA). The cells were seeded onto attachment factor-coated culture plates and maintained in CSC-complete medium according to the protocol of the manufacturer. The HBMECs formed tubular-like networks on matrigel and produced the endothelial-specific marker, von Willebrand factor, indicating that these cells maintained the general properties of endothelial cells (24). During the course of the experiment, the cells were used until passages three to seven, and checked routinely for expression of von Willebrand factor. The breast tumor cell line, MDA-MB-231, was obtained from ATCC and maintained in culture medium (DMEM containing 10% FBS, 2 mM L-glutamine). Both cell lines were incubated in 5%

CO₂ at 37 °C.

Fluorescent Labeling of MDA-MB-231 cells—MDA-MB-231 cells were incubated with 200 nM DiI for 30 min and then washed twice with PBS. DiI-labeled cells were dispersed in 0.05% trypsin solution and resuspended in culture medium. Alternatively, tumor cells were dispersed in 0.05% trypsin solution and incubated with 1 µM BCECF-AM for 15 min, then centrifuged three times to remove free BCECF-AM.

Transendothelial Migration Assay of MDA-MB-231 cells—HBMECs growing on attachment factor-coated culture plates were dispersed in 0.05% trypsin solution and resuspended in CS-C complete medium. Approximately 100,000 cells were added to fibronectin-coated 24-well Transculture inserts with pores of 8 µm (Costar Corp.) and grown for 5 days in 5% CO₂ at 37 °C. The medium was replaced every day with fresh medium. Prior to the assays, the monolayers were washed once with CS-C medium without growth factor and then 40,000 DiI-labeled MDA-MB-231 cells in 100 µl of the same medium were added to the apical chamber. To exclude the chemoattractant effect of the added growth factor, VEGF/VPF or bFGF was added evenly to the apical and basolateral chambers. In the case of inhibitor treatment, the monolayers were pre-treated for 30 min and all inhibitors, except for VEGF/VPF monoclonal antibodies and SU-1498, were removed from the monolayers by washing twice with culture medium. After incubation for 6 hours, the apical chambers were fixed with 3.7% formaldehyde and washed extensively with PBS. To remove non-migrating cells, the apical side of the

apical chamber was scraped gently with cotton wool and only the migrating tumor cells were observed under a fluorescent microscope. Migrating cells were counted from 10 random fields of 200 magnification.

Adhesion Assay of MDA-MB-231 cells—HBMECs were added to attachment factor-coated 24-well culture plates and grown for 5 days in 5% CO₂ at 37 °C. The medium was replaced every day with fresh medium. Prior to the assays, the monolayers were washed once with CS-C medium without growth factor and then 100,000 of DiI-labeled MDA-MB-231 cells in 500 µl of the same medium were added to each well with or without test samples. In the case of inhibitor treatment, the monolayers were pre-treated for 30 min and all inhibitors, except for VEGF/VPF monoclonal antibodies and SU-1498, were removed from the monolayers by washing twice with culture medium. After incubation for 2 hours, the wells were fixed with 3.7% formaldehyde and washed extensively with PBS to remove floating tumor cells. Attached tumor cells were observed under a fluorescent microscope and counted from 10 random fields of 200 magnification.

To detach the endothelial monolayer and prepare the sub-endothelial basement (SEB) membrane components, the monolayers were treated with 50 mM NH₄OH solution for 5 min as indicated previously (25), and washed extensively with PBS before adding the DiI-labeled MDA-MB-231 cells.

Retraction Assay of HBMECs—To monitor the extent of endothelial cell retraction, the amount of [³H] inulin (Amersham International) passing across an endothelial monolayer was measured as described (14). Briefly, approximately 100,000 HBMECs

were added to fibronectin-coated 24-well Transculture inserts with pores of 0.4 μm (Falcon Corp.) and grown for 5 days in 5% CO_2 at 37°C. The medium was replaced every day with fresh medium. After the removal of culture medium, 0.4 ml of the fresh culture medium containing [^3H] inulin (1 μCi) was added to the apical chamber. The basolateral chamber was filled with 0.6 ml of the same medium without [^3H] inulin and then 30 ng/ml of VEGF/VPF were added to the apical and basolateral chambers. In the case of inhibitor treatment, the monolayers were pre-treated for 30 min before VEGF/VPF treatment. After incubation for 2 hours, 30 μl of medium from the basolateral chamber was collected and the amount of [^3H] inulin across the monolayers was determined by scintillation counting.

F-Actin Staining of HBMECs—HBMECs were added to fibronectin-coated 24-well Transculture inserts with pores of 0.4 μm and grown for 5 days in 5% CO_2 at 37°C. After the assays, the cells were fixed with 3.7% formaldehyde in PBS for 20 min, and then permeabilized with 0.5% Triton X-100 for 10 min. Following a PBS washing, the cells were blocked with 20% goat serum in PBS and then incubated at room temperature with Rhodamine-Phalloidin (diluted 1:40) in PBS for 1 hour. After washing by three changes of PBS, the polycarbonate membranes were separated carefully from the apical chamber, mounted on a slide, and F-actin staining was observed under a fluorescent microscope.

VE-Cadherin staining of HBMECs—HBMECs were added to fibronectin-coated 24-well Transculture inserts with pores of 0.4 μm and grown for 5 days in 5% CO_2 at 37°C.

After the assays, the cells were fixed with 3.7% formaldehyde in PBS for 20 minutes, and then permeabilized with 0.5% Triton X-100 for 10 min. Alternatively, 1,000 BCECF-AM-labeled MDA-MB-231 cells were added to each well with or without VEGF/VPF (30 ng/ml). After incubation for 2 hours, the wells were fixed with 3.7% formaldehyde, washed extensively with PBS to remove floating tumor cells, and then permeabilized with 0.5% Triton X-100 for 10 min. Following a PBS washing, the cells were blocked with 20% goat serum in PBS for 1 hour before overnight incubation at 4°C with anti-human VE-cadherin monoclonal antibody (2 µg/ml) diluted by calcium containing serum-free DMEM. After washing by three changes of PBS, the cells were incubated for 1 hour with goat anti-mouse IgG Texas-red (diluted 1:200) in PBS. After washing by three changes of PBS, the polycarbonate membranes were separated carefully from the apical chamber, mounted on a slide, and viewed under a confocal microscope.

Generation of Stable Antisense VEGF/VPF-Transfected MDA-MB-231 Cells—

Human cDNA clones encoding VEGF/VPF were amplified by reverse transcription PCR using the following primers 5'-ACGACAGAAGGGGAGCAGAAAG-3' (forward) and 5'-GGAACGTTGCGCTCAGACACA-3' (backward). Subsequently, the 576 bp VEGF cDNA was cloned using the pBluescript αSK (+/-) vector (Stratagene, La Jolla, CA) and sequenced using the T7 promoter and primers. Both sense and antisense orientations were cloned into the Kpn1 enzyme site of the constitutive mammalian expression vector, pZeoSV (Invitrogen, Carlsbad, CA), and sequenced using the T3 and SP6 primers. MDA-MB-231 cells were transfected with antisense VEGF/VPF vector and selected in the presence of Zeocin (1 mg/ml). VEGF/VPF expression of MDA-MB-231 transfectants

was analyzed by Western blotting using polyclonal anti-VEGF/VPF antibody (Santa Cruz Biotechnology, San Diego, CA).

Western Blotting—MDA-MB-231 cells were lysed in kinase lysis buffer (New England Biolabs). Proteins were separated by sodium dodecyl sulfate-polyacrylamide gel electrophoresis (SDS-PAGE) under reducing condition, and transferred onto nitrocellulose membrane (Millipore, Boston, MA). The membranes were blocked with 5% bovine serum albumin in PBS and subsequently incubated with primary antibody for overnight incubation at 4°C. Bound antibodies were detected by horseradish peroxidase-conjugated secondary antibody and enhanced chemiluminescence (Amersham Pharmacia Biotech, Piscataway, NJ).

Adenovirus Infection—an adenoviral construct encoding VEGF/VPF₁₆₄ (VEGF-Ad) was constructed as described previously (26). MDA-MB-231 cells were starved in DMEM containing 0.5% FBS overnight and infected with VEGF-Ad or control adenovirus (CTL-Ad) at a multiplicity of infection (MOI) of 100 for 24 hours. Cells were then lysed in kinase lysis buffer for Western blotting and PI3-kinase assay.

TUNEL Assay—MDA-MB-231 cells and antisense VEGF/VPF stable clones were grown on chamber slides and stained with the fluorescein in situ cell death detection kit (Boehringer Mannheim), which is based on the TUNEL method, according to the protocol of the manufacturer. After washing with PBS, the cells were mounted and intracellular fluorescein-labeled fragmented DNA was detected by microscopic analysis.

Flow Cytometry Analysis—MDA-MB-231 cells and **antisense VEGF/VPF stable clones** were grown subconfluently in 6-well plates in culture medium containing 10% FBS. The cells were harvested, centrifuged and fixed with 70% cold ethanol for a minimum of 2 hours. Ethanol-fixed cells were centrifuged and washed once with PBS. The cell pellet was suspended in 1 ml of PI/Triton X-100 staining solution (0.1% Triton X-100, 20 µg/ml PI, 0.2 mg/ml RNase in PBS) and incubated for 15 min at 37 °C. Samples were analyzed by flow cytometry (Becton-Dickinson) and apoptosis was measured as the percentage of cells with a sub G₀/ G₁ DNA content in the PI intensity-area histogram plot (27).

Apoptosis cDNA Array—MDA-MB-231 cells and antisense VEGF/VPF stable transfected clones were grown subconfluently in 6-well plates in culture medium containing 10% FBS. Total RNA preparation and hybridization procedures were performed according to the manufacturer's protocol. Briefly, equal amounts (2 µg) of total RNA from MDA-MB-231 cells and AS-VEGF clones were used for the human apoptosis cDNA array analysis, with a commercially available membrane (R&D Systems). The membranes were prehybridized at 65°C for 2 hours in a hybrid solution (R&D Systems) containing 100 µg/ml freshly boiled salmon sperm DNA, after which the cDNA probes were hybridized onto the membranes at 65°C for 18 hours. The membranes were washed three times in low stringency washing buffer (2 x SSPE - 1% SDS) and three times in high stringency washing buffer (0.1 X SSPE - 0.5% SDS) at 65°C for 20 min each. The membranes were then exposed on a phosphorimager (Molecular Dynamics, Sunnyvale, CA) and analyzed using ArrayVisionTM software (Imaging

Research Inc., Ontario, Canada).

PI3-kinase assay—Cell lysates containing 1 mg of protein were incubated overnight at 4°C with anti-human p85 subunit specific PI3-kinase antibody and Protein G Sepharose (Pharmacia). The Sepharose beads were washed with wash buffer-1 (25 mM HEPES, 150 mM NaCl, 5 mM MgCl₂, 0.1% Triton X-100, 0.2 mM EDTA, pH 7.4) and twice with wash buffer-2 (25 mM HEPES, 150 mM NaCl, 5 mM MgCl₂, 0.2 mM EDTA, pH 7.4). The beads were resuspended in reaction buffer (25 mM HEPES, 5 mM MgCl₂, 0.2 mM EDTA, pH 7.4) containing 5 µg of phosphatidyl inositol (PI), 50 µM ATP, and 5 µCi [γ -³²P]ATP and incubated for 10 min at room temperature. After the reaction was stopped by the addition of 300 µl of 1:1 mixture of HCl and methanol, lipids were extracted by the addition of 250 µl of chloroform and were resolved on thin layer chromatography plates. The plates were then exposed to X-ray film.

RESULTS

VEGF/VPF Increases Penetration of MDA-MB-231 Cells across an HBMEC

Monolayer---To test whether VEGF/VPF increases tumor cell penetration, DiI-labeled MDA-MB-231 cells were added to an HBMEC monolayer cultured onto a Transwell apical chamber, and then penetrating MDA-MB-231 cells were assessed under a fluorescent microscope. VEGF/VPF treatment led to a dose-dependent increase in the penetration of MDA-MB-231 cells across the HBMEC monolayer as compared to the untreated control (Fig. 1). However, basic fibroblast growth factor (bFGF), which is also known as a potent endothelial cell growth factor that does not increase vascular permeability (28), failed to significantly increase the transendothelial migration of the cells. These data indicate the possibility that increased transmigration of MDA-MB-231 cells is due to the endothelial cell retraction induced by VEGF/VPF and not due to the mitogenic effect of VEGF/VPF.

MDA-MB-231 cells failed to migrate toward either the basolateral side of the formaldehyde-fixed HBMEC monolayer or the fibronectin-coated polycarbonate filter without the HBMEC monolayer (data not shown), indicating that the living endothelial monolayer is needed to induce the migration of tumor cells toward the basolateral side of the filter as reported previously (29). To further characterize whether VEGF/VPF is related directly to the increased transendothelial migration of MDA-MB-231 cells, the HBMEC monolayer was treated with VEGF/VPF monoclonal antibodies and with SU-1498, an antagonist of VEGF/VPF receptor (Flk-1/KDR). As shown in Fig. 3, both treatments against VEGF/VPF significantly inhibited the transendothelial migration of MDA-MB-231 cells at 20 μ g/ml and 50 μ M, respectively.

VEGF/VPF Increases the Adhesion of MDA-MB-231 Cells to an HBMEC Monolayer—Metastatic tumor cells attach more preferentially to SEB membrane components than to the apical surface of an intact endothelial monolayer (30). The same phenomenon was observed in this study with MDA-MB-231 cells which attached preferentially to areas where the SEB of the endothelial cell was exposed (Fig. 2, right panel). Therefore, the increased transendothelial migration of MDA-MB-231 cells induced by VEGF/VPF might result from increased adhesion of the cells to the SEB membrane components of endothelial cells which were exposed. To test this possibility, DiI-labeled MDA-MB-231 cells were added to an HBMEC monolayer cultured onto 24-well plates with or without VEGF/VPF and cell adhesion was then assessed under a fluorescent microscope. At a concentration of 30 ng/ml, VEGF/VPF increased the adhesion of MDA-MB-231 cells to the HBMEC monolayer by 3-fold as compared to the untreated control (Fig. 2, left panel), and this effect was blocked by VEGF/VPF monoclonal antibodies and SU-1498 (Fig. 4). However, bFGF failed to significantly increase the adhesion of tumor cells to the monolayer as compared to the untreated control (Fig. 2). These results indicate that the increased transendothelial migration of MDA-MB-231 cells induced by VEGF/VPF was at least in part derived from enhanced tumor cell adhesion onto the exposed SEB membrane components.

VEGF/VPF Increases the Transendothelial Migration and Adhesion of MDA-MB-231 Cells through Calcium Signaling—VEGF/VPF stimulates several molecules mediating intracellular signals in endothelial cells, including mitogen-activated protein/extracellular signal-regulated kinase (ERK) kinase (MEK), phosphatidylinositol

3-kinase (PI3-kinase), and calcium (11). To examine which signaling pathways of VEGF/VPF in endothelial cells are responsible for the increased transendothelial migration and adhesion of MDA-MB-231 cells, the effects of specific inhibitors for various VEGF/VPF signaling pathways were tested. As shown in Figs. 3 and 4, the intracellular calcium chelator (BAPTA-AM) inhibited the increased transendothelial migration and adhesion of MDA-MB-231 cells stimulated by VEGF/VPF while the MEK inhibitor (PD98059) and the PI3-kinase inhibitor (Wortmannin) had no effect, indicating that VEGF/VPF increases the transendothelial migration and adhesion of MDA-MB-231 cells through activation of endothelial calcium signaling.

VEGF/VPF Increases the Permeability of the HBMEC Monolayer—Endothelial cell retraction induces the breakdown of intercellular junctions and leads to an increase in vascular permeability. Therefore, we measured the extent of endothelial cell retraction induced by VEGF/VPF as the degree of permeability change of [³H] inulin through the HBMEC monolayer. As expected, VEGF/VPF meaningfully increased the permeability of the monolayer as compared to the untreated control, and this effect was blocked by VEGF/VPF monoclonal antibody and SU-1498 (Fig. 5). Furthermore, the increased vascular permeability caused by VEGF/VPF was abolished by BAPTA-AM but not by PD98059 and Wortmannin (Fig. 5), indicating that calcium signaling mediates the increased permeability induced by VEGF/VPF.

VEGF/VPF Induces Cytoskeletal Rearrangement of HBMECs—We then assessed the mechanism that leads to increased endothelial cell permeability. One important

regulatory mechanism for the integrity of endothelial cell junction maintenance is the distribution of actin to a cortical pattern, precluding stress fiber formation. As shown in Fig. 6A, VEGF/VPF caused a marked redistribution of actin fibers which condensed toward the center of the cell, with resulting stress fiber formation. The actin condensation in the endothelial cells occurred within 15 min after VEGF/VPF treatment. Actin redistribution induced by VEGF/VPF was substantially reversed by co-incubation with VEGF/VPF monoclonal antibody and SU-1498 (data not shown). These data indicated that VEGF/VPF was responsible for the architectural change within the endothelial cell, leading to increased vascular permeability. Since we found that calcium signaling contributed to the increased permeability stimulated by VEGF/VPF, we assessed its contribution to the redistribution of actin. We found that BAPTA-AM potently blocked the effect of VEGF/VPF in stimulating actin redistribution (Fig. 6A), suggesting a molecular mechanism for the role of calcium in modulating the permeability of the HBMEC monolayer.

We also examined adherens junction protein alignment at the HBMEC monolayer (Fig. 6B). The specific endothelial adherens junctional protein VE-cadherin has been shown to maintain and perhaps regulate endothelial barrier properties (31). VE-cadherin was disrupted to a zig-zag form within 15 min after treatment with VEGF/VPF. After 2 hours, gaps between adjacent endothelial cells could be seen where junctional protein staining was lost (Fig. 6B). Co-incubation of monolayers with BAPTA-AM failed to show disorganization of VE-cadherin or promote the appearance of inter-endothelial gap formation (Fig. 6B), indicating that calcium signaling governs the endothelial junction disorganization produced by VEGF/VPF.

These data suggest that the increased transendothelial migration of MDA-MB-231 cells induced by VEGF/VPF occurs through the loss of junctional proteins, with concomitant gap formation in endothelial monolayer, as shown in Fig. 6C.

Down-Regulation of VEGF/VPF Expression Induces Apoptosis and Inhibits the Transendothelial Migration of MDA-MB-231 Cells —In addition to its vascular permeability activity in endothelial cells, VEGF/VPF induces intracellular signaling that mediates the proliferation and invasion of breast cancer cells (22, 23). To examine the possibility that the endogenous VEGF/VPF in MDA-MB-231 cells modulates the transendothelial migration of these cells, we have generated MDA-MB-231 clones stably transfected with antisense VEGF/VPF cDNA constructs (AS-VEGF-C1 and -C2). In these clones, VEGF/VPF expression was down-regulated significantly as compared to the parental cells (Fig. 7A). When these cells were added to the HBMEC monolayer and examined for transendothelial migration, the two stable clones showed reduced migration toward the bottom of the HBMEC monolayer as compared to the parental or control vector expressing cells (pZeoSV, Fig. 7B). Next, using cell cycle analysis and TUNEL assay, we investigated whether the reduced transendothelial migration of AS-VEGF-C1 and -C2 clones resulted from the increased apoptosis of these cells. As shown in Fig. 8A and B, the apoptosis rates of AS-VEGF-C1 and -C2 clones were significantly increased over the parental or pZeoSV cells, indicating that endogenous VEGF/VPF acts as a survival factor in MDA-MB-231 cells. Furthermore, apoptosis gene array analysis revealed that apoptosis-related genes such as TRAIL, Cox-2, caspase-7, and -8 were up-regulated significantly in AS-VEGF-C1 and -C2 clones as compared to the parental or

pZeoSV cells (Fig. 8C, Table 1), strongly suggesting that the reduced transendothelial migration of AS-VEGF-C1 and -C2 resulted from the increased apoptosis of these cells.

VEGF/VPF Promotes the Survival of MDA-MB-231 Cells Through the PI3-kinase Pathway—Since VEGF/VPF can stimulate the PI3-kinase pathway (11), we examined whether VEGF/VPF mediates the survival of MDA-MB-231 cells through phosphorylation of the serine/threonine kinase Akt/PKB, a downstream target of PI3-kinase. To test this possibility, the AS-VEGF-C1 clone was treated with VEGF/VPF (100 ng/ml) for 15 min and the phosphorylation of Akt was analyzed by Western blotting. VEGF/VPF increased significantly the phosphorylation of Akt as compared to the untreated control (Fig. 9A), but failed to increase the phosphorylation of ERK (data not shown). Epidermal growth factor (EGF) did not increase significantly the phosphorylation of Akt as compared to the untreated control. In addition, VEGF-Ad-infected cells showed increased PI3-kinase activity and Akt phosphorylation as compared to the parental or CTL-Ad-infected cells (Fig. 9B, C, and D). However, no change in the ERK phosphorylation of VEGF-Ad-infected cells was observed (Fig. 9E). These data indicate that VEGF/VPF mediates the survival of MDA-MB-231 cells via the PI3-kinase/Akt pathway.

DISCUSSION

A key event in cancer metastasis is the transendothelial migration of tumor cells. Metastasizing tumor cells should penetrate blood vessels twice, by intravasation and extravasation. These tumor cells may possess an "offensive ability" to penetrate blood vessels. It is well known that increased endothelial cell retraction is closely associated with the enhanced adhesion of tumor cells and their invasion into the endothelial monolayer. Metastasizing tumor cells can induce endothelial cell retraction through the secretion of soluble factors (32, 33) and/or through direct adhesion to the endothelial monolayer where intracellular signals are transduced to induce morphological changes (29). For example, Honn et al. reported that 12(S)-hydroxyeicosatetraenoic acid produced by tumor cells induces retraction of endothelial cells and can enhance tumor cell adhesion to the SEB membrane components of the exposed endothelial monolayer (32). Kusama et al. also reported that endothelial-cell-retraction factor secreted by tumor cells increases the transendothelial migration of tumor cells through enhanced tumor cell adhesion (33).

In this report, we examined whether VEGF/VPF, which is expressed highly in breast cancer cells, enhances the transendothelial migration of MDA-MB-231 cells across a monolayer of brain microvascular endothelial cells. VEGF/VPF has been shown to potently induce the retraction of endothelial cells. As expected, VEGF/VPF significantly increased the transendothelial migration of MDA-MB-231 cells across a monolayer of HBMECs. Our data indicate that enhanced transendothelial migration by VEGF/VPF, at least in part, is derived from the increased adhesion of these cells onto exposed SEB membrane components of the monolayer. The mitogenic effect of VEGF/VPF on endothelial cells does not seem to be related to the increased transendothelial migration

and adhesion of the MDA-MB-231 cells, because bFGF and the MEK inhibitor PD98059 failed to stimulate the transendothelial migration and adhesion of these cells. bFGF has been shown to stimulate the growth of endothelial cells through the ERK pathway as does VEGF/VPF, but does not increase vascular permeability (33). However, the permeability effect of VEGF/VPF seems to be related to the increased transendothelial migration and adhesion of MDA-MB-231 cells, because inhibition of VEGF-induced vascular permeability by the calcium chelator BAPTA-AM significantly prevented the transendothelial migration and adhesion of these cells.

Calcium, as a multifunctional modulator, also regulates permeability in the vascular system (34). Many inflammatory agents including histamine and thrombin as well as VEGF/VPF are known to increase vascular permeability through calcium up-regulation in endothelial cells (35-37). Although the mechanism of how this transient increase in calcium concentration alters vascular permeability has not been fully elucidated, increased calcium in endothelial cells can induce the activation of myosin light chain (MLC) kinase and that phosphorylated MLC contributes to the contraction of endothelial cells from the increased actin-myosin interaction (36). Our data as well as other studies have shown that VEGF-induced actin rearrangement and gap formation in inter-endothelial junctions result in increased permeability (38), and that these effects were significantly blocked by the intracellular calcium chelator BAPTA-AM (Fig. 6B). Interestingly, after adhesion to the endothelial monolayer, malignant tumor cells can transiently increase the calcium concentration of endothelial cells in the contact area and stimulate endothelial cell retraction by breaking the intercellular junctions (28). In the case of the transendothelial migration of leukocytes, leukocytes migrate across the

endothelial monolayer by inducing an enhanced intracellular calcium concentration of the endothelial cells (39-42), and pretreatment of endothelial monolayer with BAPTA-AM did potently block the transendothelial migration of the leukocytes (42). These studies suggest the possibility that cells penetrating through blood vessels have the ability to elicit changes in intracellular calcium concentration in endothelial cells.

VEGF/VPF may also enhance the transendothelial migration of MDA-MB-231 cells through increased adhesion onto the apical surface of endothelial cells as well as onto exposed SEB membrane components. Recently, Kim et al. reported the VEGF/VPF significantly increased expression of E-selectin in human umbilical vein endothelial cells (43, 44). Endothelial E-selectin has been shown to mediate increased adhesion onto endothelial monolayer and the transendothelial migration of some tumor cells across the layer (45, 46). These studies suggest the possibility that VEGF/VPF increases transendothelial migration and adhesion of MDA-MB-231 cells through up-regulation of adhesion molecules such as E-selectin in endothelial cells. However, tumor cells have been reported to attach with higher affinity to SEB membrane components than to the apical surface of an intact endothelial monolayer (29). Thus, we suggest that the vascular permeability of VEGF/VPF might contribute predominantly to the transendothelial migration of tumor cells as compared to the up-regulation of endothelial adhesion molecules by VEGF/VPF.

The hepatoprotective agent Malotilate intensifies the cell-to-cell contact of endothelial cells and increases the integrity of the endothelial monolayer (47, 48). Interestingly, this compound inhibits significantly the *in vitro* transendothelial migration and *in vivo* metastasis of some carcinoma cells (47, 48). Furthermore, some peptides and antibodies

that are able to block the adhesion of tumor cells to SEB membrane components have exerted anti-metastatic effects (49-51). Taken together, our data as well as other studies indicate that the integrity of blood vessels and the progression of tumor metastasis are closely related.

In addition to its vascular permeability activity in endothelial cells, VEGF/VPF has been shown to act as an autocrine survival factor for VEGF/VPF receptor-expressing breast cancer cells (20, 21). Thus, it is possible that endogenous VEGF/VPF affects the transendothelial migration of breast cancer cells through regulation of tumor survival. To test this possibility, we transfected anti-sense VEGF/VPF cDNA into MDA-MB-231 cells and selected two stable clones (AS-VEGF-C1 and -C2). In these clones, VEGF/VPF expression was significantly down-regulated as compared to the parental cells (Fig. 7A). When the cells were seeded onto the endothelial monolayer and examined for transendothelial migration, the two stable clones showed reduced migration toward the bottom of the endothelial monolayer as compared to the parental or control vector expressing cells (Fig. 7B). Using cell cycle analysis and TUNEL assay, we observed that the reduced transendothelial migration of AS-VEGF-C1 and -C2 resulted from the reduced survival of these cells (Fig. 8A and B). We also observed that apoptosis-related genes were up-regulated highly in AS-VEGF-C1 and -C2 clones as compared to the parental or pZeoSV cells (Fig. 8C, Table 1), indicating that endogenous VEGF/VPF is important in maintaining the survival of MDA-MB-231 cells. Next, we examined whether VEGF/VPF induces phosphorylation of Akt, a downstream target of PI3-kinase, in MDA-MB-231 cells since the PI3-kinase pathway is a major survival signaling pathway in several cell types. As shown in Fig. 9A, VEGF/VPF increased significantly

the phosphorylation of Akt in the AS-VEGF-C1 clone. However, the parental cells responded poorly to the exogenously added VEGF/VPF (data not shown). It is possible that parental cells might be governed by the autocrine signaling of endogenously expressed VEGF/VPF. In fact, when MDA-MB-231 cells were allowed to constitutively overexpress VEGF/VPF upon infection with adenovirus encoding VEGF/VPF (Fig. 9B), VEGF-Ad-infected cells showed increased PI3-kinase activity and Akt phosphorylation as compared to the parental cells (Fig. 9C and D). These data indicate that VEGF/VPF acts as an autocrine survival factor via the PI3-kinase pathway in MDA-MB-231 cells. Recently, VEGF/VPF antisense oligodeoxynucleotide was reported to down-regulate VEGF/VPF expression in MDA-MB-231 cells and induced apoptosis through inhibition of PI-3 kinase activity (20). In this study, we obtained similar results by using cells stably transfected with antisense VEGF/VPF cDNA constructs and cells that overexpressed VEGF/VPF upon infection with adenovirus encoding VEGF/VPF. From these results as well as the above-mentioned study, it is possible that VEGF/VPF can act as a survival factor in MDA-MB-231 cells via PI-3 kinase pathway.

To date, VEGF/VPF has been shown to exert an essential role in tumor angiogenesis. However, its role as a vascular permeability factor or tumor survival factor in metastatic processes, such as transendothelial migration, has not been defined. Melnyk et al. reported that neutralization of the function of VEGF/VPF potently blocked tumor metastasis irrespective of its angiogenic property (52). However, their study did not demonstrate the inter-relationship between tumor metastasis and the functions of VEGF/VPF in vascular permeability and tumor cell survival. Thus, functional blocking of VEGF/VPF is a potentially effective therapeutic approach to delay or prevent tumor

metastasis through inhibition of multiple steps of tumor progression, such as neo-vascularization (angiogenesis) in tumor bearing tissue, survival and transendothelial migration of tumor cells.

In conclusion, we report that VEGF/VPF enhances the transendothelial migration of tumor cells through down-regulation of endothelial integrity via a paracrine mode and promotion of tumor cell survival via an autocrine mode.

ACKNOWLEDGEMENTS

We thank Dr. Harold Dvorak for providing the adenoviral construct encoding VEGF/VPF. We also thank Dr. Tae Kim for valuable advice during this study, Janet Delahanty for editing, Daniel Kelley for preparation of the figures, and Mikyung Kim-Park for typing the manuscript.

This work was supported in part by National Institutes of Health Grants HL55445 (SA), (R2)CA87200 (HA), DAMD17-99-1-9078 (HA), CA76226 (HA), The experienced Breast Cancer research Grant 34080057089 (HA), Massachusetts Department of Public Health Grant (HA), Milheim Foundation (SA), Claudia Sargent Breast Cancer Fellowship, and Diana Michelis Fellowship (T-H, L). This work was done during the term of an established investigatorship from the American Heart Association (HA). This paper is dedicated to Ronald Ansin and Charlene Engelhard for their continuing friendship and support for our research program.

FOOTNOTES

The abbreviations used are:

Human brain microvascular endothelial cells (HBMECs); vascular endothelial growth factor (VEGF); vascular permeability factor (VPF); fetal bovine serum (FBS); blood-brain barrier (BBB); basic fibroblast growth factor (bFGF); propidium iodide (PI); sodium dodecyl sulfate-polyacrylamide gel electrophoresis (SDS-PAGE); extracellular signal-regulated kinase (ERK); mitogen-activated protein/extracellular signal-regulated kinase kinase (MEK); phosphatidylinositol 3-kinase (PI3-kinase); myosin light chain (MLC); C-terminal SRC kinase (Csk);

REFERENCES

1. Orr, F. W., Wang, H. H., Lafrenie, R. M., Scherbarth, S., and Nance, D. M. (2000) *J. Pathol.* **190**, 310-329
2. Nicolson, G. L., Menter, D. G., Herrmann, J., Cavanaugh, P., Jia, L., Hamada, J. I., Yun, Z., Nakajima, M., and Marchetti, D. (1994) *Oncogenesis*. **5**, 451-471
3. Nicolson, G. L. (1988) *Cancer Metastasis Rev.* **7**, 143-188
4. Akiyama, S.K., Olden, K., and Yamada, K. M. (1995) *Cancer Metastasis Rev.* **14**, 173-189
5. Thurston, G., Suri, C., Smith, K., McClain, J., Sato, T. N., Yancopoulos, G. D., and McDonald, D. M. (1999) *Science*. **286**, 2511-2514
6. Thurston, G., Rudge, J. S., Ioffe, E., Zhou, H., Ross, L., Croll, S. D., Glazer, N., Holash, J., McDonald, D. M., and Yancopoulos, G. D. (2000) *Nat. Med.* **6**, 460-463
7. Olesen, S. P. (1986) *Brain Res.* **368**, 24-29.
8. Tanno, H., Nockels, R. P., Pitts, L. H., and Noble, L. J. (1992) *J. Neurotrauma* **9**, 335-347.
9. Ikeda, E., Achen, M. G., Breier, G., and Risau, W. (1995) *J. Biol. Chem.* **270**, 19761-19766.
10. Gleadle, J. M., Ebert, B. L., Firth, J. D., and Ratcliffe, P. J. (1995) *Am. J. Physiol.* **268**, C1362-C1368.
11. Neufeld, G., Cohen, T., Gengrinovitch, S., and Poltorak, Z. (1999) *FASEB J.* **13**, 9-22
12. Ferrara, N., and Davis-Smyth, T. (1997) *Endocr. Rev.* **18**, 4-25
13. Kim, K. J., Li, B., Winer, J., Armanini, M., Gillett, N., Phillips, H. S., and Ferrara, N. (1993) *Nature*. **362**, 841-844

14. Brekken, R. A., Overholser, J. P., Stastny, V. A., Waltenberger, J., and Minna, J. D., and Thorpe, P. E. (2000) *Cancer Res.* **60**, 5117-5124
15. Senger, D. R., Perruzzi, C. A., Feder, J., and Dvorak, H. F. (1986) *Cancer Res.* **46**, 5629-5632.
16. Brown, L. F., Berse, B., Jackman, R. W., Tognazzi, K., Guidi, A. J., Dvorak, H. F., Senger, D. R., Connolly, J. L., and Schnitt, S. J. (1995) *Hum. Pathol.* **26**, 86-91
17. Berkman, R. A., Merrill, M. J., Reinhold, W. C., Monacci, W. T., Saxena, A., Clark, W. C., Robertson, J. T., Ali, I. U., and Oldfield, E. H. (1993) *J. Clin. Invest.* **91**, 153-159
18. Boockvar, C. A., Charnock-Jones, D. S., Sharkey, A. M., McLaren, J., Barker, P. J., Wright, K. A., Twentyman, P. R., and Smith, S. K. (1995) *J. Natl. Cancer Inst.* **87**, 506-516
19. De Jong, J. S., van Diest, P. J, van der Valk, P., and Baak, J. P. (1998) *J. Pathol.* **184**, 53-57
20. Bachelder, R. E., Crago, A., Chung, J., Wendt, M. A., Shaw, L. M., Robinson, G., and Mercurio, A. M. (2001) *Cancer Res.* **61**, 5736-5740
21. Masood, R., Cai, J., Zheng, T., Smith, D. L., Hinton, D. R., and Gill, P. S. (2001) *Blood.* **98**, 1904-1913
22. Miralem, T., Steinberg, R., Price, D., and Avraham, H. (2001) *Oncogene.* **20**, 5511-5524
23. Price, D. J., Miralem, T., Jiang, S., Steinberg, R., and Avraham, H. (2001) *Cell Growth Differ.* **12**, 129-135

24. Lee, T. H., Avraham, H., Lee, S. H., and Avraham, S. (2002) *J. Biol. Chem.* **277**, 10445-10451
25. Gospodarowicz, D., Massoglia, S., Cheng, J., and Fujii, D. K. (1986) *J. Cell. Physiol.* **127**, 121-136
26. Sundberg, C., Nagy, J. A., Brown, L. F., Feng, D., Eckelhoefer, I. A., Manseau, E. J., Dvorak, A. M., and Dvorak, H. F. (2001) *Am. J. Pathol.* **158**, 1145-1160
27. Alvarez-Tejado, M., Naranjo-Suarez, S., Jimenez, C., Carrera, A. C, Landazuri, M. O, and del Peso, L. (2001) *J. Biol. Chem.* **276**, 22368-22374
28. Friesel, R. E., and Maciag, T. (1995). *FASEB J.* **9**, 919-925.
29. Lewalle, J. M., Caltaldo, D., Bajou, K., Lambert, C. A., and Foidart, J. M.(1998) *Lin. Exp. Metastasis.* **16**, 21-29
30. Kramer, R. H., Gonzalez, R., and Nicolson, G. L. (1980) *Int. J. Cancer.* **26**, 639-645
31. Dejana, E., Bazzoni, G., and Lampugnani, M. G. (1999) *Exp. Cell Res.* **252**, 13-19
32. Honn, K. V., Grossi, I. M., Diglio, C. A., Wojtukiewicz, M., and Taylor J. D. (1989) *FASEB J.* **3**, 2285-2293
33. Kusama, T., Nakamori, S., Ohigashi, H., Mukai, M., Shinkai, K., Ishikawa, O., Imaoka, S., Matsumoto, Y., and Akedo, H. (1995) *Int. J. Cancer.* **63**, 112-118
34. Curry, F. E. (1992) *FASEB J.* **6**, 2456-2466
35. Morel, N. M, Petruzzo, P. P., Hechtman, H. B., and Shepro, D. (1990) *Inflammation.* **14**, 571-583
36. van Nieuw Amerongen, G. P., Draijer, R., Vermeer, M. A., and van Hinsbergh, V. W. (1998) *Circ. Res.* **83**, 1115-1123
37. Bates, D. O., and Curry, F. E. (1997) *Am. J. Physiol.* **273**, H687-H694

38. Kevil, C. G., Payne, D. K., Mire, E., and Alexander, J. S. (1998) *J. Biol. Chem.* **273**, 15099-15103
39. Huang, A. J., Manning, J. E., Bandak, T. M., Rataui, M. C., Hanser, K. R., and Silverstein, S. C. (1993) *J. Cell Biol.* **120**, 1371-1380
40. Ziegelstein, R. C., Corda, S., Pili, R., Passaniti, A., Lefer, D., Zweier, J. L., Fraticelli, A., and Capogrossi, M. C. (1994) *Circulation.* **90**, 1899-1907
41. Pfau, S., Leitenberg, D., Rinder, H., Smith, B. R., Pardi, R., and Bender, J. R. (1995) *J. Cell Biol.* **128**, 969-978
42. Etienne-Manneville, S., Manneville, J. B., Adamson, P., Wilbourn, B., Greenwood, J., and Couraud, P. O. (2000) *J. Immunol.* **165**, 3375-3383
43. Kim, I., Moon, S. O., Kim, S. H., Kim, H. J., Koh, Y. S., and Koh, G. Y. (2001) *J. Biol. Chem.* **276**, 7614-7620.
44. Kim, I., Moon, S. O., Park, S. K., Chae, S. W., and Koh, G. Y. (2001) *Circ. Res.* **89**, 477-479
45. Brodt, P., Fallavollita, L., Bresalier, R. S., Meterissian, S., Norton, C. R., and Wolitzky, B. A. (1997) *Int. J. Cancer.* **71**, 612-619
46. Laferriere, J., Houle, F., Taher, M. M., Valerie, K., and Huot J. (2001) *J. Biol. Chem.* **276**, 33762-33772
47. Nagayasu, H., Hamada, J., Kawano, T., Konaka, S., Nakata, D., Shibata, T., Arisue, M., Hosokawa, M., Takeichi, N., and Moriuchi T. (1998) *Br. J. Cancer.* **77**, 1371-1377
48. Shibata, T., Nagayasu, H., Hamada, J., Konaka, S., Hosokawa, M., Kawano, T., Kitajo, H., and Arisue, M. (2000) *Tumour Biol.* **21**, 299-308

49. Gehlsen, K. R., Argraves, W. S., Pierschbacher, M. D., and Ruoslahti, E. (1988) *J. Cell Biol.* **106**, 925-930
50. Yi, M., and Ruoslahti, E. (2001) *Proc. Natl. Acad. Sci. U. S. A.* **98**, 620-624
51. Fujita, S., Suzuki, H., Kinoshita, M., and Hirohashi S. (1992) *Jpn. J. Cancer Res.* **83**, 1317-1326
52. Melnyk, O., Shuman, M. A., and Kim, K. J. (1996) *Cancer Res.* **56**, 921-924

FIGURE LEGENDS

Fig. 1. VEGF/VPF increases transendothelial migration of MDA-MB-231 cells across an HBMEC monolayer. HBMECs were added to fibronectin-coated 24-well Transculture inserts with pore sizes of 8 μ m (Costar Corp.) and grown for 5 days in 5% CO₂ at 37 °C. 40,000 DiI-labeled MDA-MB-231 cells were added to the apical chamber. To exclude the chemoattractant effect of the added growth factor, bFGF or VEGF/VPF was added evenly to the apical and basolateral chambers. After incubation for 6 hours, the apical chamber was fixed with 3.7% formaldehyde and washed extensively with PBS. The apical side of the apical chamber was scraped gently with cotton wool. Only the migrating tumor cells were observed by a fluorescent microscope and counted from 10 random fields of 200 magnification. The results are presented as the mean \pm SD of duplicate samples and are representative of 5 individual studies. CTL, control

Fig. 2. VEGF/VPF increases Adhesion of MDA-MB-231 cells onto the HBMEC monolayer. HBMECs were added to attachment factor-coated 24-well culture plates and grown for 5 days in 5% CO₂ at 37 °C. 100,000 DiI-labeled MDA-MB-231 cells in 500 μ l of the same medium were added to each well with or without test samples. After incubation for 2 hours, the wells were fixed with 3.7% formaldehyde and washed extensively with PBS to remove floating tumor cells. Attached tumor cells were observed by a fluorescent microscope and counted from 10 random fields of 200 magnification. Alternatively, to detach the endothelial monolayer, the monolayers were treated with 50 mM NH₄OH solution for 5 min and washed extensively with PBS before adding the DiI-

labeled MDA-MB-231 cells. The results are presented as the mean \pm SD of triplicate samples. CTL, control; EC, endothelial cells; SEB, sub-endothelial basement

Fig. 3. BAPTA/AM inhibits transendothelial migration of MDA-MB-231 cells across an HBMEC monolayer. HBMECs were added to fibronectin-coated 24-well Transculture inserts with pore sizes of 8 μ m (Costar Corp.) and grown for 5 days in 5% CO₂ at 37 °C. The monolayers were pre-treated for 30 min with the indicated inhibitors and washed twice with culture medium. 40,000 DiI-labeled MDA-MB-231 cells were added to the apical chamber. To exclude the chemoattractant effect of the added growth factor, VEGF/VPF was added evenly to the apical and basolateral chambers. After incubation for 6 hours, the apical chamber was fixed with 3.7% formaldehyde and washed extensively with PBS. The apical side of the apical chamber was scraped gently with cotton wool. Only the migrating tumor cells were observed by a fluorescent microscope and counted from 10 random fields of 200 magnification. The results are presented as the mean \pm SD of triplicate samples. CTL, control; VEGF-Ab, VEGF/VPF antibody (20 μ g/ml); SU, SU-1498 (50 μ M); PD, PD98059 (10 μ M); WM, Wortmannin (1 μ M); BAPTA, BAPTA-AM (10 μ M)

Fig. 4. BAPTA/AM inhibits adhesion of MDA-MB-231 cells onto the HBMEC monolayer. HBMECs were added to attachment factor-coated 24-well culture plates and grown for 5 days in 5% CO₂ at 37 °C. The monolayers were pre-treated for 30 min with the indicated inhibitors and all inhibitors except VEGF/VPF monoclonal antibodies and SU-1498 were removed from the monolayers by washing twice with culture medium.

100,000 DiI-labeled MDA-MB-231 cells in 500 μ l of the same medium were added to each well with or without VEGF/VPF. After incubation for 2 hours, the wells were fixed with 3.7% formaldehyde and washed extensively with PBS to remove floating tumor cells. Attached tumor cells were observed by a fluorescent microscope and counted from 10 random fields of 200 magnification. The results are presented as the mean \pm SD of triplicate samples. CTL, control; VEGF-Ab, VEGF/VPF antibody (20 μ g/ml); SU, SU-1498 (50 μ M); PD, PD98059 (10 μ M); WM, Wortmannin (1 μ M); BAPTA, BAPTA-AM (10 μ M)

Fig. 5. VEGF/VPF increases the permeability of the HBMEC monolayer.

Approximately 100,000 HBMECs were added to fibronectin-coated 24-well Transculture inserts with pore sizes of 0.4 μ m (Falcon Corp.) and grown for 5 days in 5% CO₂ at 37°C. After the removal of culture medium, 0.4 ml of the fresh culture medium containing [³H] inulin (1 μ Ci) was added to the apical chamber. The basolateral chamber was filled with 0.6 ml of the same medium without [³H] inulin and then VEGF/VPF (30 ng/ml) was added to the apical and basolateral chambers. For the inhibitor treatment, the monolayers were pre-treated for 30 min with various inhibitors as indicated before VEGF/VPF treatment. After the incubation for 2 hours, 30 μ l of medium from the basolateral chamber were collected and the amount of [³H] inulin across the monolayers was determined by scintillation counting. The data represent the mean values of total cpm of three separate experiments. CTL, control; VEGF-Ab, VEGF/VPF antibody (20 μ g/ml); SU, SU-1498 (50 μ M); PD, PD98059 (10 μ M); WM, Wortmannin (1 μ M); BAPTA, BAPTA-AM (10 μ M)

Fig. 6. VEGF/VPF induces actin redistribution and VE-cadherin disruption in HBMECs. *Panel A*, HBMECs were added to fibronectin-coated 24-well Transculture inserts with pore sizes of 0.4 μm and grown for 5 days in 5% CO_2 at 37°C. After assaying for 2 hours, the cells were fixed with 3.7% formaldehyde in PBS, and then permeabilized with 0.5% Triton X-100. The F-actin in the cells was stained according to the method described under “EXPERIMENTAL PROCEDURES” and observed by a fluorescent microscope. *Panel B*, HBMECs were grown as in A. After assaying, the cells were fixed with 3.7% formaldehyde in PBS, and then permeabilized with 0.5% Triton X-100. The VE-Cadherin of the cells was stained according to the method described under “EXPERIMENTAL PROCEDURE” and viewed under a confocal microscope. *Panel C*, HBMECs were grown as in A. Approximately 1,000 BCECF-AM-labeled MDA-MB-231 cells were added to each well with or without VEGF/VPF. After incubation for 2 hours, the cells were fixed with 3.7% formaldehyde in PBS. VE-cadherin in the HBMECs was stained as described under “EXPERIMENTAL PROCEDURES” and viewed under a confocal microscope. MDA-MB-231 cells are visualized by green color, whereas VE-cadherin is viewed as red color, respectively. CTL, control; VEGF/VPF, 30 ng/ml; BAPTA-AM, 10 μM

Fig. 7. Down-regulation of endogenous VEGF/VPF induces the reduced transendothelial migration of MDA-MB-231 cells. *Panel A*, antisense VEGF/VPF transfectants were stably generated as described in “EXPERIMENTAL PROCEDURES”. MDA-MB-231 cells were transfected with antisense VEGF vector and selected in the presence of Zeocin (1 mg/ml). VEGF/VPF expression of MDA-MB-231

transfectants was analyzed by Western blotting using a polyclonal anti-VEGF/VPF antibody. Total protein extracts were analyzed by Western blotting using anti-Csk antibody as an internal control. *Panel B*, HBMECs were added to fibronectin-coated 24-well Transculture inserts with pore sizes of 8 μ m (Costar Corp.) and grown for 5 days in 5% CO₂ at 37 °C. 40,000 DiI-labeled parental or transfected MDA-MB-231 cells were added to the apical chamber. After incubation for 6 hours, the apical chamber was fixed with 3.7% formaldehyde and washed extensively with PBS. The apical side of the apical chamber was scraped gently with cotton wool. Only the migrating tumor cells were observed by a fluorescent microscope and counted from 10 random fields of 200 magnification. The results are presented as the mean \pm SD of triplicate samples.

Fig. 8. Down-regulation of endogenous VEGF/VPF induces apoptosis of MDA-MB-231 cells. *Panel A*, parental or transfected MDA-MB-231 cells were grown subconfluently in 6-well plates in culture medium containing 10% FBS. The cells were harvested, centrifuged and fixed with 70% cold ethanol. Ethanol-fixed cells were centrifuged and suspended in 1 ml of PI/Triton X-100 staining solution and incubated for 15 min at 37 °C. Samples were analyzed by flow cytometry, and apoptosis was measured as the percentage of cells with a sub G₀/ G₁ DNA content in the PI intensity-area histogram plot. *Panel B*, parental or transfected MDA-MB-231 cells were grown on chamber slides and stained with the fluorescein in situ cell death detection kit (Boehringer Mannheim) according to the protocol of the manufacturer. After washing with PBS, the cells were mounted and intracellular fluorescein-labeled fragmented DNA was observed by a fluorescent microscope. *Panel C*, parental or transfected MDA-MB-

231 cells were grown subconfluently in 6-well plates in culture medium containing 10% FBS. Total RNA preparation and hybridization were performed as described under "EXPERIMENTAL PROCEDURES." The hybridized membranes were exposed on a Phosphorimager and analyzed by using ArrayVisionTM software. 1, TRAIL; 2, Cox-2

Fig. 9. VEGF/VPF induces PI3-kinase activation in MDA-MB-231 cells. *Panel A*, the AS-VEGF-C1 clone was grown subconfluently in 6-well plates in culture medium containing 10% FBS. The medium was replaced by culture medium containing 0.5% FBS and, after starvation for 24 hours, the cells were stimulated by VEGF/VPF (100 ng/ml) or EGF (100 ng/ml) for 15 min. The cells were then lysed, and 50 µg of total protein was resolved by 12% SDS-PAGE and subjected to Western blot analysis by using anti-human phospho-Akt antibody. To verify the amount of loaded proteins, blots were reprobed with anti-human Akt antibody. *Panels B-E*, MDA-MB-231 cells were grown subconfluently in 6-well plates in culture medium containing 10% FBS. The medium was replaced by culture medium containing 0.5% FBS and after starvation overnight, the cells were infected with VEGF-Ad. After incubation for 24 hours, the cells were lysed, and 50 µg of total protein was resolved by 12% SDS-PAGE and subjected to Western blot analysis by using anti-human VEGF/VPF antibody (B), anti-human phospho-Akt antibody (D), or anti-mouse phospho-ERK antibody (E). Total protein extracts were analyzed by Western blotting using anti-Csk antibody (B), anti-human Akt antibody (D), or anti-mouse ERK monoclonal antibody (E) as an internal control. Alternatively, a PI3-kinase assay was performed as described under "EXPERIMENTAL PROCEDURES." Briefly, cell lysates containing 1 mg of protein were incubated overnight at 4°C with anti-human p85 subunit

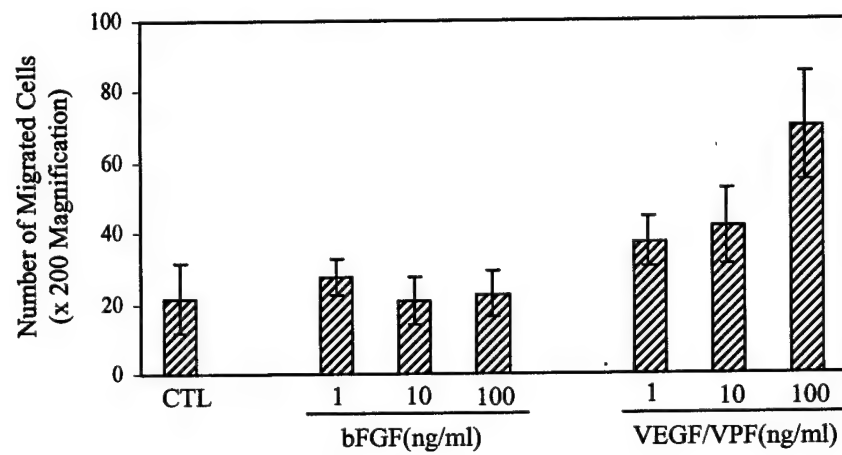
specific PI3-kinase antibody and Protein G Sepharose. After washing, the beads were incubated in reaction buffer containing 5 μ g of PI, 50 μ M ATP, and 5 μ Ci [γ - 32 P]ATP for 10 min at room temperature. Lipid extracts were resolved on thin layer chromatography plates and then the plate was exposed to X-ray film (C, upper panel). The PI3-P was eluted from the plate and the amount was determined by scintillation counting (C, lower panel). CTL, control; PI3-P, phosphatidyl inositol-3 phosphate

Table 1. Expression of apoptosis related-genes in antisense VEGF/VPF transfected MDA-MB-231 cells

The human apoptotic cDNA membranes were hybridized with total RNA isolated from antisense VEGF/VPF-transfected MDA-MB-231 cells. The membranes were exposed on a Phosphorimager and analyzed using ArrayVision™ software. The sVOL is the subtracted volume value derived by subtracting the background volume value from the volume value of the spot. Genomic DNA and GAPDH represent the positive controls for the hybridizations.

Apoptosis related-genes	Control sVOL [(Parental + PzeoSV)/2]	Data sVOL [(VEGF-C1+ C2)/2]	Data/Control ratio (VOL)
TRAIL	0.38	10.30	27.10
Cox-2	0.48	5.91	12.31
GM-CSF	0.38	2.06	5.42
IL-1beta	1.32	5.11	3.87
DAP kinase	0.84	3.17	3.77
VEGI	0.80	2.85	3.56
p27	1.42	4.83	3.40
IAP-1	3.68	11.81	3.20
M-CSF	8.84	27.75	3.13
P21	1.23	3.40	2.76
BimEL	1.17	3.15	2.69
Caspase-7	2.93	7.86	2.68
Rb2/p130	2.34	6.19	2.63
NAIP	2.07	5.37	2.59
GALECTIN-3	7.77	19.86	2.55
IGF-I R	1.71	4.18	2.44
IL-12 p35	1.02	2.46	2.41
Caspase-8	2.23	5.18	2.32
RAR-epsilon	1.97	4.57	2.31
TANK	3.42	7.55	2.20
HLA hc	20.14	43.79	2.17
IFN-gamma R1	3.17	6.85	2.16
BDNF	3.98	8.57	2.15
p100/NF-kappa B2	10.01	21.39	2.13
GAPDH	175.01	226.77	1.29
Genomic DNA	88.79	102.63	1.15

Fig.1



CTL



VEGF/VPF(100 ng/ml)

Fig. 2

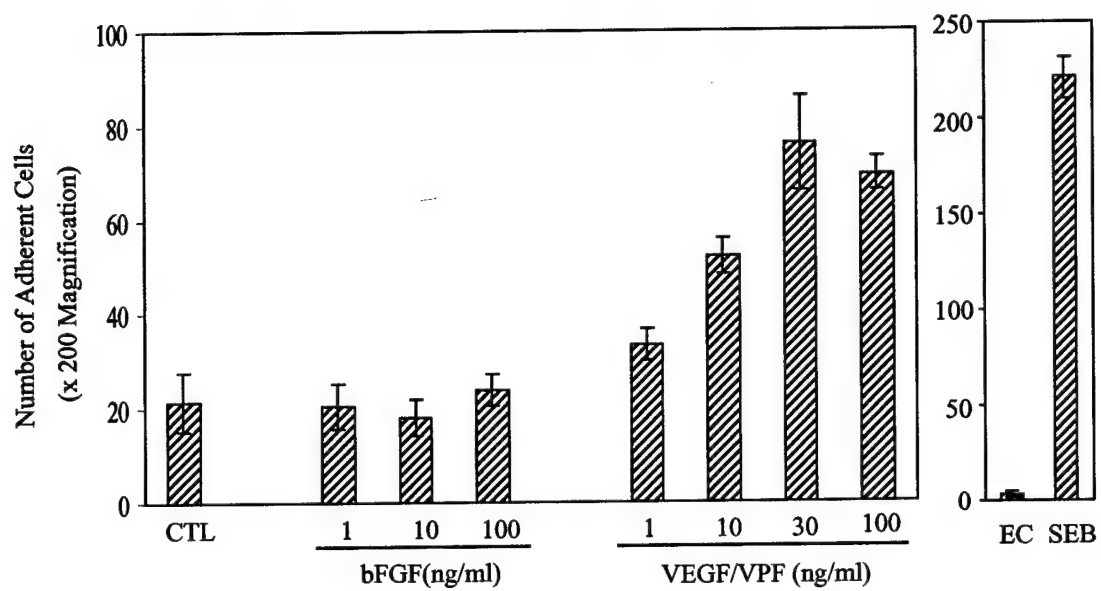


Fig. 3

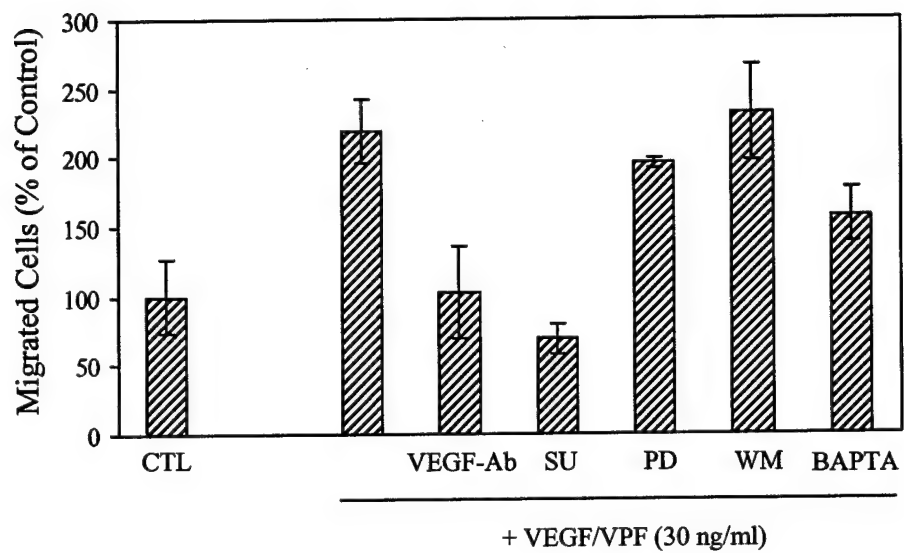


Fig. 4

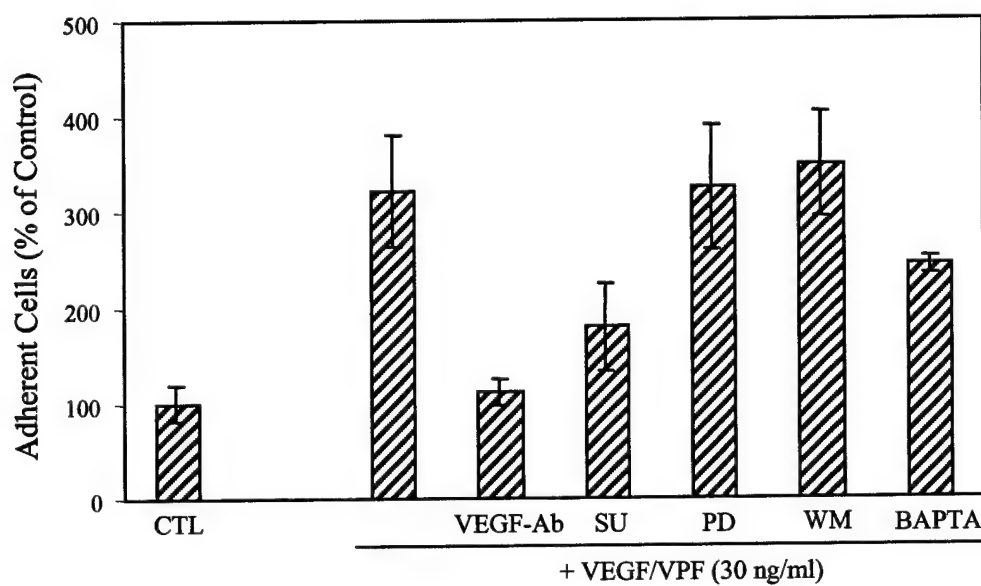


Fig. 5

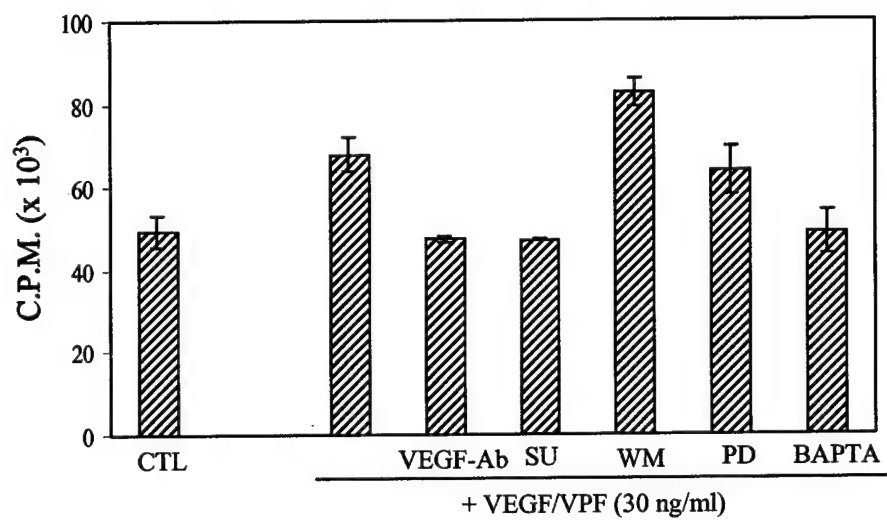
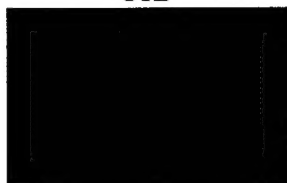


Fig. 6

A



CTL



VEGF/VPF



VEGF/VPF
+ BAPTA-AM

B

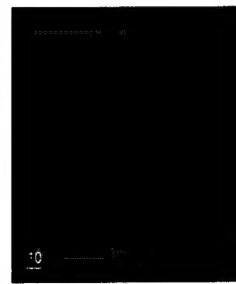
15 min



CTL

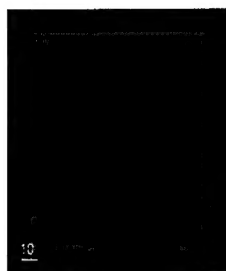


VEGF/VPF



VEGF/VPF
+ BAPTA-AM

120 min

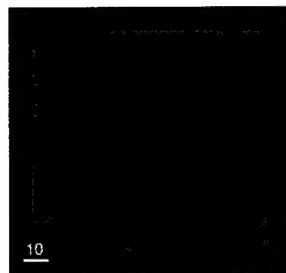


C

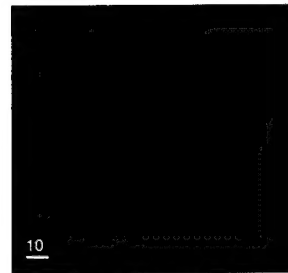
CTL



MDA-MB-231



HBMEC



Overlay

VEGF/VPF

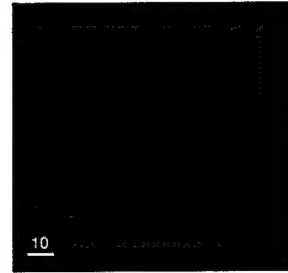
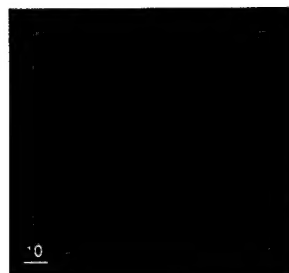
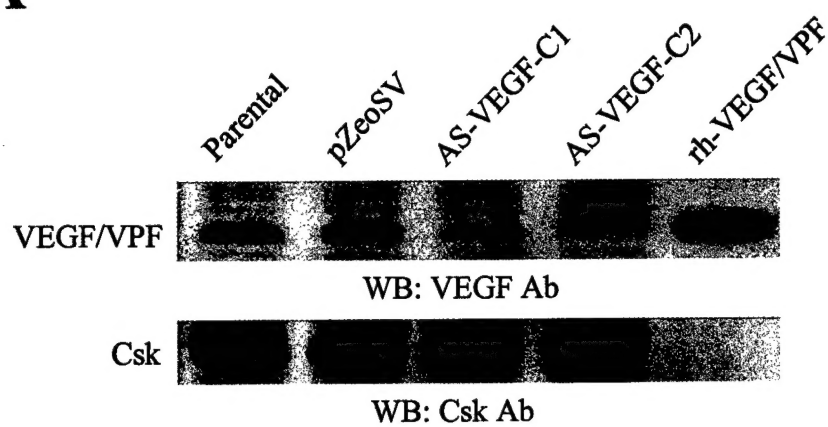


Fig. 7

A



B

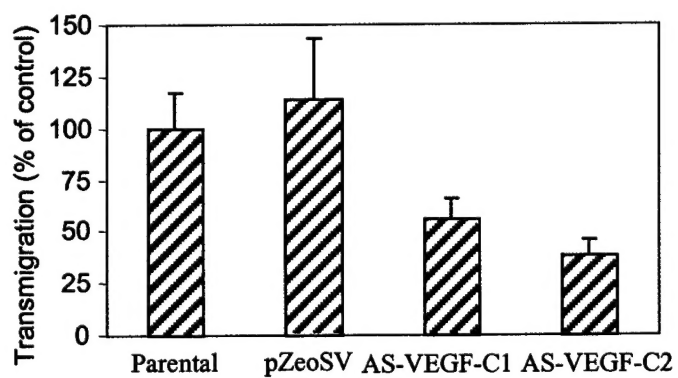


Fig. 8

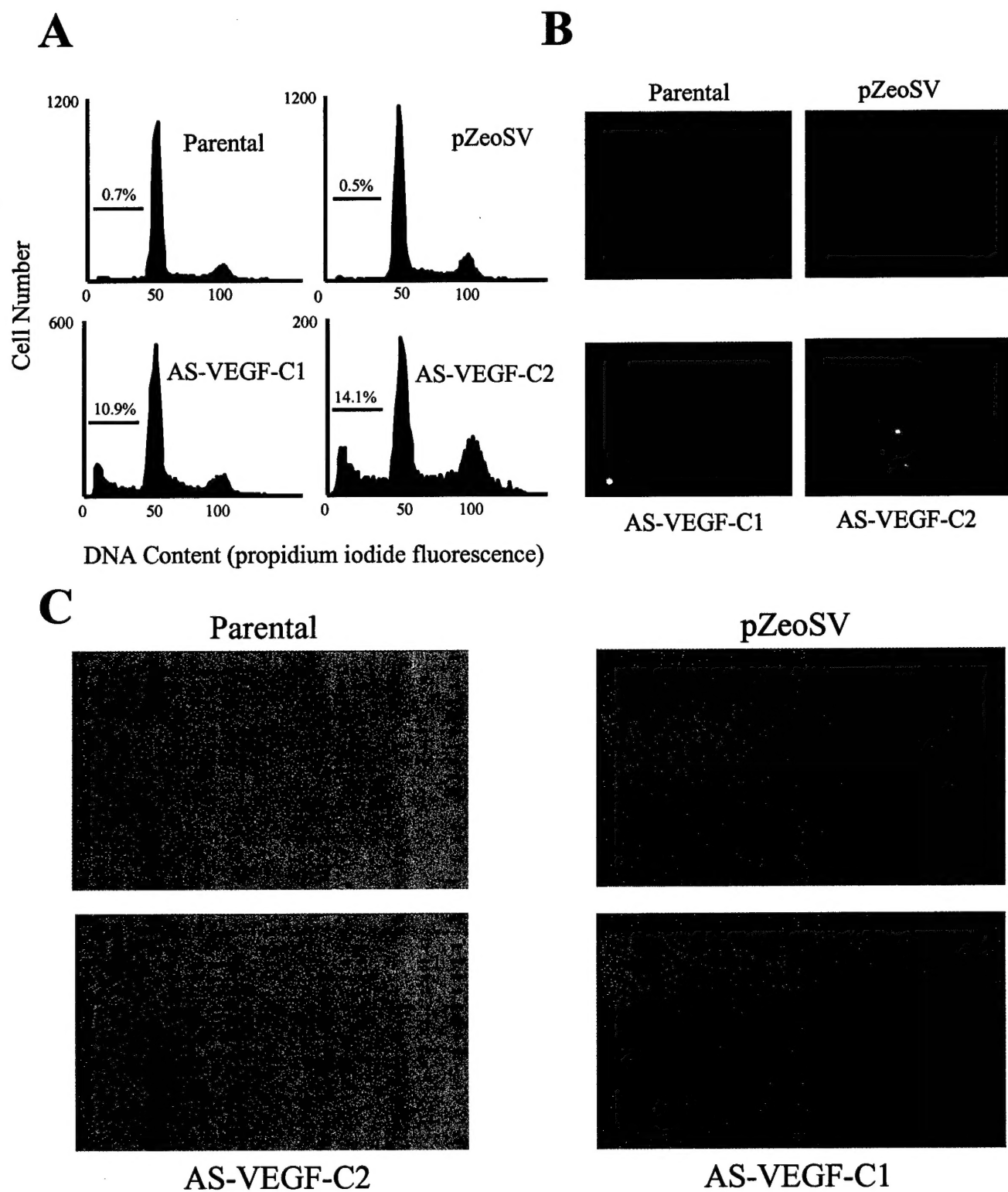
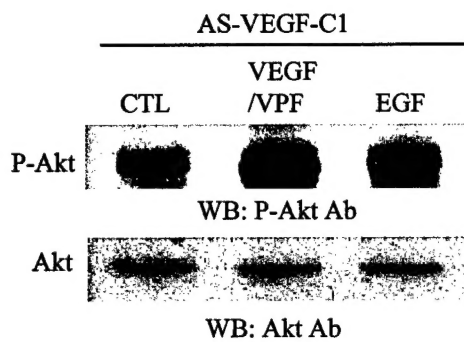
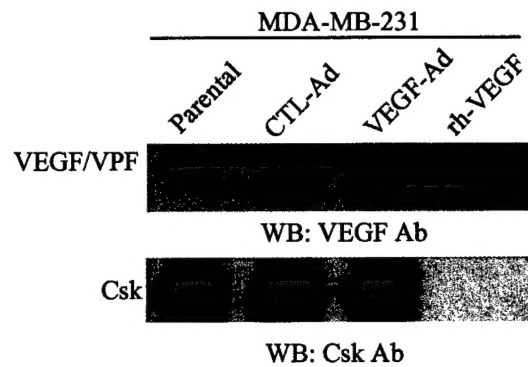


Fig. 9

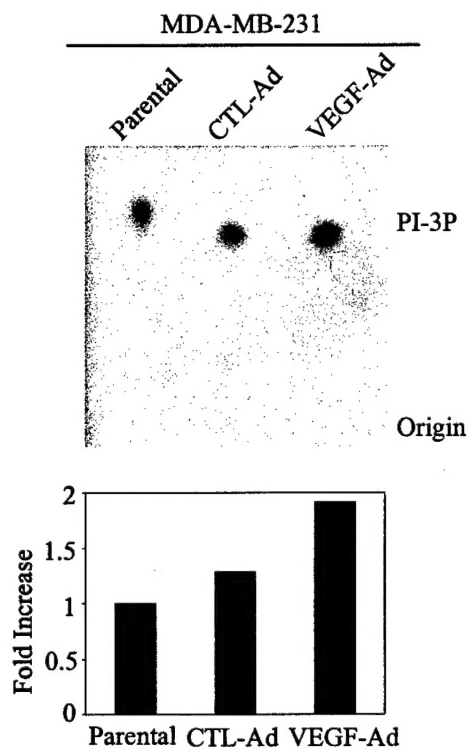
A



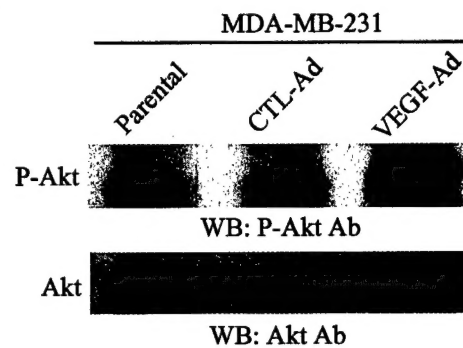
B



C



D



E

